San Jose State University
SJSU ScholarWorks

Master's Theses | Master's Theses and Graduate Research

1991

Physical modelling of transpressional strike-slip faulting : implications for deformational styles surrounding the San Andreas Fault zone

John M. (John Michael), 1940- Wallace
San Jose State University

Follow this and additional works at: https://scholarworks.sjsu.edu/etd_theses

Recommended Citation
Wallace, John M. (John Michael), 1940-, "Physical modelling of transpressional strike-slip faulting : implications for deformational styles surrounding the San Andreas Fault zone" (1991). *Master's Theses*. 175.
DOI: https://doi.org/10.31979/etd.vm9w-fpgs
https://scholarworks.sjsu.edu/etd_theses/175

This Thesis is brought to you for free and open access by the Master's Theses and Graduate Research at SJSU ScholarWorks. It has been accepted for inclusion in Master's Theses by an authorized administrator of SJSU ScholarWorks. For more information, please contact scholarworks@sjsu.edu.

INFORMATION TO USERS

This manuscript has been reproduced from the microfilm master. UMI films the text directly from the original or copy submitted. Thus, some thesis and dissertation copies are in typewriter face, while others may be from any type of computer printer.

The quality of this reproduction is dependent upon the quality of the copy submitted. Broken or indistinct print, colored or poor quality illustrations and photographs, print bleedthrough, substandard margins, and improper alignment can adversely affect reproduction.

In the unlikely event that the author did not send UMI a complete manuscript and there are missing pages, these will be noted. Also, if unauthorized copyright material had to be removed, a note will indicate the deletion.

Oversize materials (e.g., maps, drawings, charts) are reproduced by sectioning the original, beginning at the upper left-hand corner and continuing from left to right in equal sections with small overlaps. Each original is also photographed in one exposure and is included in reduced form at the back of the book.

Photographs included in the original manuscript have been reproduced xerographically in this copy. Higher quality 6" x 9" black and white photographic prints are available for any photographs or illustrations appearing in this copy for an additional charge. Contact UMI directly to order.

UMI

University Microfilms International
A Bell & Howell Information Company
300 North Zeeb Road, Ann Arbor, MI 48106-1346 USA
313/761-4700 800/521-0600

Order Number 1344321

Physical modelling of transpressional strike-slip faulting: Implications for deformational styles surrounding the San Andreas fault zone

Wallace, John M., M.S.

San Jose State University, 1991

U·M·I
300 N. Zeeb Rd.
Ann Arbor, MI 48106

PHYSICAL MODELLING OF TRANSPRESSIONAL STRIKE-SLIP FAULTING: IMPLICATIONS FOR DEFORMATIONAL STYLES SURROUNDING THE SAN ANDREAS FAULT ZONE

A Thesis

Presented to

The Faculty of the Department of Geology

San Jose State University

In Partial Fulfillment

of the Requirements for the Degree

Master of Science

By

John M. Wallace

May, 1991

APPROVED FOR THE DEPARMENT OF GEOLOGY

Dr. John W. Williams

Dr. Deborah R. Harden

Dr. Robert B. Miller

APPROVED FOR THE UNIVERSITY

TABLE OF CONTENTS

	Page
ABSTRACT	viii
INTRODUCTION	1
STRESS FIELD NEAR THE SAN ANDREAS FAULT ZONE	4
Stress Indicators	7
Geologic Evidence For Fault-normal Compression	9
Plate Motion	10
Earthquake Evidence	15
Fault Zone Characteristics	19
EXPERIMENTAL MODELLING	26
Previous Work	26
Limitations of the Wilcox Model	33
PHYSICAL MODELLING	35
Apparatus	35
Modelling Materials	38
Modelling Methods and Techniques	38
Gelatin Experiments	38
Limitations	42
Experiment 1	43
Experiment 2	48
Experiment 3	51
Experiment 4	54
Interpretation of Experimental Results	54
Sand Experiments	58
Experiment 5	59

Experiment 6 68
Experiment 7 76
Experiment 8 78
Sand Sections 87
Summary 95
NATURAL EXAMPLES 99
Coalinga, California 99
Newport-Inglewood Fault, California 103
Alpine Fault, New Zealand 106
DISCUSSION 109
REFERENCES CITED 112

LIST OF ILLUSTRATIONS

Figure		Page
1.	Strike-slip Strain Ellipse	5
2.	Fold Axes, Borehole Breakouts, and Relation to the San Andreas Fault Zone (SAFZ)	8
3.	Fold Axes Flanking the Central Segment of the SAFZ	11
4.	Geologic Section, Fault Orientations Near the Central Segment of the SAFZ	13
5.	Wrench Tectonic Deformational Features	14
6.	Seismicity of Central Coast Ranges	16
7.	Principal Stress Directions, Coalinga Earthquake	17
8.	San Francisco Region Geologic Structures	18
9.	Cross Section Through San Francisco Region	20
10.	Coupled Versus Decoupled Fault Zones	24
11.	Wilcox Clay Experiment	29
12.	Oil Traps Along the Central SAFZ	31
13.	Model Apparatus, Photograph	36
14.	Model Fault Interface, Photograph	37
15.	Model Fine Adjustments, Photograph	39
16.	Photograph of Model Gelatin, No Deformation	41
17.	Photograph of Wilcox Model Simulation	44
	a) Line Drawing	45
18.	Transpression in Gelatin, Photograph	46

a) Line Drawing 46
b) Advanced Deformation, Photograph 47
c) Line Drawing 47

19. Photograph of Separate Gelatin Plates, Oblique View 49
a) Transpression, Photograph 50
b) Line Drawing 50

20. Photograph of High-drag Fault, Transpression 52
a) Line Drawing 52
b) Advanced Deformation, Photograph 53
c) Line Drawing 53

21. Photograph of Low-drag Fault, Transpression 55
a) Line Drawing 55
b) Continued Deformation, Photograph 56
c) Advanced Deformation, Photograph 57
d) Line Drawing 57

22. Naylor Strike-slip Sand Features 60

23. Strike-slip Sand Deformation, Photograph 61
a) Line Drawing 61
b) Continued Deformation, Photograph 62
c) Line Drawing 62
d) Advanced Deformation, Photograph 63
e) Line Drawing 63

24. Photograph of the Central Segment of the SAFZ 65

25. Borrego Mountain Earthquake, Photograph 66
a) Line Drawing 67

26. Unconsolidated Sand Deformation, Photograph 70
a) Line Drawing 70
b) Continued Deformation, Photograph 71
c) Line Drawing 71
d) Advanced Deformation, Photograph 72
e) Line Drawing 72

27. Block Diagram, Santa Cruz Mountains 74

28. Thrust Box Photograph 77
a) Initial Thrusting, Photograph 79
b) Line Drawing 79

c) Continued Thrusting, Photograph 80
d) Line Drawing 80
e) Advance Thrusting, Photograph 81
f) Line Drawing 81

29. Cohesive Sand Deformation For Sections, Photograph 84
a) Line Drawing 84
b) Continued Deformation, Photograph 85
c) Line Drawing 85
d) Advance Deformation, Photograph 86
e) Line Drawing 86
f) Final Deformation, Photograph 88
g) Line Drawing 88

30. Location of Sand Sections 89

31. Section #1, Photograph 90
a) Line Drawing 90
b) Section #2, Photograph 91
c) Line Drawing 91
d) Section #3, Photograph 92
e) Line Drawing 92
f) Section #4, Photograph 93
g) Line Drawing 93
h) Close-up of Thrust Faulting, Photographs 94

32. Three-dimensional Geometry of Sand Sections 96

33. Thrust-ramp Mechanism, Block Diagram 100

34. Shaded-relief Map, Showing Faults, Folds, and Seismicity, Central California 102

35. Newport-Inglewood Fault Zone 104

36. Newport-Inglewood Alquist-Priolo Zone 105

37. Alpine Fault, Block Diagram 107

Tables

1. Summary of Experiments 98

ABSTRACT

PHYSICAL MODELLING OF TRANSPRESSIONAL STRIKE-SLIP FAULTING: IMPLICATIONS FOR DEFORMATIONAL STYLES SURROUNDING THE SAN ANDREAS FAULT ZONE

by John M. Wallace

Thrust faults and folds parallel to the central and northern portions of the San Andreas fault zone are not consistent with the expected orientation of deformational features stemming from a high friction, coupled, pure right-lateral strike-slip fault.

Physical modelling of the San Andreas fault zone, in this study, incorporates the most recent stress field, fault zone, and plate motion data that suggest the San Andreas fault zone is a low-friction, decoupled, transpressional fault zone. Gelatin modelling experiments indicate that fault-parallel thrust faults and folds are related to the convergent component of transpression acting perpendicular to the model plate boundary. Sand models indicate that deformation occurs along low-angle detachment faults in response to fault-normal maximum horizontal stress. The correlation of gelatin and sand models is consistent with observed deformation along the central and northern portions of the San Andreas fault zone.

The genetic relationship between compressional subsurface faulting and surface folding surrounding the San Andreas fault has important implications for seismic hazard zonation. The ability to recognize potentially hazardous compressive stress regimes is enhanced through the use of this modelling study.

INTRODUCTION

Since the advent of the plate tectonic theory in the mid-1920's, a number of geologic structures stemming from strike-slip deformation along the central and northern portions of the San Andreas fault zone (SAFZ) could not be explained in terms of a pure right-lateral, transform fault. These features include a 50 to 100 km wide zone of folds and thrust faults, oriented nearly parallel to the trace of the San Andreas fault (Mount and Suppe, 1987). If these structures are, in fact, associated with the SAFZ, then the maximum horizontal stress must be oriented nearly perpendicular to the SAFZ. A fault-parallel fold and thrust belt is indicative of crustal shortening, which is not consistent with a pure strike-slip fault zone. The San Andreas fault has been characterized as a classic wrench fault with substantial friction, coupling, and drag, with a zone of distributed shear characterized by en echelon folds and faults flanking the throughgoing master strike-slip fault (Wilcox and others, 1973; Harding, 1976). Wilcox used the term "wrench fault," taken from Kennedy (1946), to describe "high-angle strike-slip faults of great linear extent, along which horizontal translation may be tens of miles or considerably more." The presence of en echelon folds adjacent to the SAFZ is well documented; however, their numbers are limited, and their ages suggest development under a different stress regime than the one currently acting across the plate boundary. Through the use of experiments involving models, the discrepancy between the actual field orientation of folds and faults flanking the SAFZ and the expected orientation of deformational features stemming from a right-lateral strike-slip fault will be addressed.

Recent stress field studies along the SAFZ have yielded additional data that are not consistent with classical wrench faulting theory. Through the use of borehole breakouts and earthquake focal mechanisms, Zoback and others (1987) have determined that the maximum horizontal stress surrounding the plate boundary is oriented nearly perpendicular to the trend of the SAFZ. A fault-normal maximum horizontal stress orientation would produce contractional features oriented roughly parallel to the trend of the SAFZ. Additionally, heatflow studies have determined that there is no appreciable frictionally induced heat along the SAFZ. The lack of such heat, combined with a stress field indicating fault-normal compression, indicates that shear stresses along the fault zone are being reduced. For shear stress reduction to occur, fault zone materials must be weak, allowing for sliding at extremely low shear stresses (Zoback and others, 1987).

Because the stress field data across the SAFZ indicate fault-normal compression, and numerous folds and thrust faults suggest crustal shortening, then relative motions between the Pacific and Northern American plates must be consistent with these data and show a component of compression. Plate motion studies performed by Cox and Engebretson (1985) and Harbert (1991) indicate that the Pacific plate underwent a clockwise rotation approximately 2.5-3.9 million years ago, resulting in five degrees of convergence across the central segment of the SAFZ. Therefore, the nature of the boundary between the Pacific and North American plates can best be described as a transpressional plate boundary. Variations in strike of the SAFZ will predictably alter the amount of convergence and the resultant geologic features surrounding these fault bends.

The primary emphasis of this study is to physically model a transpressional plate boundary such as the SAFZ, using the most recent stress field and plate motion data, in order to analyze the relationship between imposed movements and associated stresses across the fault zone and the resultant deformational features developed in response to these stresses. Wilcox and others (1973) performed similar modelling experiments where clay was deformed by strike-slip motion. The resulting structures were related to those features seen along the SAFZ. However, with newly acquired data regarding fault zone characteristics, plate motions, stress orientations, and a more accurate portrayal of fault zone parameters, physical modelling of the SAFZ can be accomplished in a much more representative manner. The structures derived from this type of modelling more closely match the geologic features surrounding the central and northern portions of the SAFZ. The application of this type of modelling to the SAFZ and analogue fault zones will aid in the recognition of structures and may help delineate areas capable of generating potentially hazardous earthquakes.

STRESS FIELD NEAR THE SAN ANDREAS FAULT

The SAFZ in central California has been classified as a classic active wrench fault (Wilcox and others, 1973; Harding, 1976). Harding (1976) and Wilcox and others (1973) identified en echelon folds and faults surrounding the SAFZ that appeared to mimic the structural patterns that are explained by classical frictional faulting theory. The strain ellipse best illustrates the relationship between the relative motion along a throughgoing master strike-slip fault (wrench fault), stress orientations, and the resultant deformational features (fig. 1). A hypothetical strain ellipse, deformed by dextral shear, originally a circle which attained its shape due to right-lateral motion, graphically illustrates how the maximum and minimum stresses become oriented in response to strike-slip motion. The X-axis of the ellipse (short axis) corresponds to the direction of maximum compressive stress, and the Z-axis (long axis) corresponds to the direction of minimum compressive stress. Superimposed upon the strain ellipse are the expected orientations of geologic features related to the dextral slip. The direction of maximum compression is oriented approximately 40° from the trend of the throughgoing fault.

Geologic structures stemming from this stress regime include conjugate strike-slip faults bisected by the compressional vector; they are oriented approximately 30° to 40° from the direction of maximum compression. Conjugate strike-slip faults are also referred to as synthetic Riedel (R) and antithetic Riedel (R') shears. Synthetic Riedel shears have similar motion as, and are oriented at low angles to the primary fault zone, whereas antithetic

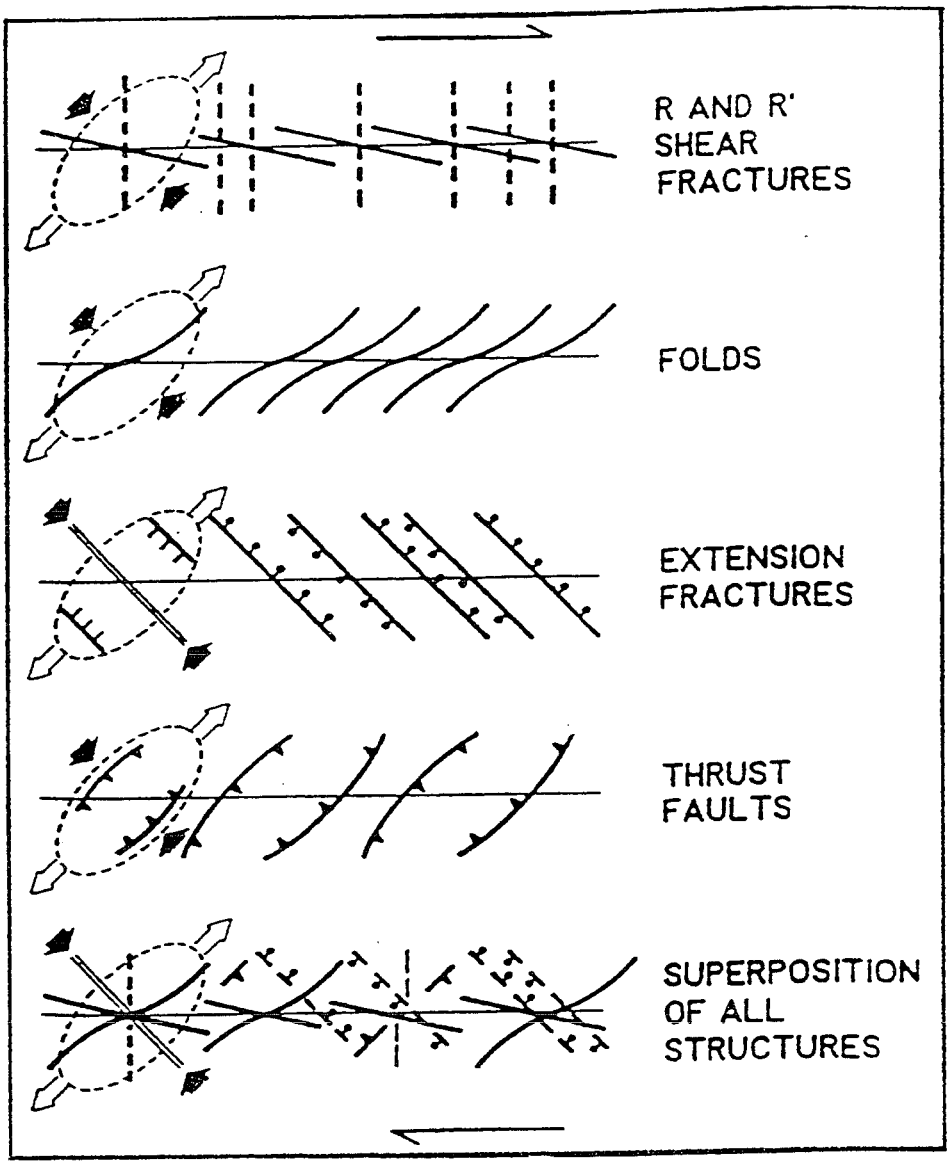

Figure 1. Strain ellipse diagram illustrating stress orientations and deformational features resulting from pure right-lateral shear (modified from Sylvester, 1988).

Riedel shears have the opposite sense of motion and are oriented at high angles to the primary fault zone. Thrust faults, reverse faults, and folds are oriented perpendicular to the direction of maximum compression, forming a right-stepping en echelon array of folds and thrust faults oriented approximately 30° to 40° from the trend of the throughgoing strike-slip fault. In this paper, thrust faults and reverse faults will be included under the term "thrust faults." Normal faults are oriented perpendicular to the direction of maximum extension, forming a left-stepping en echelon array, with individual fault traces oriented approximately 40° from the trend of the throughgoing strike-slip fault (Sylvester, 1988).

If, instead of assuming pure strike-slip motion along a throughgoing fault, a component of compression is involved, then the simple shear model predicts a clockwise rotation of the stress vectors, depending upon the magnitude of the compressional component. Therefore, thrust faults and folds are oriented at slightly lower angles to the throughgoing fault, and extensional faults are oriented at slightly higher angles to the throughgoing fault.

Recent evidence suggests that a large proportion of the geologic features surrounding the SAFZ in central and northern California do not have orientations similar to those seen in the simple shear, strain ellipse model for pure strike-slip or transpressional motion. A large proportion of the thrust faults and folds are oriented nearly parallel to the San Andreas fault (Aydin and Page, 1984; Zoback and others, 1987; Mount and Suppe, 1987). This fault-parallel

orientation cannot be explained in terms of classic simple shear on wrench faults.

Stress Indicators

Through the use of wellbore breakouts, earthquake focal plane mechanisms, hydraulic fracturing, and surface mapping, the orientation of the maximum horizontal compression can be derived. Zoback and others (1987) have compiled a map that shows the orientations of these stress indicators relative to surface trace of the SAFZ (fig. 2).

Vertical boreholes can be used to determine the direction of maximum horizontal stress by measuring the orientation of borehole elongation, also termed breakouts and spalls. Borehole breakouts are thought to occur in response to the concentration of compressive stress on the borehole wall and can be measured with downhole, four-arm calipers, or ultrasonic borehole televiewers (Zoback, 1985). Breakouts are enlargements of the borehole, aligned along the direction of minimum horizontal compression, that can be used to determine the orientation of the principal horizontal in situ stresses. Borehole breakout data are limited to the upper 4 km of the Earth's crust because most exploratory wells fall within this depth.

Earthquake focal plane mechanisms also indicate the direction of maximum horizontal compression, by depicting the sense of motion along fault rupture zones. The typical depth of the seismogenic zone along the SAFZ is 18

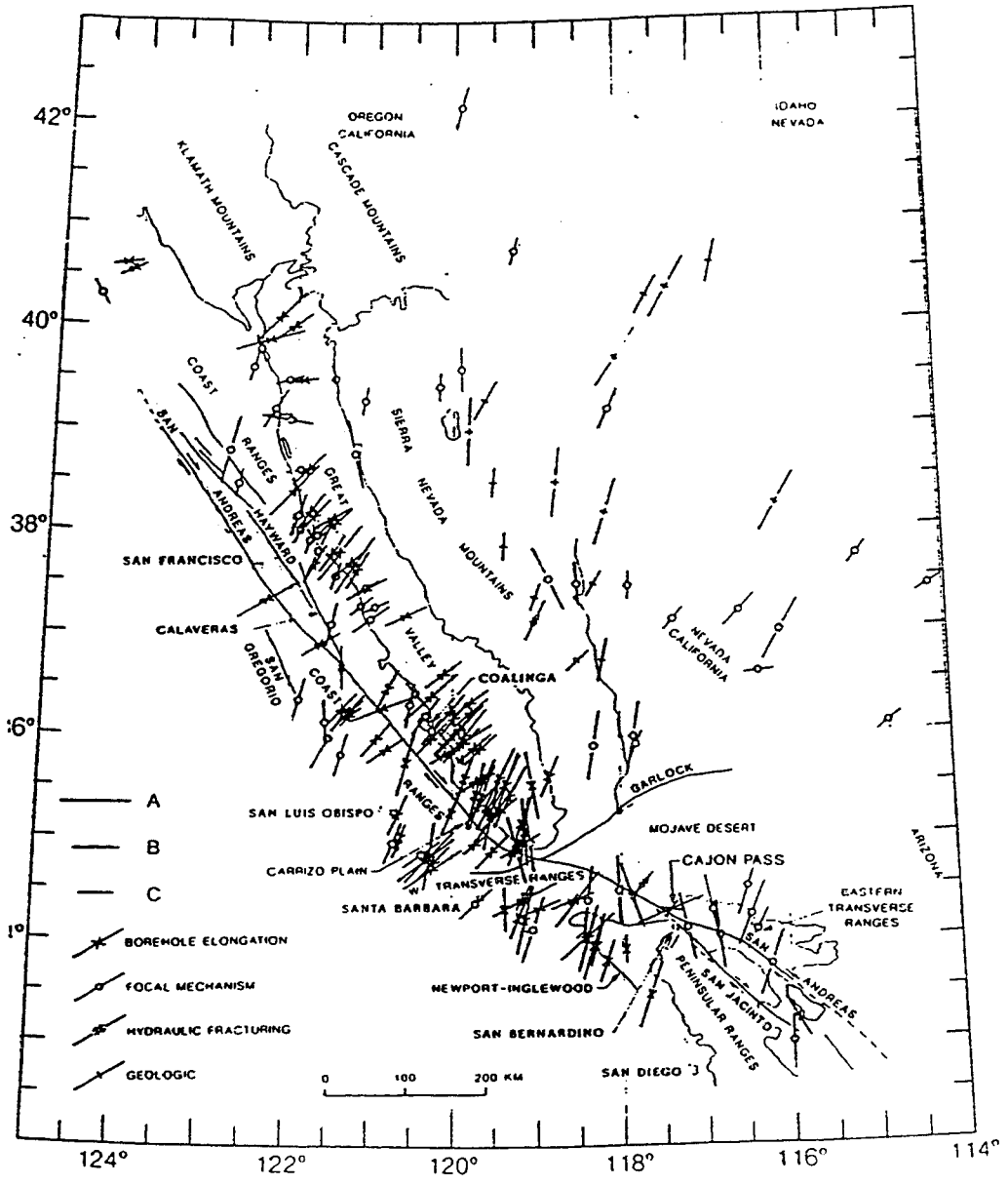

Figure 2. A schematic diagram showing the angular relation between the strike of the San Andreas fault, borehole breakout data, and fold axis orientation along the central segment of the SAFZ (modified from Zoback and others, 1987).

km ± 3 km (Working Group, 1990); therefore, earthquake focal mechanism data are confined to this depth.

Additionally, maximum horizontal stresses can be determined through the use of hydraulic fracturing data. Pore pressure elevation, theoretically, can only rise to the level of the minimum horizontal stress before hydraulic fracturing of the rock occurs along the azimuth of the least principal stress. Therefore, the maximum horizontal stress can be determined from the orientation of hydraulic fractures, just as with the borehole breakout data.

Analysis of Figure 2 indicates that borehole breakout, hydraulic fracturing, and geologic data are in general agreement, suggesting that the stress field surrounding the SAFZ is characterized by fault-normal compression. Previous studies indicated that the maximum horizontal stress in California was oriented mostly in a north-south direction (Zoback, 1980). Far-field stress indicators do indeed delineate a north-south orientation of the maximum horizontal stress, whereas the near-field maximum stress (surrounding the SAFZ) is oriented approximately N 50° E (fig. 2). Maximum horizontal stresses appear to remain nearly fault-normal despite bends in the San Andreas fault, indicating that fault zone characteristics may be responsible for re-orienting stresses across the SAFZ (Zoback and others, 1987).

Geologic Evidence For Fault-Normal Compression

A steadily growing body of geologic evidence suggests that recent structures along the central and northern portions of the SAFZ formed as a

result of compression. The ages of structures, their orientation with respect to the SAFZ, and the timing of plate motion changes of the Pacific plate relative to the North American plate, suggest that a fault-normal fold and thrust belt characterizes the San Andreas transform fault zone. This differs from the widely held perception that the SAFZ predominantly consists of features developed in a purely translational tectonic regime.

Plate Motion

The Hawaiian island hotspot and associated seamount chain has recorded a clockwise rotation of the Pacific plate between 2.5 and 3.9 Ma, resulting in increased convergence along the Pacific-North American plate boundary (Cox and Engebretson, 1985; Harbert, 1991). Cox and Engebretson (1985) have determined that the Pacific plate rotation has created 5° of convergence across the Pacific-North American plate boundary.

Considerable geologic evidence supports a Pliocene onset of compression, the most convincing being the Coast Range uplift, which initiated at approximately 3.0 to 3.5 million years before present. The Coast Ranges are characterized by numerous sub-ranges oriented mostly parallel to the trace of the SAFZ, such as the Santa Cruz, Diablo, Temblor, and Gabilan ranges. Adjacent alluviated depressions, including the Salinas Valley, Santa Clara Valley, and Carrizo Plain are oriented nearly parallel to the San Andreas fault (Zoback and others, 1987). Further evidence is expressed by a 50- to 100-km-wide zone of folded Pliocene and Pleistocene strata with axial planes oriented subparallel to the SAFZ (fig. 3). Numerous thrust and high-angle reverse faults oriented

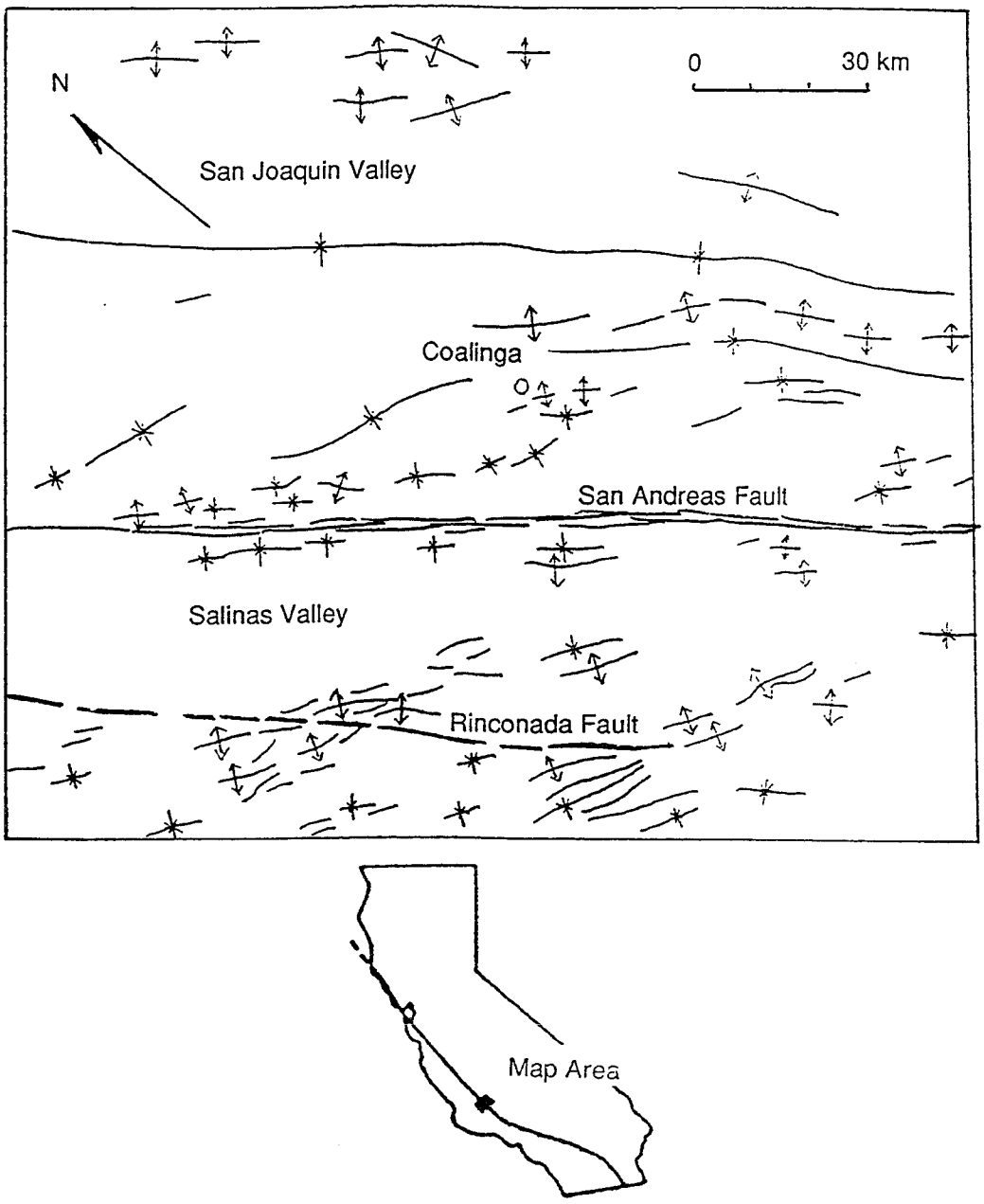

Figure 3. The central segment of the SAFZ near Coalinga with mostly fault-parallel, Pliocene and younger fold axes. Two Miocene folds located north of Coalinga are oriented at higher angles. This line drawing illustrates the wide zone of deformational features surrounding the central segment of the SAFZ (modified from Mount and Suppe, 1987).

nearly parallel to the SAFZ are located within this deformed zone (figs. 3 and 4). These features cannot be explained by deformation within a zone of wrench (strike-slip) deformation.

A zone of wrench deformation is ideally characterized by right-stepping en echelon folds flanking a throughgoing master wrench fault, as shown schematically in Figure 5 (Wilcox and others, 1973; Harding, 1976). Within the zone of distributed shear, continued strike-slip movement would be expected to rotate the existing folds toward parallelism with the wrench fault, and newly developed folds would form at the expected 30° to 40° orientation. However, along the SAFZ near Coalinga, just the opposite is observed. Folds oriented at low angles to the SAFZ are Plio-Pleistocene in age, whereas Miocene folds are oriented more closely to the expected en echelon wrench orientation (Zoback and others, 1987). This could indicate that the SAFZ initially behaved as a zone of wrench deformation, and has since undergone progressive strain softening, resulting in a drop in shear stress and a re-orientation of the principal stress direction. Shear stress reduction along the transpressional plate boundary would result in a re-orientation of the maximum horizontal stress to a near fault-normal direction. Shear stress reduction results in a low friction, decoupled fault zone with translation and contraction occurring simultaneously, but mostly independently (Zoback and others, 1987). Therefore, the development of a fault-parallel fold and thrust belt outside the zone of distributed shear is consistent with the most recent stress data gathered in central and northern California.

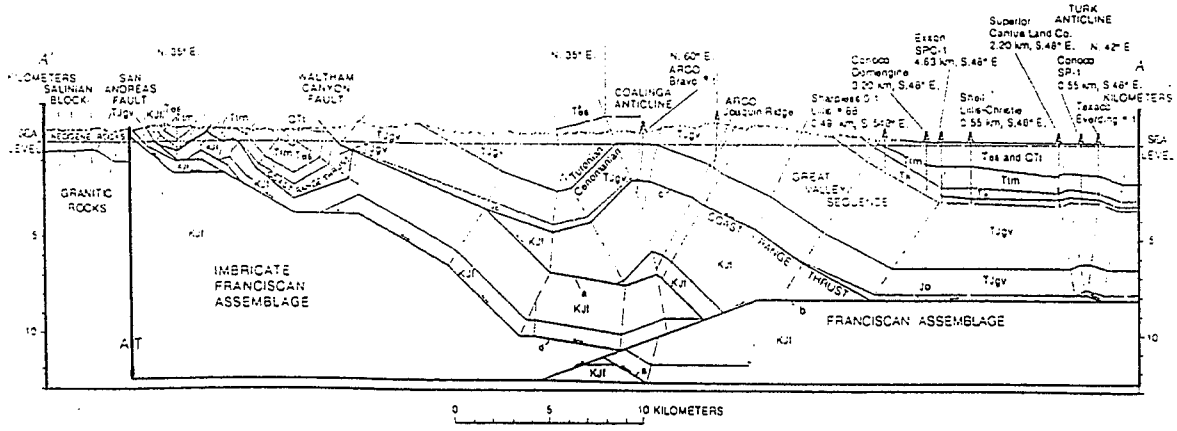

EXPLANATION

QTt	Tulare Formation (Pleistocene and Pliocene)
Tes	Etchegoin and San Joaquin Formations, undivided (Pliocene and Miocene) — Represents late Miocene-Pliocene facies
Tim	Temblor, Monterey, Big Blue, Santa Margarita, and Reef Ridge Formations, undivided (Miocene) — Represents Miocene facies
Tk	Kreyenhagen Formation and lower Eocene and Paleocene rocks, undivided (Eocene and Paleocene) — Represents Paleocene-Eocene facies
Tgv	Great Valley sequence (Paleocene to Jurassic)
Kfr	Franciscan assemblage (Cretaceous and Jurassic)
Jo	Coast Range ophiolite (Jurassic)
———	Contact
———	Fault — Half-arrow indicates direction of relative movement: T, toward; A, away
~~	Unconformity
	Dip of bedding at surface

Figure 4. Area surrounding the central segment of the SAFZ near Coalinga, showing the presence of numerous fault-parallel thrust and high-angle reverse faults. These orientations are not consistent with a high friction, wrench tectonic style of deformation (modified from Namson and others, 1990).

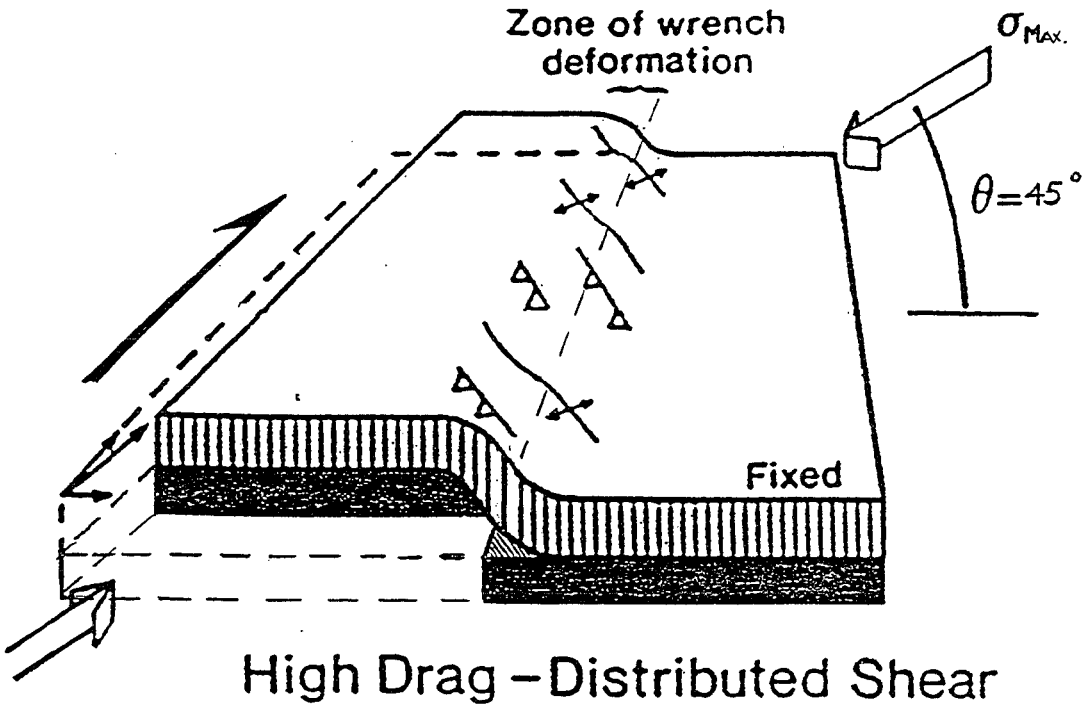

Figure 5. A block diagram illustrating the deformational structures developed within the zone of distributed shear in a high-drag, wrench tectonic style of deformation (modified from Mount and Suppe, 1987).

Earthquake Evidence

An active fold and thrust belt flanks the central segment of the SAFZ and is characterized by structures oriented sub-parallel to the SAFZ, suggesting that crustal shortening is taking place across the Pacific-North American plate boundary. This is supported by Minster and Jordan's (1987) conclusion that 9 ± 3 mm/yr of fault-normal shortening is occurring across the San Andreas fault system. Active thrust faults are located along nearly the entire length of the west side of the Central Valley, as indicated by the 1983 Coalinga (M = 6.7), 1985 North Kettleman Hills (M = 5.7), 1976 Avenal (M = 4.7), and 1982 Idria (M = 5.5) earthquakes (fig. 6). Earthquake focal mechanisms from these and many other smaller earthquakes along the east flank of the southern Coast Ranges suggest that a component of compression is acting across the SAFZ. The inferred P-axis directions of the Coalinga mainshock and large aftershocks are shown in relation to the generalized geology of the Coalinga region, indicating that the maximum average horizontal compressive stress is oriented nearly perpendicular to the trace of the SAFZ (fig. 7) (Eaton, 1990).

In the more structurally complex San Francisco Bay region, the presence of additional active strike-slip fault zones, including the Hayward, Calaveras, Greenville, and San Gregorio fault zones, complicate the deformational picture. These secondary strike-slip fault zones have their own localized stress fields and resultant deformational features, thus eliminating the ability to attribute one deformational mechanism as being responsible for all off-fault deformation. However, when viewed on a large scale, the abundance of thrust faults and folds oriented sub-parallel to the SAFZ is striking (fig. 8). The orientation of structures

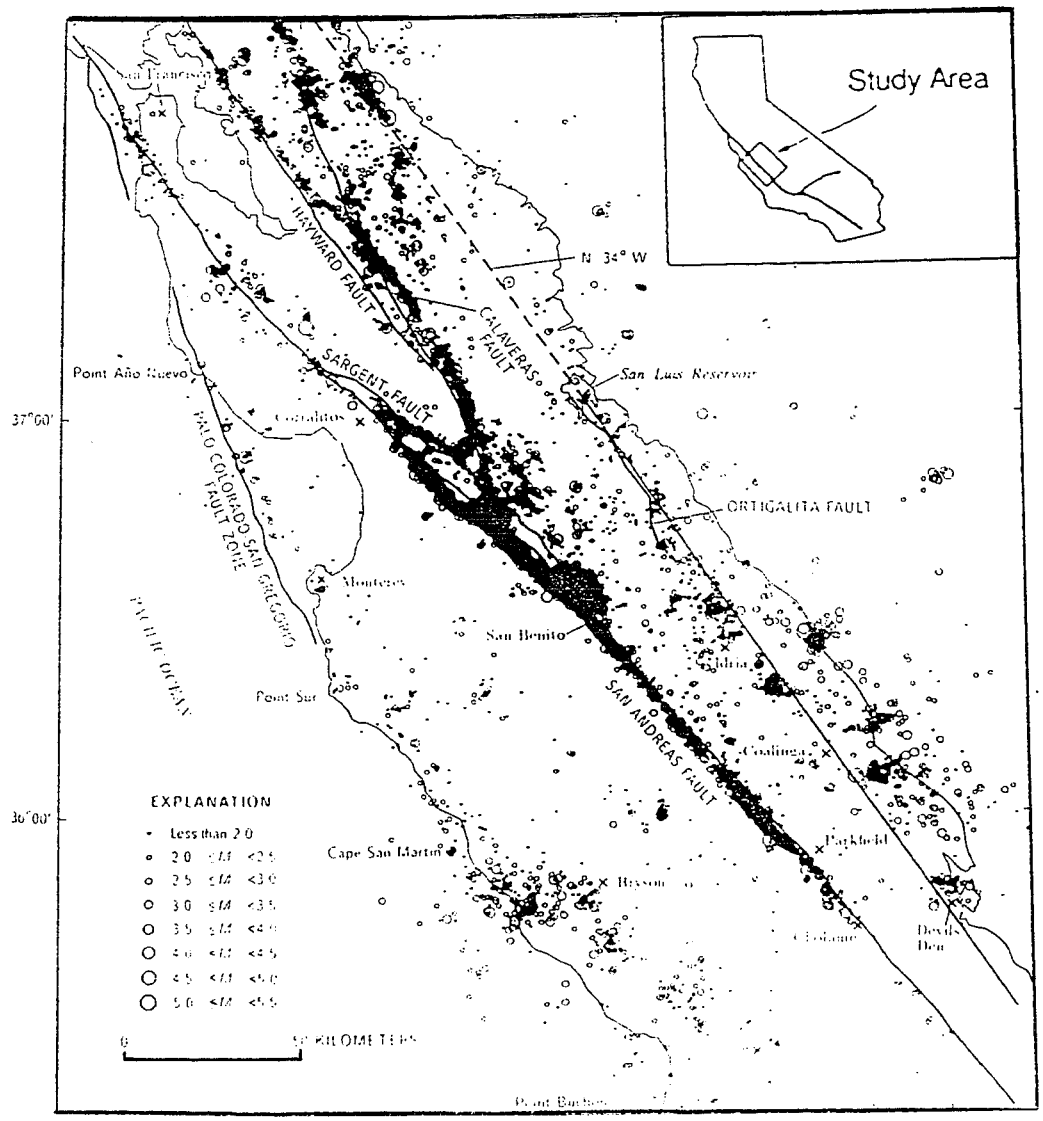

Figure 6. Seismicity (greater than M = 1.5) in the central California Coast Ranges between 1972 and 1983 (prior to the Coalinga event). Note the correlation between the creeping central segment of the SAFZ and the active seismic area located along the eastern flank of the Coast Ranges (modified from Eaton and Rymer, 1990).

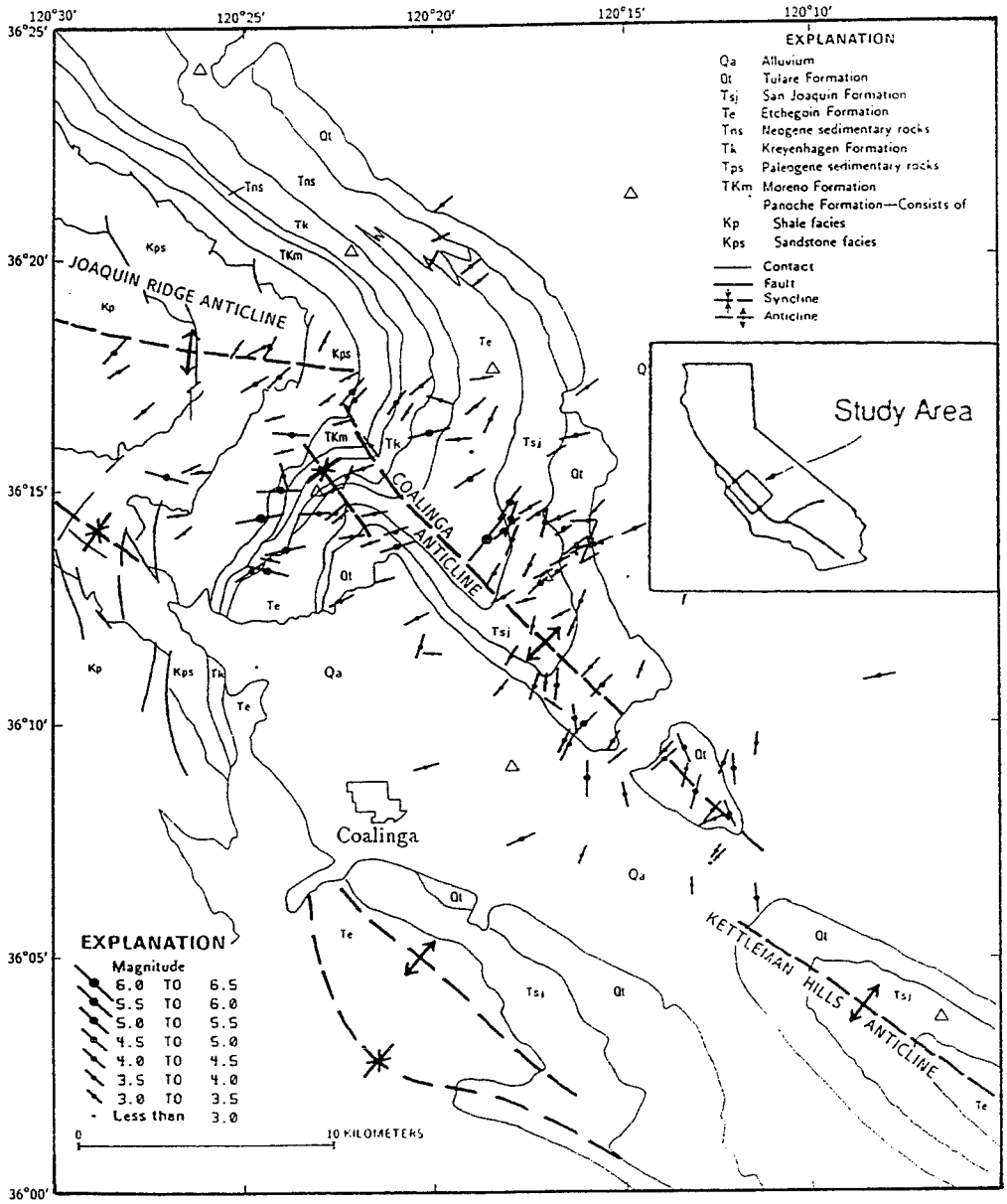

Figure 7. The inferred P-axis directions from the May 2, 1983, Coalinga earthquake and aftershocks. P-axes are superimposed upon the generalized geology of the region. The compressional direction matches the orientation of the fold axes in the region, indicating a probable genetic relationship between earthquakes and folding (modified from Eaton, 1990).

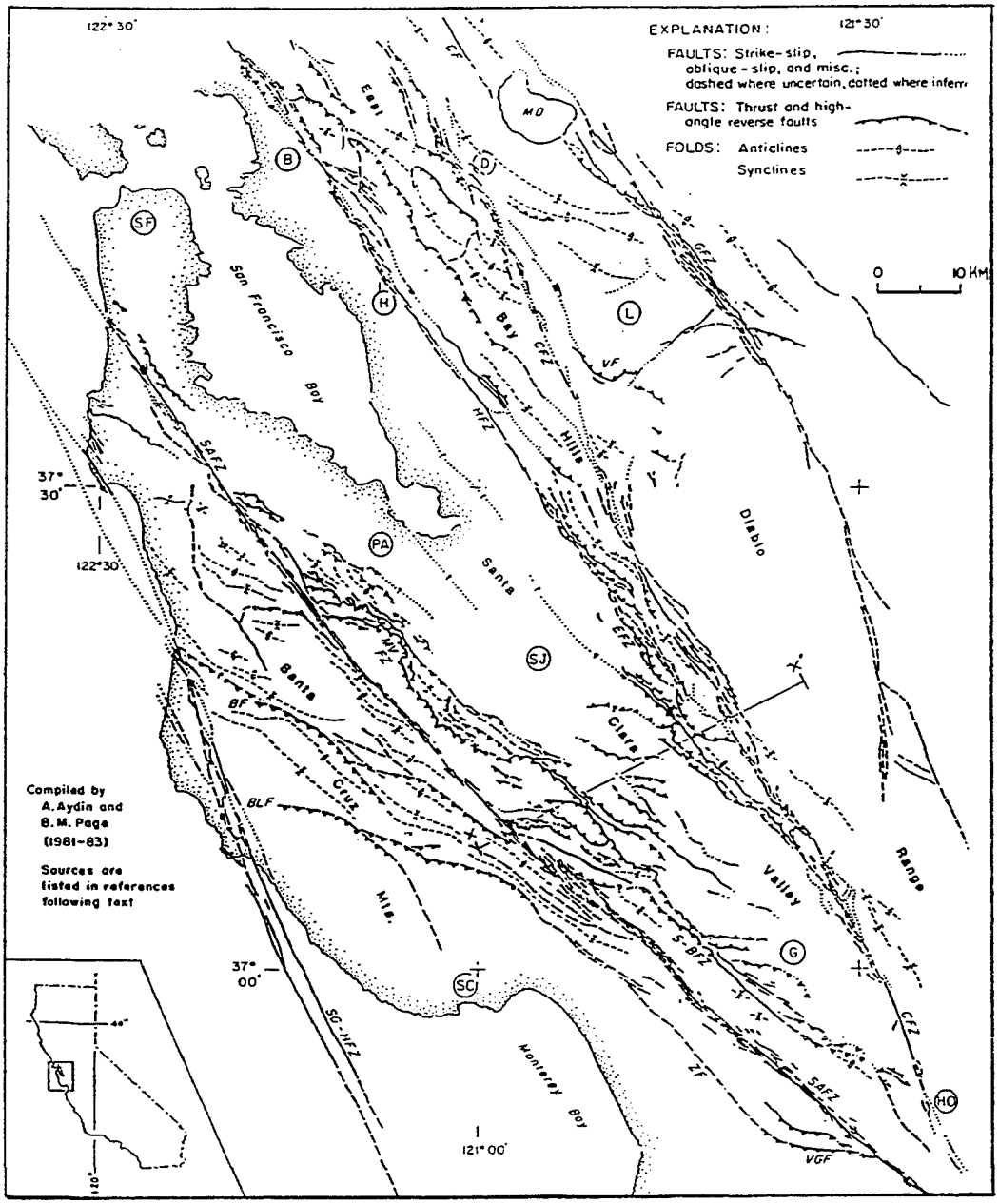

Figure 8. A map of the San Francisco Bay region showing the primary structural features in relation to major cities. The abundance of fault-parallel thrust faults and folds surrounding the San Andreas (SAFZ), Hayward (HFZ), and Calaveras fault zones (CFZ) is striking. It is interesting to note the deformational features oriented at high angles to the SAFZ located in the Salinian block, southwest of the SAFZ. The major faults include the Greenville (GFZ), Evergreen (EFZ), Sargent-Berrocal (S-GFZ), Monte Vista (MVFZ), Vergales (VGF), Concord (CF), Butano (BF), Ben Lomond (BLF), Verona (VF), and the Zayante fault (ZF). The major cities shown are San Francisco (SF), Berkeley (B), Hayward (H), Dublin (D), Livermore (L), Palo Alto (PA), San Jose (SJ), Santa Cruz (SC), Gilroy (G), and Hollister (HO) (modified from Aydin and Page, 1984).

shown in the accompanying cross-section is indicative of a crustal shortening fold and thrust belt surrounding the throughgoing San Andreas and Calaveras strike-slip fault zones (fig. 9).

Focal mechanisms associated with the 1984 Morgan Hill (magnitude M = 6.2) earthquake mainshock and aftershocks provide specific examples of fault-normal compression flanking the Calaveras fault zone. The mainshock focal mechanism illustrates strike-slip movement and associated principal stress directions that are consistent with those expected in a dextral-slip, simple shear environment. However, off-fault focal mechanisms associated with pre- and post-earthquake events show fault-normal compression both east and west of the Calaveras fault trace (Zoback and others, 1987). Therefore, the SAFZ does not appear to be the only fault zone capable of re-orienting the maximum horizontal stress to a fault-normal orientation. The mechanism responsible for re-orienting the maximum horizontal stress is unclear; however, certain fault zone characteristics may be critical in lowering the shear stresses that accommodate translational motion.

Fault Zone Characteristics

Studies along the SAFZ within the past 20 to 25 years, beginning with Henyey (1968), have been unable to detect anomalously high heat flow developed in response to frictional faulting (Working Group, 1990). However, a broad zone of high heat flow has been recognized throughout the entire Coast Ranges, although not in response to frictional faulting along the SAFZ (Lachenbruch and Sass, 1973; Lachenbruch and McGarr, 1990). The lack of

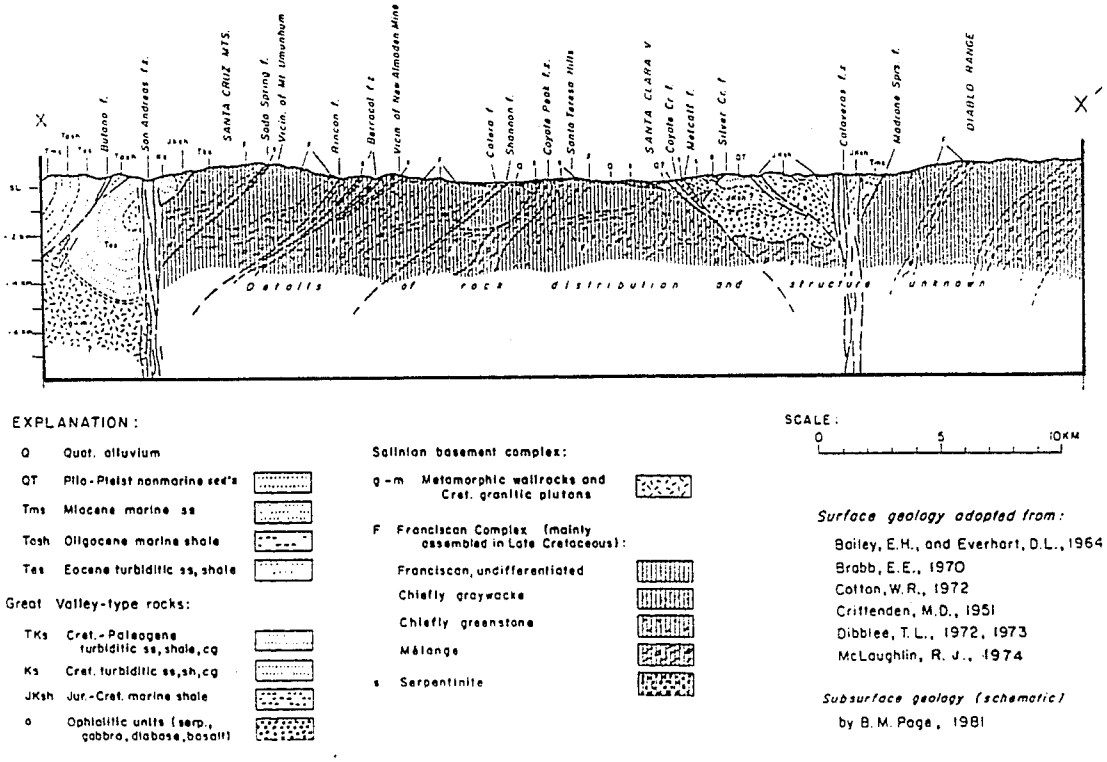

Figure 9. Geologic cross-section X-X', from Figure 13. The major structural deformational features are low-angle thrust faults diverging from the primary throughgoing strike-slip faults. The geologic units and surface expression of deformational and topographic features are represented (modified from Aydin and Page, 1984).

frictionally induced heat along the SAFZ contrasts sharply with laboratory experiments that indicate high frictional strength should be developed in the upper 15 to 20 km (Stesky and Brace, 1973). The lack of frictional heating is puzzling considering that the SAFZ is characterized by hundreds of kilometers of translational offset, is associated with repeated large seismic events, and is currently a transpressional boundary between large lithospheric plates. The transpressional nature of the Pacific-North American plate boundary, as opposed to a pure strike-slip plate boundary, would be expected to increase the friction along the SAFZ due to the added component of compression. Large seismic events suggest that asperities and/or barriers repeatedly impede the horizontal translation between the Pacific and North American plates, resulting in periodic seismic events when the translational plate forces exceed the strength of the fault zone "stuck spots." This type of fault behavior implies that a high friction interface is a critical factor controlling fault motion. The central creeping segment of the SAFZ is characterized by a lack of large earthquakes, but produces numerous, shallow, and small earthquakes. The fact that a well-developed, active fold and thrust belt is located adjacent to the creeping central segment, suggests that shear stresses along the fault may be reduced, transferring convergent motion across the SAFZ into a fault-parallel fold and thrust belt.

Structures surrounding the San Andreas, Hayward, and Calaveras faults do not show the high seismic activity as do those adjacent to the central segment of the SAFZ; however, the short historical seismic record may prevent accurate assessments of these features if earthquakes recur less frequently than every 150 years. Orientations of these structures indicate that both fault-parallel and high-

drag features are present. Subsurface data, although lacking in the San Francisco region, indicates that fault-parallel thrust faults and folds may originate from a "positive flower" or high-friction type of deformation. However, the possible presence of low-angle detachment faults splaying from a low-friction San Andreas fault should not be discounted. The presence of fault-parallel contractional features surrounding the creeping (central segment SAFZ) and non-creeping (Santa Cruz and Peninsula segments) segments of the SAFZ suggests that, despite the fundamental difference in the translational mechanism of the SAFZ, off-fault deformational features may be forming in response to a common stimulus. Therefore, whether a fault zone is involved in repeated stick-slip cycles or continual creep, the factor common to both is a large amount of translational movement. During fault movement, shear stresses along the fault may become reduced, resulting in the re-orientation of the compressional component of plate motion to a fault-normal direction. It is possible that immediately prior to or during an earthquake, fluid pressures become elevated and significantly reduce the shear stresses accommodating translational motion. Zoback and others (1987) indicate that a number of recent studies suggest the SAFZ has low seismic velocity, density, and resistivity, which indicates that it is highly pulverized and possibly overpressured. Highly compressible and highly impermeable fault zone materials, combined with fault-normal compression, could significantly reduce fault strength (Zoback and others, 1987).

Progressive strain-softening of the SAFZ may be one of the primary causes of the fault-normal compressional tectonic environment surrounding the fault. In the early stages development of the SAFZ, prior to the presence of a well

defined, throughgoing fault zone, fault gouge would have yet to be formed. This results in a high drag, high friction fault zone that develops en echelon folds and faults within the zone of wrench deformation (fig. 10). As progressive deformation of the fault zone materials occurs, along with the development of a throughgoing fault zone, frictional drag is reduced and a fault-parallel fold and thrust belt is generated. The continuously creeping central segment may be at a more advanced stage of deformation than other SAFZ segments, to the point of no longer being able to generate large seismic events. If a weak fault zone and fault-normal compression are intimately related in a transpressional environment, then it is not surprising that the most well-developed fault-parallel compressional features can be found flanking the central segment of the SAFZ.

Progressive fault deformation that reaches such an advanced stage of deformation as that which has apparently occurred along the central segment of the SAFZ, may be the consequence of a unique, or at least highly unlikely set of circumstances. Achieving this advanced stage of deformation apparently requires large amounts of translation across the fault interface, a consistent and appropriate degree of convergence across the fault, and a relatively straight, uninterrupted fault segment. Other factors that may be critical for reducing shear stresses along the fault may be the mineralogic characteristics of the fault zone materials, and the introduction of fluids into the fault zone. These, as well as other characteristics, may be complexly interrelated. The fact that more decoupled, low-friction fault zones are not observed may attest the low probability of all these characteristics occurring along one fault zone. However, it

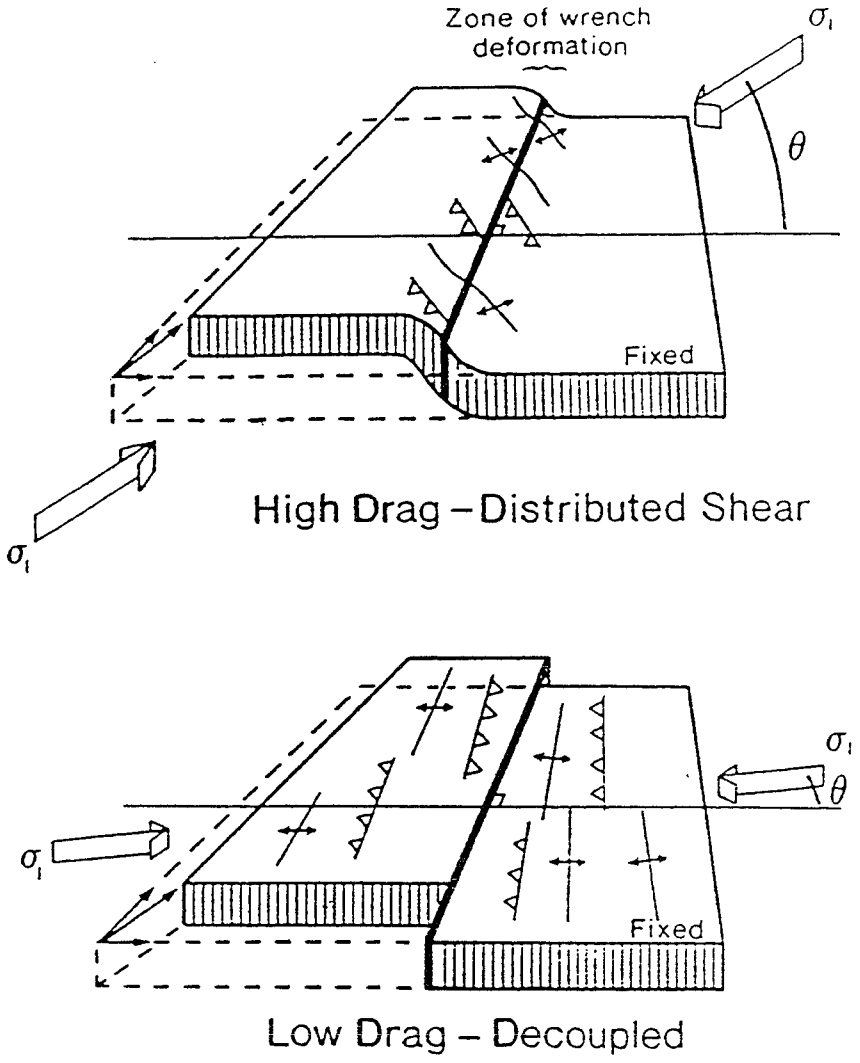

Figure 10. A comparison between structures developed along a relative young fault zone, illustrated by en echelon features surrounding a high-drag fault zone, and a well-developed fault zone, illustrated by the low-drag, strain-softened fault zone. Geologic structures flanking a low-drag fault develop along a wide zone of fault-parallel compression. Geologic structures surrounding a high-drag fault develop only within the narrow zone of distributed shear (modified from Mount and Suppe, 1987).

is possible that decoupled, low-friction fault zones are more widespread, only that they have yet to be recognized.

EXPERIMENTAL MODELLING

The physical modelling of the San Andreas transpressional plate boundary in this study incorporates the most recent stress field and plate motion data and simulates the general plate boundary characteristics that are critical for attaining meaningful results.

Physical modelling of this nature is not intended to precisely scale the Earth's crustal materials or to predict exact locations of folds or faults, but is intended to help visualize large-scale features, just as aerial photographs aid in the recognition of large-scale geologic features that are initially inconspicuous during field investigations. Scale modelling has been performed since the 1920's and has been highly valuable in helping to formulate general theories that aid in the three-dimensional recognition of geologic structures in the field. A full discussion of scaling parameters is beyond the scope of this paper, but previous modelling experiments using similar materials and methods to those of this experiment, have been widely accepted for their general application toward the field recognition of geologic structures.

Previous Work

Some of the earliest physical modelling was performed by Cloos (1928) and Riedel (1929), who employed clay-cake models to study wrench faulting. Subsequent modelling involved the shearing of clay (Cloos, 1955; Oertel, 1965; Tchalenko, 1970; Lowell, 1972; Wilcox and others, 1973; Courtillot, 1974; Hempton, 1985) and collectively reproduced most of the en echelon arrays of

folds and fractures observed in natural wrench fault zones. These studies determined that the greatest principal compressive stress across the shear zone boundary is oriented at approximately 45° to the throughgoing wrench fault (Bartlett, 1981). Experimental modelling performed with clay is particularly valuable when folds are the desired deformational structure. Scaling problems become evident when using clay to simulate fault deformation because of excessive cohesive forces and the inability of water to drain from the clay during experimental modelling (Naylor, 1986). Wilcox and others (1973) published the best-known study of experimental wrench faulting which resulted in their classic paper "Basic Wrench Tectonics."

The Wilcox study, which used clay as the deformational material, was used as a basic guideline for the modelling that was performed in this study. Details of the Wilcox experiment will be outlined in subsequent sections of this paper.

Physical modelling using sand has a long and respected history in geological and soil mechanical modelling (Hubbert, 1937, 1951; Emmons, 1969; Mandl, 1977; Naylor, 1986). Horsfield (1977) has shown that the use of dry sand allows appropriate downscaling of frictional strength of natural rocks. Naylor (1986) has published the most extensive account of experimental wrench faulting using sand, the details of which will be outlined in subsequent sections of this paper. Numerous other modelling materials have been used to simulate various tectonic environments, including plasticine (McClay, 1976; Tapponnier, 1982), wax (Odonne, 1983; Oldenburg, 1972), and rock (Bartlett, 1981).

Wilcox and others (1973) performed wrench fault experiments and related the deformational patterns developed in the clay to actual field examples observed surrounding strike-slip fault zones. The structural orientations observed within the clay models were used to predict the locations of structural oil traps developed in response to movement along the strike-slip fault. The development of deformational features within the model material was related to the imposed principal stress orientations. The maximum and minimum horizontal stresses could be inferred through the use of circles drawn on the clay surface that, when deformed, acted as a lattice of strain ellipses which provided visual confirmation of the resulting strain (fig. 11). The orientation of experimental deformational features, and the related horizontal stress, was applied to similarly oriented geologic structures observed along portions of the SAFZ.

Experimental results of the Wilcox and others (1976) modelling showed that right-stepping en echelon folds and thrust faults developed flanking a dextral-slip wrench fault. The orientation of these en echelon structures was approximately 30° to 40° to the strike of the throughgoing fault and suggested that the maximum horizontal compressive stress was oriented at 90° to these features. Therefore, the maximum compressive stress acting across the model fault zone should have an orientation of approximately 30° to 40° to the wrench fault trace, and is expected to be oriented perpendicular to the thrust faults and folds. These results were applied to folded and faulted rock observed along the west side of the San Joaquin valley, east of the central segment of the SAFZ (fig.

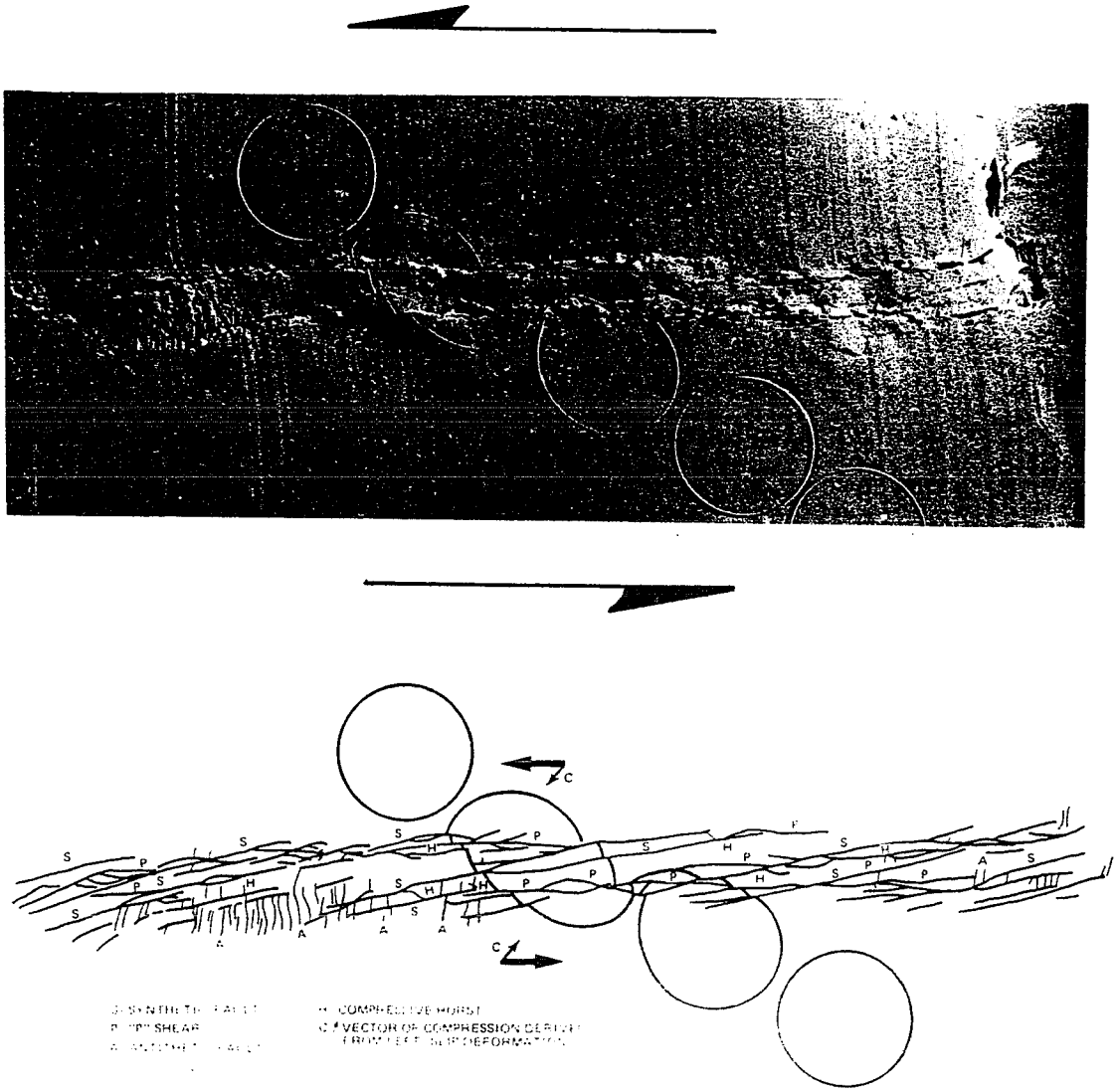

Figure 11. An illustration of the Wilcox model. Clay was deformed by an underlying basement strike-slip fault and the deformational features that developed in the clay were used to correlate with natural field examples. Circles drawn on the clay depict the imposed stresses upon the clay (Modified from Wilcox and others, 1973).

12). This area is characterized by a number of oil-bearing anticlines oriented in a right-stepping, en echelon manner; however, the majority of the folds are oriented sub-parallel to the SAFZ. Wilcox and others postulated that some of these naturally occurring structures developed in much the same way as those of the experimental model. Therefore, the experimental model could be used as a predictive tool for oil exploration. No other modelling experiment had been able to combine mechanical theory, physical modelling, and "real-world" examples into a working hypothesis where each was in fundamental agreement with the other. The ability, through the use of modelling, to associate en echelon folds and related oil traps to strike-slip faults was a highly valuable tool. Wilcox analyzed other major strike-slip fault zones and compared them to his model results, including the Barisan Mountains fault, Sumatra, the Alpine fault, New Zealand, and the Newport-Inglewood fault zone, California.

As previously stated, in central and northern California the majority of the deformational features observed along the SAFZ do not fit the expected 30° to 40°, right-stepping en echelon pattern. In fact, a large proportion of the thrust faults and folds are oriented nearly parallel to the trace of the SAFZ. This phenomenon was not addressed in "Basic Wrench Tectonics." Structures such as folds with near fault-parallel orientations within the zone of distributed shear, can be explained by progressive strike-slip deformation and rotation of en echelon fold axes into parallism with the throughgoing shear zone. Therefore, folds oriented at high angles to the wrench fault should be younger than the folds having near fault-parallel orientations. Just the opposite is seen along the eastern side of the southern Coast Ranges where en echelon folds are thought to

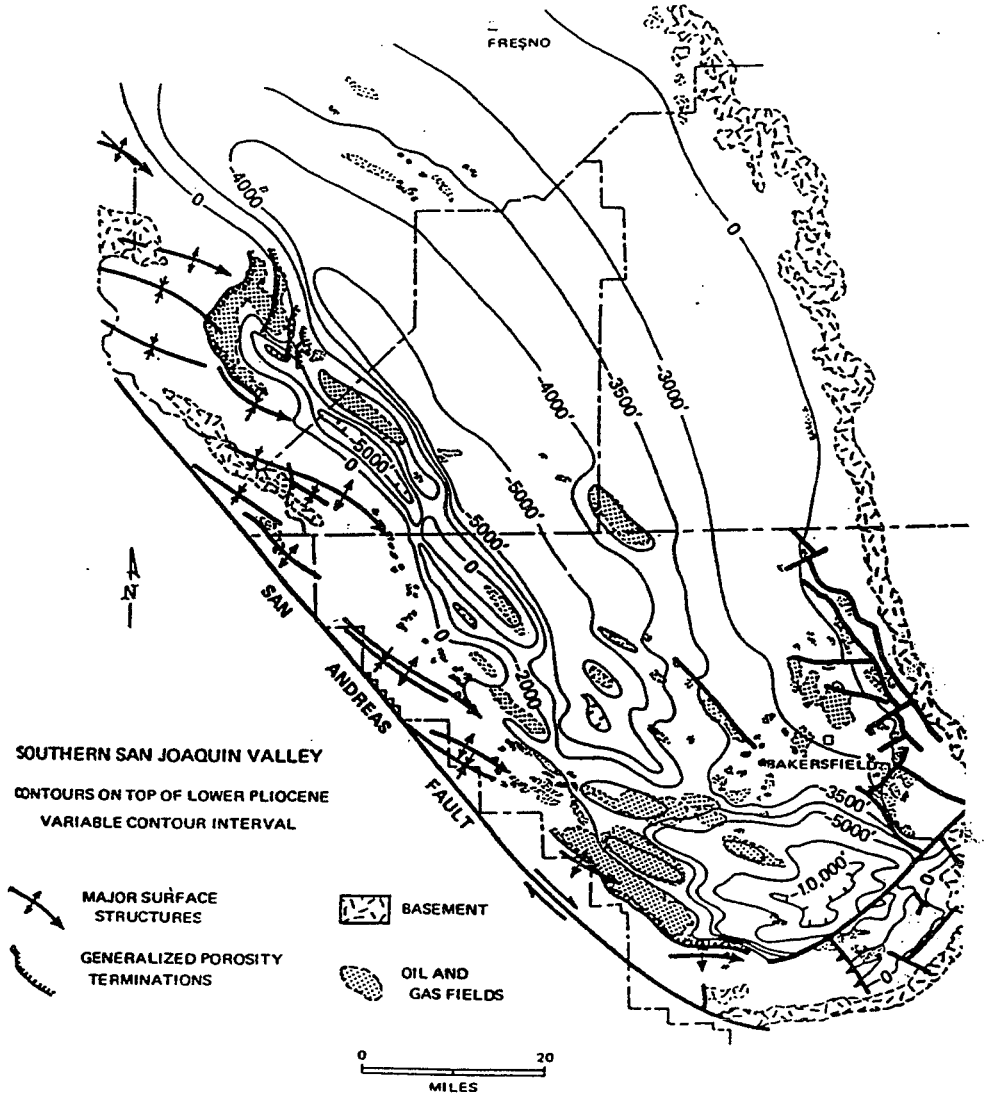

Figure 12. Wilcox correlated his model structures with natural field structures. En echelon folds surrounding the central segment of the SAFZ were used as field examples to support his wrench tectonic theory. Because the Wilcox model did seem to predict the en echelon folds, the majority of the fault-parallel structures located in the region were unexplainable in terms of wrench tectonic deformation (modified from Wilcox and others, 1973).

have developed in Miocene time, whereas fault-parallel folding initiated in early Pliocene time and continues today (Zoback and others, 1987).

The Wilcox model cannot account for this progression of folds or for the en echelon and fault-parallel folds observed along the SAFZ. The fact that their model does not precisely match the current structural configuration surrounding the SAFZ does not necessarily invalidate their results, but indicates that they may reproduce a deformational stage prior to that of the current developmental stage of the SAFZ.

Although the Wilcox model does not accurately portray the current SAFZ characteristics, it does provide highly valuable insights into the early stages of fault development. Prior to initiation of a fault zone, it can be assumed that shallow crustal materials are relatively undisturbed and internally coherent. This is the stage that the Wilcox model seems to have portrayed. Therefore, their model predicts the orientations of deformational structures developed at the incipient stages of fault development, and explains why oil traps could be accurately correlated with wrench faults. If en echelon folds and faults result from the initial stages of fault development, as predicted in the Wilcox experiment, then any mobile hydrocarbons would tend to migrate to the first trap developed in the area. If en echelon folds develop during the initial stages of wrench faulting, the recognition and dating of these features could constrain the time at which translational fault movement began. This is potentially a very valuable tool in areas where dormant extensional and/or thrust faults become reactivated as strike-slip faults. The recognition of these en echelon features may

aid in constraining episodes of translational movement that become overprinted by structures developed during a subsequent stress regime.

As strike-slip deformation proceeds, a crustal weakness is developed along the fault interface and subsequent deformation preferentially exposes this area due to the inherent weakness. Continued movement along this weak zone progressively deforms the rock and generates a highly sheared fault gouge. Progressive strain-softening of the fault gouge materials could result in a material that has very low friction, yield strength, and permeability. These characteristics represent a fault zone in an advanced stage of development, and must be incorporated into any model that attempts to simulate the current developmental stage of the SAFZ.

Limitations of the Wilcox Model

Wilcox and others (1973) performed their wrench fault modelling experiments by placing a uniform clay cake atop two adjacent plates that represented the basement wrench fault at depth. Translational movement between the two plates simulated motion along a strike-slip fault zone. The overlying clay material represented shallow sedimentary crust above the master wrench fault. This type of modelling, which Wilcox applied to the SAFZ, suggests that the SAFZ is not a throughgoing strike-slip fault but a structure that has yet to deform the overlying sedimentary package. The SAFZ is clearly a well-defined, throughgoing strike-slip fault zone with surficial expressions characterized by highly sheared fault materials, linear troughs, shutter ridges, pressure ridges, and distinctive rock types across the fault zone. Surface faulting associated with the 1906 San Francisco earthquake, numerous offset stream

drainages along the trace of the SAFZ (Wallace, 1990), and evidence of hundreds of kilometers of right-lateral displacement along the fault (Stanley, 1987; Graham, 1989) provide ample evidence to suggest that the SAFZ is a throughgoing feature. Therefore, using results of the Wilcox experiment to draw conclusions about the current deformational stage of the SAFZ does not seem relevant. In order to more accurately model the SAFZ and the current stresses and deformational characteristics, a throughgoing fault zone should be incorporated into the modelling scheme. The use of a throughgoing fault zone has been incorporated into this study, along with new modelling techniques, materials, and results, which are presented in the following sections.

PHYSICAL MODELLING

Apparatus

The fault modelling apparatus developed for this study is comprised of two conveyor belts oriented orthogonally to each other. The longitudinal belt moves in what will be described as a north-south direction, and the latitudinal belt moves in an east-west direction (fig. 13). The interface between the two moving belts represents the basement fault zone. Movement of the conveyors, with various modelling materials placed atop the belts, deforms the materials along the model fault zone.

Pure strike-slip movement can be achieved by moving the longitudinal conveyor belt only, which can create either dextral or sinistral slip. Extensional and contractional fault zones can be generated by conveyance of the latitudinal belt away from or toward the longitudinal belt, respectively. By moving the belts simultaneously, varying degrees of transtension or transpression can be developed across the model fault zone, depending upon the magnitude of translation of each belt with respect to the other. The curvature of the belt as it moves around the roller at the end of the latitudinal conveyor prevents a flush joining between the interface of the two belts. Therefore, one end of the latitudinal conveyor has been designed to slip beneath the longitudinal conveyor to provide a near flush interface between the two moving belts (fig. 14). In addition to achieving a flush interface, regardless of the type of motion, no voids are created during tensional or transtensional movement because the belt is the

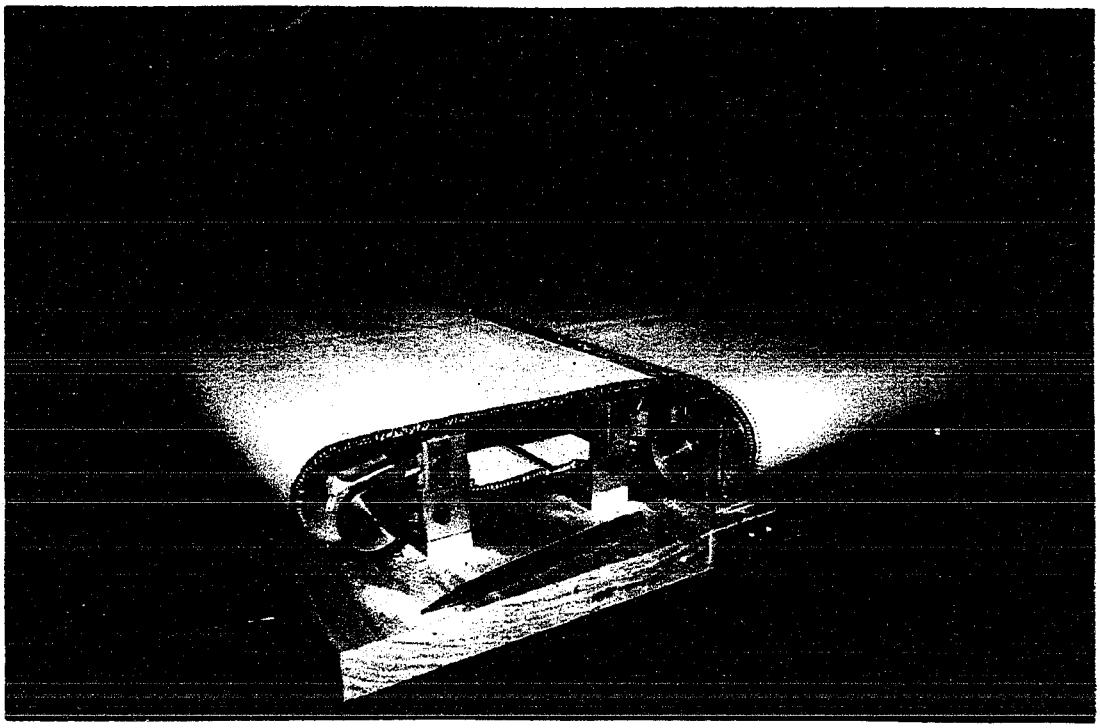

Figure 13. Model apparatus developed for this study. Heavy canvas belts act as conveyor belts to passively transport model material. Relative movements of the belts enable any component of transpression, transtension, pure strike-slip, and/or pure compression to be generated. Apparatus is approximately 1.5 feet long (0.46 m) and 1.5 feet wide (0.46 m).

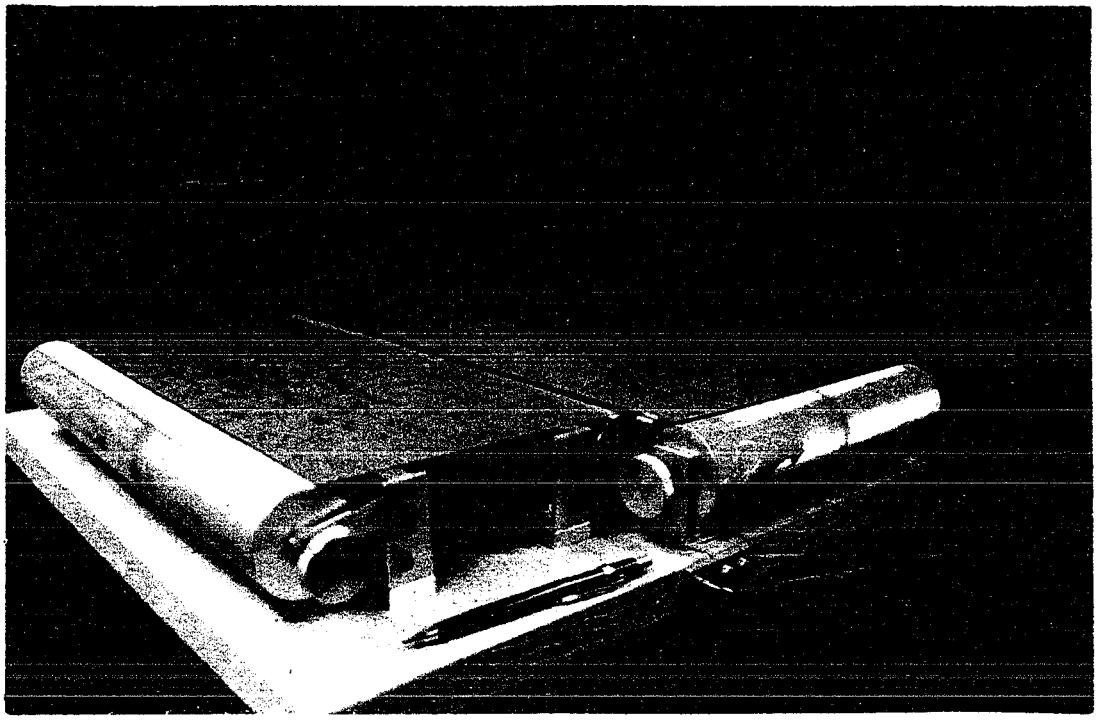

Figure 14. Close-up of fault interface showing flush joining as latitudinal roller is placed within longitudinal conveyor. This type of fault interface allows continual movement without developing space problems across the fault interface.

only moving part. This model also eliminates problems of earlier transpressional models that had to start with the plates at some distance apart and then bring them together, which limited the amount of shortening to the initial distance of plate separation. Fine adjustments have also been incorporated into the model design to accommodate vertical belt movements, and to provide for belt tightening or loosening (fig. 15) should the belts stretch or shrink.

Modelling Materials

Clay, gelatin, and sand were used in this study. Initial clay modelling simulated the Wilcox and others (1973) experiments; however, gelatin was ultimately favored over clay because of its uniform consistency, consistent transference of stresses, and its ability to depict strain. The majority of the experiments involve the deformation of gelatin, which, like clay, is particularly good at generating folds. Sand is valuable for generating faults, and is used in this study to analyze the timing of faulting, and the orientations of secondary faults stemming from deformation along the master basement fault.

Modelling Methods and Techniques

Gelatin Experiments

The primary goal of this experiment is to model a transpressional fault zone and describe the surface and subsurface deformational structures which develop in the model materials stemming from movement along the basement fault.

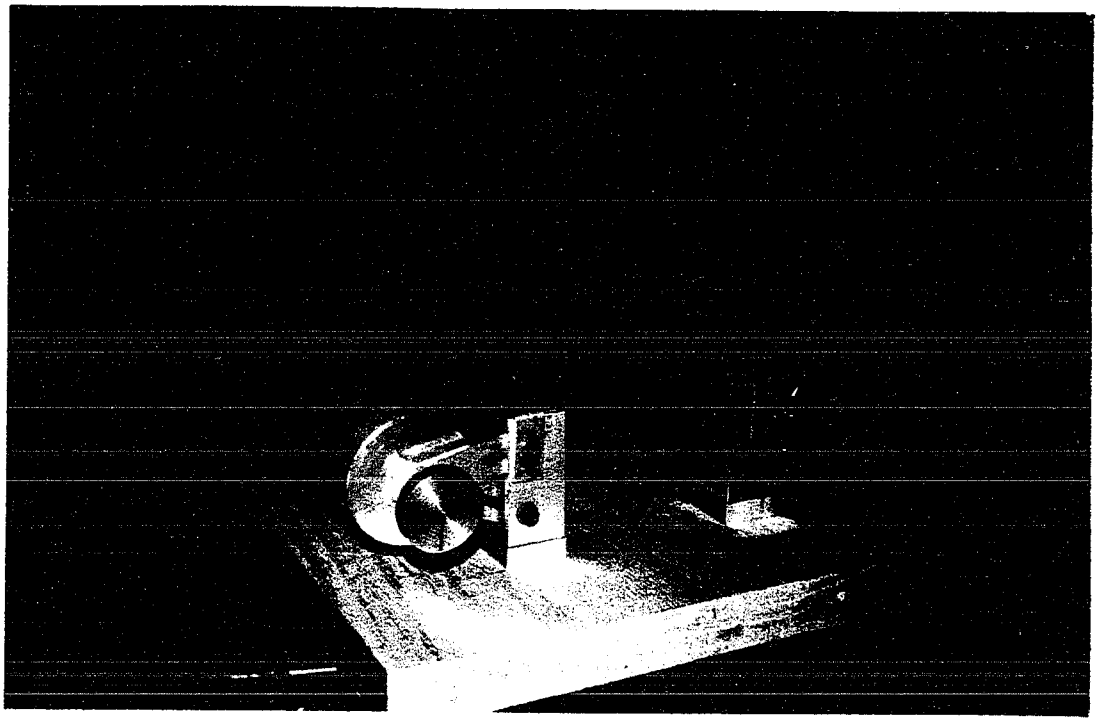

Figure 15. Close-up of bracket showing fine adjustments that allow the belts to be tightened to prevent slippage between the rollers and the belts.

This study attempts to incorporate the latest stress-field, plate motion, and fault zone data to more accurately describe the structures seen along the SAFZ today. A more accurate portrayal of these parameters may help account for a wider range of structures along the SAFZ, whereas the Wilcox model accounted for the en echelon folds, but ignored the profusions of fault-parallel folds and thrust faults.

Initial experiments performed with the new model were aimed at reproducing Wilcox and others' (1973) results to verify that the new modelling methods and mechanics were consistent with those of Wilcox. A uniform clay cake was placed across the model wrench fault and subjected to pure right-lateral strike-slip movement. The results indicated that en echelon folds developed in a right stepping pattern, oriented approximately 30° to 40° from the trace of the master wrench fault, similar to the Wilcox results. However, problems with the clay's inhomogeneities, workability, and reproducibility, instigated the use of different materials.

A stiff gelatin proved to be the material with the most desirable modelling characteristics. Gelatin can be consistently reproduced as a homogeneous layer of any thickness, color, or consistency, and shows up well in photographs. A key advantage of gelatin over clay in this type of modelling experiment is that the basement fault can be seen through the gelatin layer, enabling visual correlation between the surficial deformational structures and the underlying wrench fault (fig. 16). The surface of the gelatin is covered with a layer of cellophane that responds to the strained gelatin quickly, and reflects light in such a way that the

Figure 16. Plan view of model with undeformed gelatin material placed atop the fault interface, which is visible as the dark lineament through the gelatin. Cellophane layer is placed atop the gelatin, arrows show the relative direction of movement between the belts once deformation begins.

deformational patterns are easily visible in photographs. Wilcox also used cellophane in his clay experiments for similar reasons. Modelling without cellophane produces similar features as modelling with cellophane, but the amount of movement along the wrench fault needed to produce visible structures exceeds the longitudinal capacity of the model. Gelatin provides a uniform top surface that is ideal for cellophane to conform to without developing numerous irregularities that disrupt the surface prior to deformation, as is the case with clay.

Limitations

The limitations, and possible sources of error stemming from the modelling apparatus and the sand and gelatin material include boundary effects, inhomogeneities within the modelling material, variable rates of deformation, inconsistent plate motion, and possible slippage between the modelling material and the basal plates.

The boundary effects are derived from the limited size of the modelling apparatus. There is only a limited amount of motion that can take place between the plates before the deformational interface is translated to its entirety. Boundary effects stem from the outer edges of the material that are not exposed to equal transpressional forces. Possible sources of error stem from inconsistent rates and angles of deformation, which could be eliminated by attaching a motor to drive the plates. Variable rates of deformation were used, but did not seem to affect the experimental results. Basal slippage, which is a problem when modelling with clay, does not occur with gelatin or sand.

A rectangular frame has been placed over the modelling material to aid in mapping deformational features. Arrows placed upon the model indicate the relative direction of movement of the individual plates; parallel arrows pointing in opposite directions indicate strike-slip movement, and perpendicular arrows indicate transpression.

Experiment 1

A uniform gelatin layer, approximately 1.25 cm thick, has been placed atop the basement fault prior to strike-slip deformation (fig. 16). This model configuration simulates the Wilcox experiment which placed a uniform cake atop a wrench fault, without a pre-existing, throughgoing fault zone.

A photograph taken directly above the model distinctly shows that right-stepping en echelon folds are developed in response to dextral slip along the basement wrench fault (fig. 17). A line drawing of the photograph shows the 30° to 40° angular relationship between the folds and the trace of the strike-slip fault (fig. 17a). A small strain ellipse diagram illustrates the orientation of the principal stress directions. Using the same gelatin plate configuration, a transpressional motion is applied, and the resulting folds develop in much the same way as in the strike-slip experiment (figs. 18 and 18a). As predicted by frictional faulting theory, and represented in the modelling line drawing (figs. 18b and 18c), the angle of the folds with respect to the wrench fault trace has been reduced. The strain ellipse line drawing indicates that the maximum horizontal stress has rotated approximately 10°. These deformational patterns, although

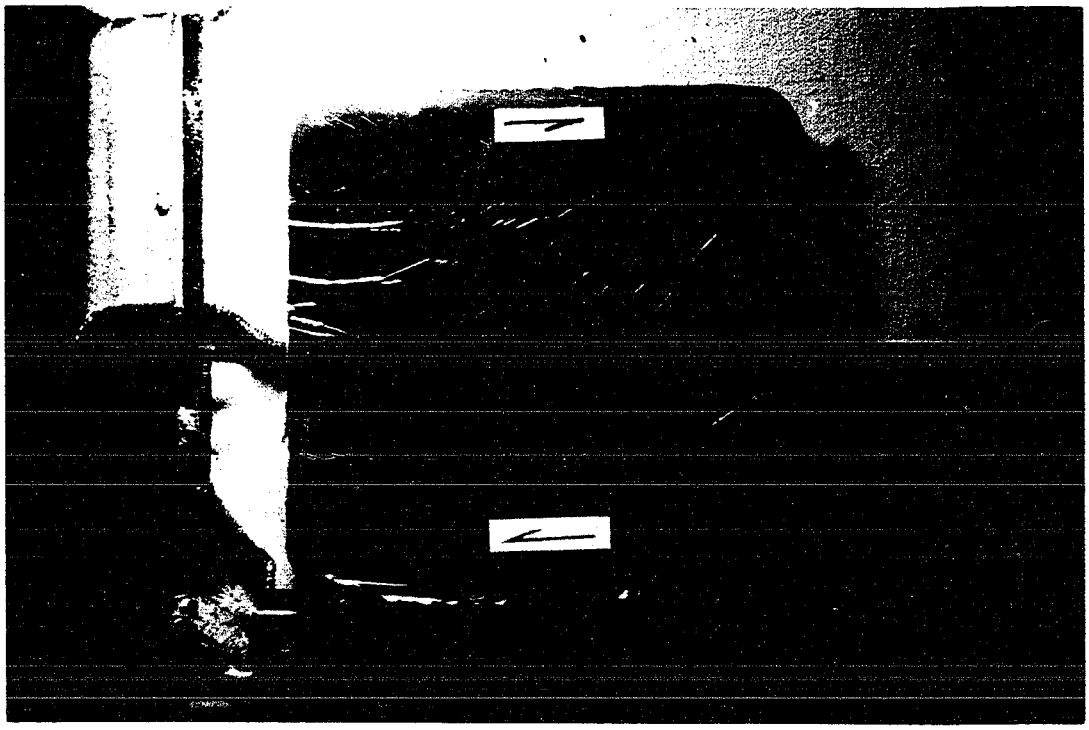

Figure 17. Incipient translational motion quickly produces en echelon folds oriented approximately 40° to the trace of the basement wrench fault, after only 1/4 inch of strike-slip motion. The longitudinal belt (top of photo) has been translated to the right, with the latitudinal belt (bottom of photo) held stationary to achieve pure dextral slip.

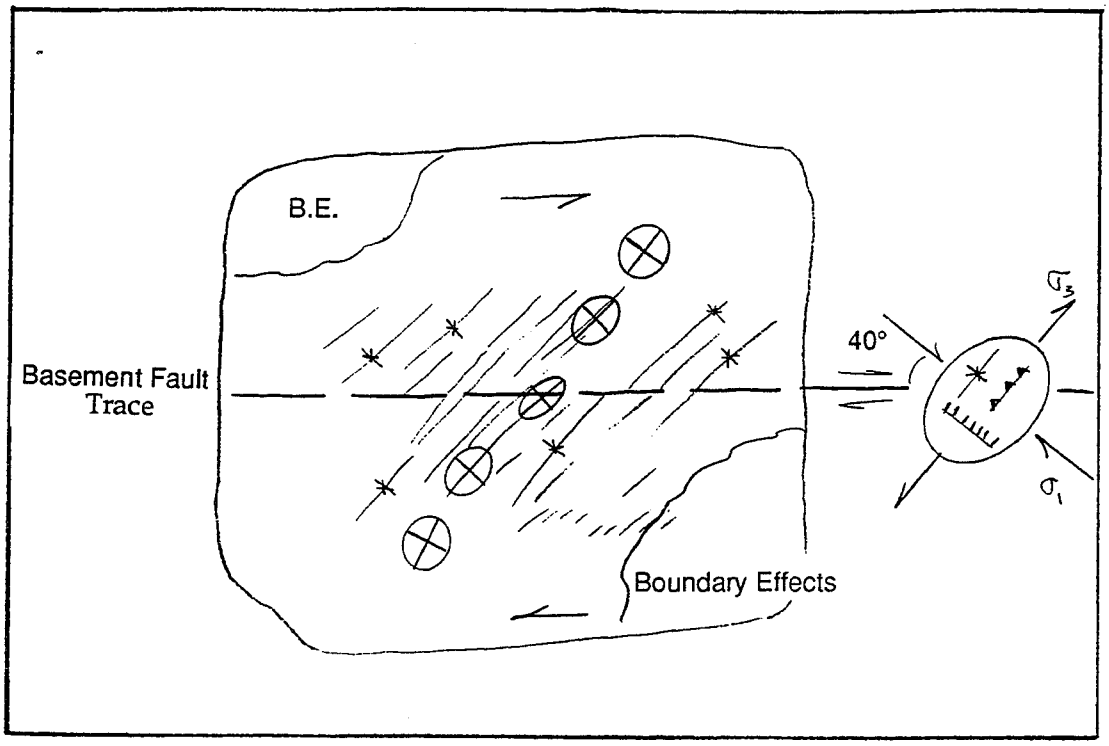

Figure 17a. Line drawing of Figure 24 illustrating the fold geometries and associated stress orientations. The strain ellipses indicate the relative amount of shear displacement across the zone of distributed shear. Fold orientations match those of the Wilcox and others (1973) indicating high-drag, wrench tectonic deformation.

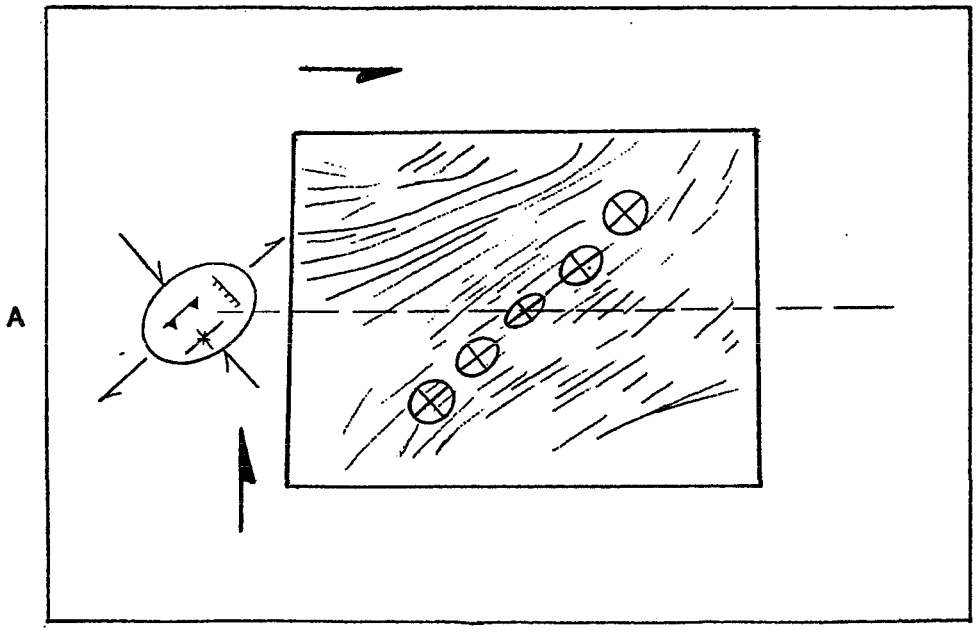

Figures 18 and 18a. Incipient transpressional motion across the fault interface; 1/4 inch of translation, 10° of transpression. Folds initiate at 40°, then begin to rotate to lower angles with respect to the basement fault. a) Line drawing of Figure 25 illustrating fold geometries and stress orientations through the use of the strain ellipse.

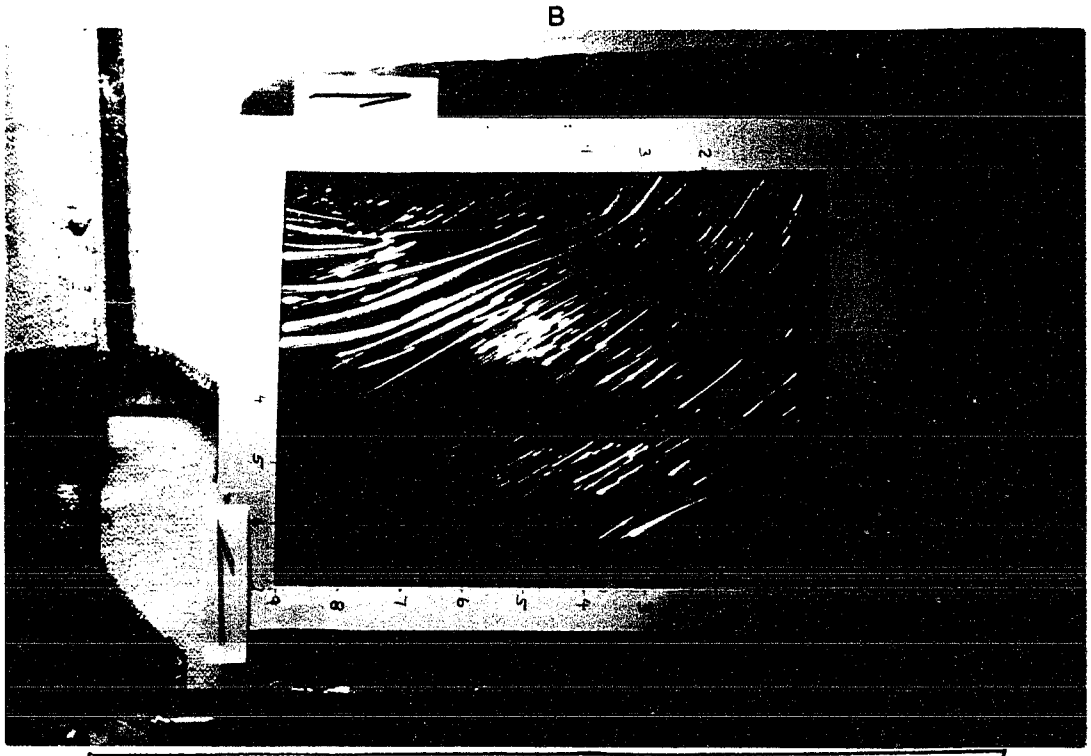

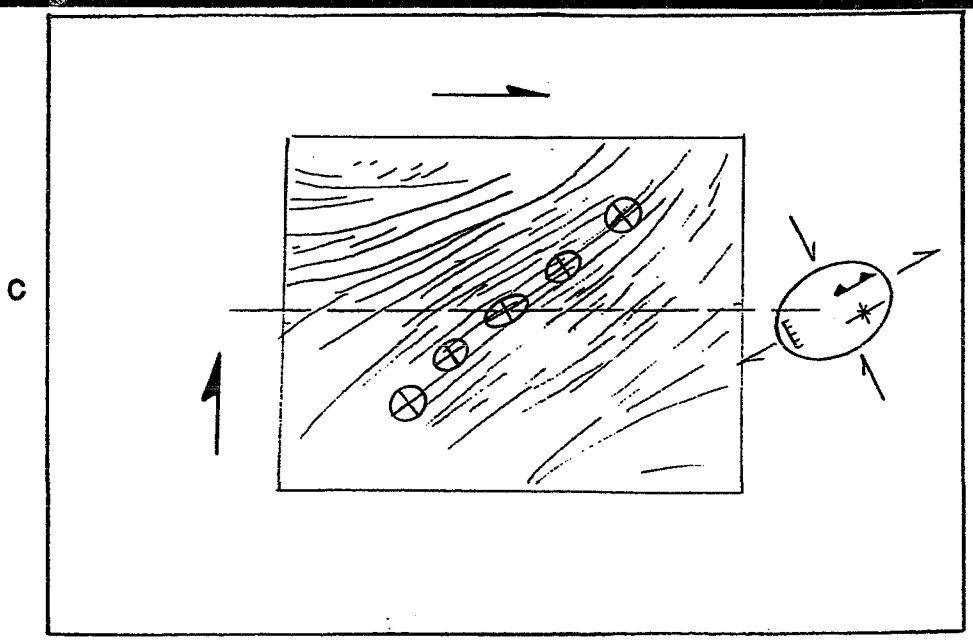

Figures 18b and 18c. b) Advanced transpressional deformation shows that folds are now oriented 25° to 35° to the basement fault; 1/2 inch of translational motion, 10° of transpression. c) Line drawing illustrating fold geometries and stress orientations; notice the rotation of the principal stress direction from the pure strike-slip experiment.

more closely resembling fault-parallel features, still cannot explain the abundant fault-parallel folds and thrust faults observed along the SAFZ.

Experiment 2

A more accurate modelling portrayal of the SAFZ must incorporate the latest fault parameters, fault zone characteristics, and overall geomorphic expression. These have been incorporated one at a time so that the determining variables controlling deformation may be deciphered. The first new fault parameter to be added is a throughgoing fault zone. Two separate gelatin plates, each a different color, have been placed adjacent to each other with their interface aligned along the basement strike-slip fault (fig. 19). A single cellophane layer has been placed across both of the gelatin plates. This configuration is more representative of the SAFZ, in that the separate plates simulate the Pacific and North American plates, with their interface representing the transform fault zone. However, the continuous cellophane layer prevents this from being distinguished as a full plate separation. In response to pure right-lateral fault movement, en echelon folds are developed at 30° to 40° orientations to the trace of the basement wrench fault (figs. 19a and 19b). These results indicate that despite the gelatin plate separation, the cellophane is still the controlling variable. This suggests that the continuous cellophane layer, which represents a homogeneous sedimentary unit, is deformed in a similar manner regardless of how close to the surface the wrench fault terminates. Transpressional motion across this plate boundary produces the same 10° reduction in the angle of the en echelon folds with respect to the basement fault.

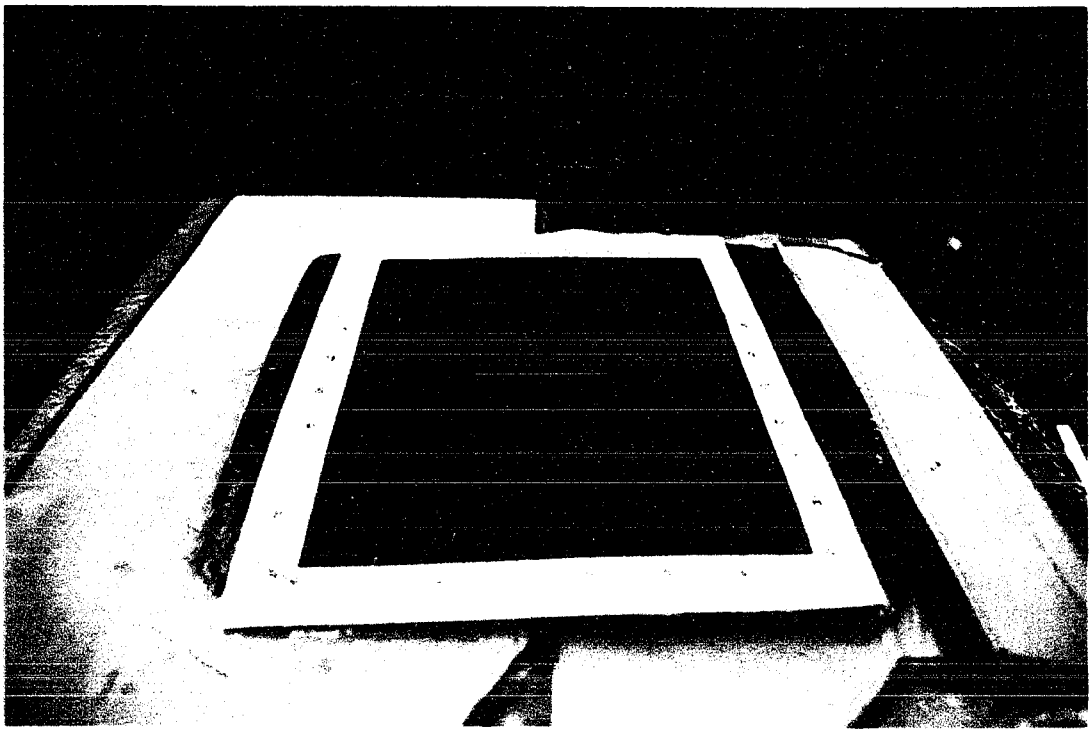

Figure 19. Oblique view of model with separate gelatin plates aligned atop the basement fault. Frame atop the material is for mapping purposes. Longitudinal belt (left of picture) translates material toward the top of the picture, while the latitudinal belt moves right to left.

A

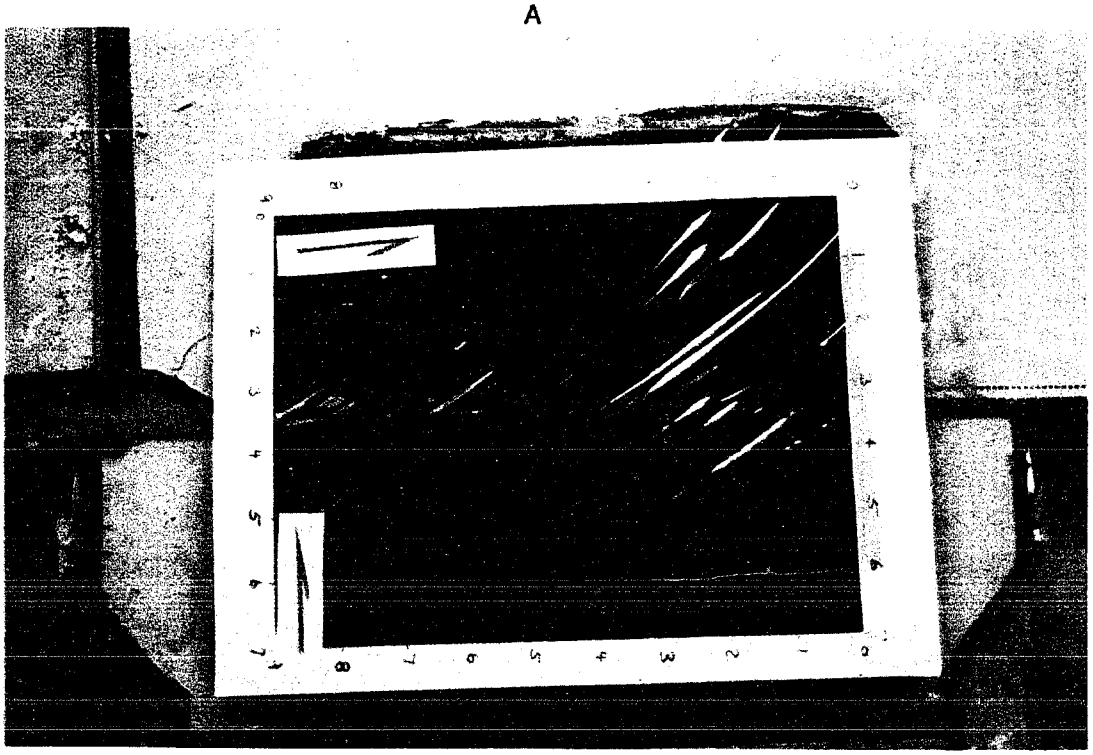

B.

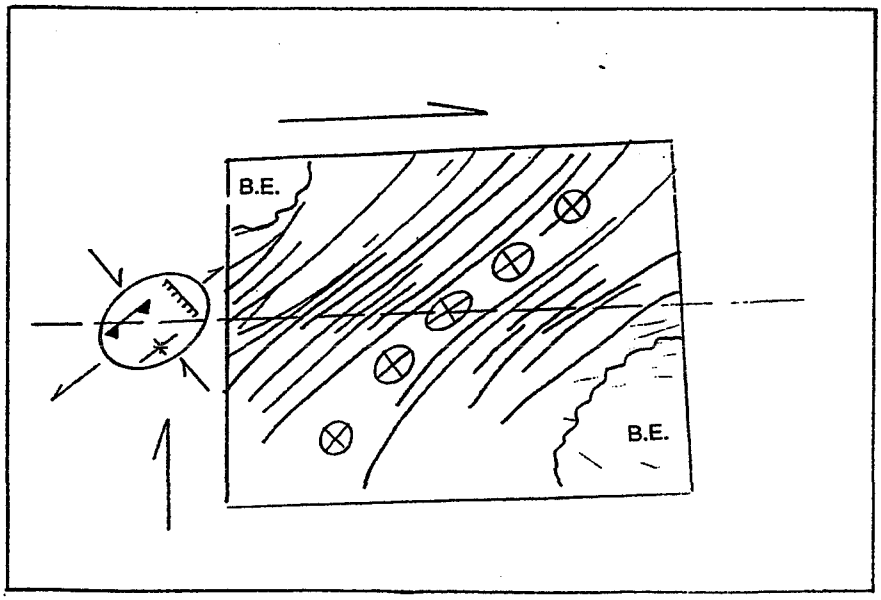

Figures 19a and 19b. a) Transpressional deformation of separate gelatin plates with a single cellophane layer atop the two plates. Fold orientations, 30° to 40° from the fault trace, suggest high-drag deformation. b) Line drawing illustrating fold geometries and stress orientations with respect to the basement fault.

Experiment 3

If the cellophane layer is separated and placed individually atop the two gelatin plates, then the basement wrench fault can be considered a throughgoing fault. Therefore, structures stemming from transpressional motion across the wrench fault are not a function of the mechanical properties and wrenching characteristics of the overlying material, but a product of the deformational characteristics and stress transfer of the fault interface. The frictional resistance and strength of the fault zone material controls the transfer of the imposed stresses to the material surrounding the fault zone. Experiment #3 models a high friction, decoupled, throughgoing, transpressional fault zone. The dry gelatin plate interface has high frictional resistance to translation, producing repeated stick-slip fault movement when exposed to translational or transpressional movement. Figure 20 shows transpressional motion across the model fault interface and the resulting structures. The orientation of the folds, oriented 20° to 40° from the main fault trace, indicates that the principal stresses are acting in much the same manner as in Experiments #1 and #2. As deformation proceeds, the angles of the existing folds decrease with respect to the main fault trace, suggesting that the folds are gradually rotating toward parallelism within the zone of distributed shear (figs. 20 and 20a-c). Therefore, despite the presence of a decoupled plate boundary separated by a throughgoing fault zone, transpressional motion still results in the development of en echelon folds oriented at relatively high angles (20° to 40°) to the main wrench fault trace.

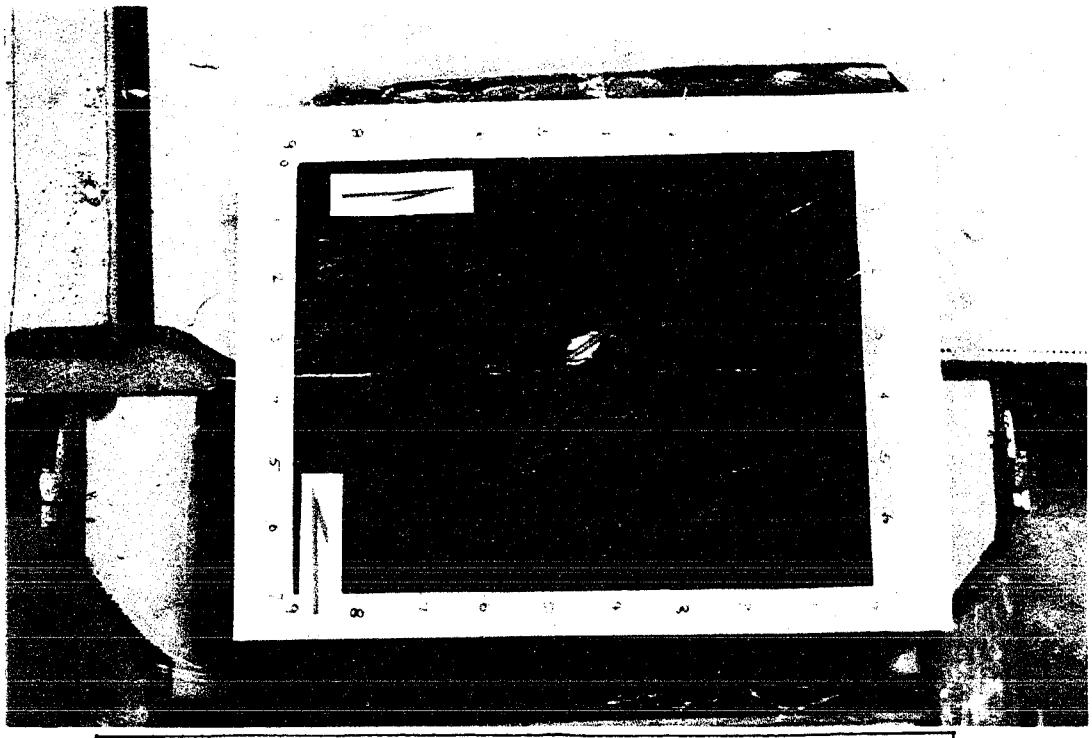

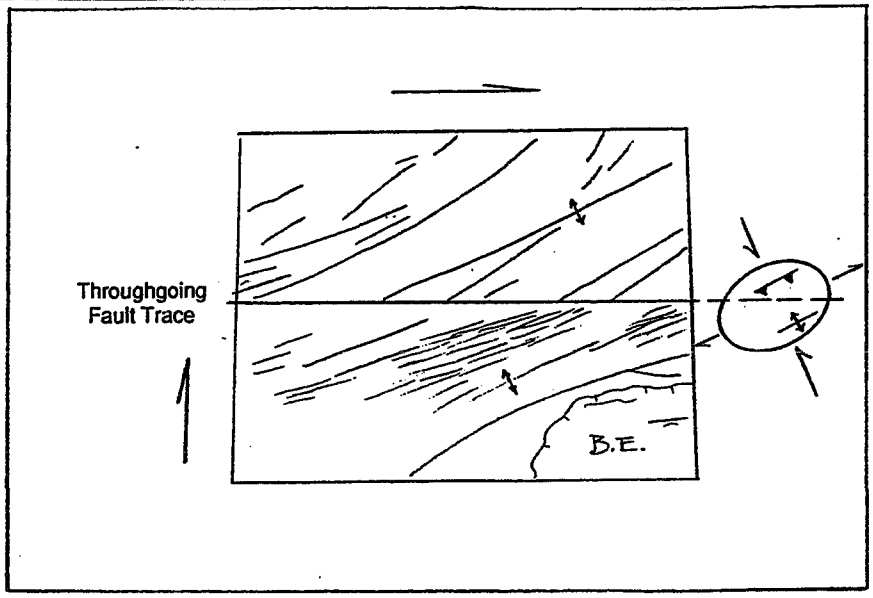

Figures 20 and 20a. Transpressional deformation of separate gelatin plates with individual cellophane layers atop each plate, simulating a throughgoing fault zone. Fold orientations are suggestive of high-drag wrench deformation. a) Line drawing illustrating 20° to 30° fold orientations. Folds retain an en echelon pattern, as in previous high-drag experiments, except the fault interface disrupts the continuity of the folds.

B

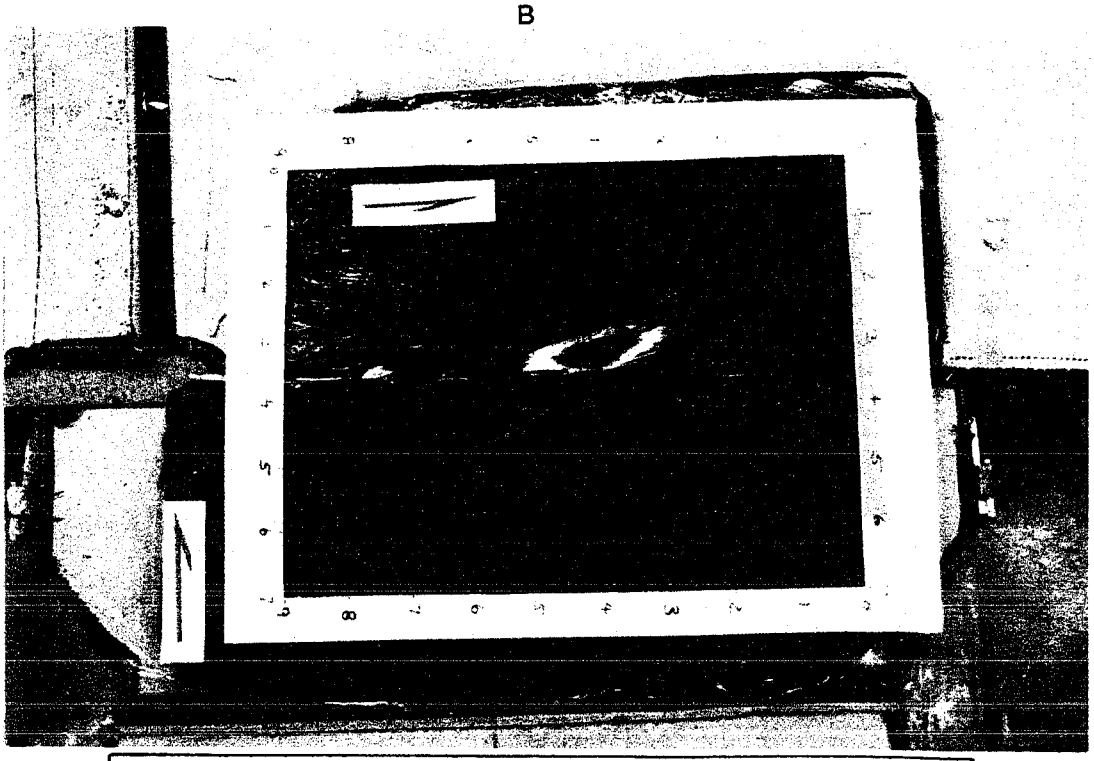

C

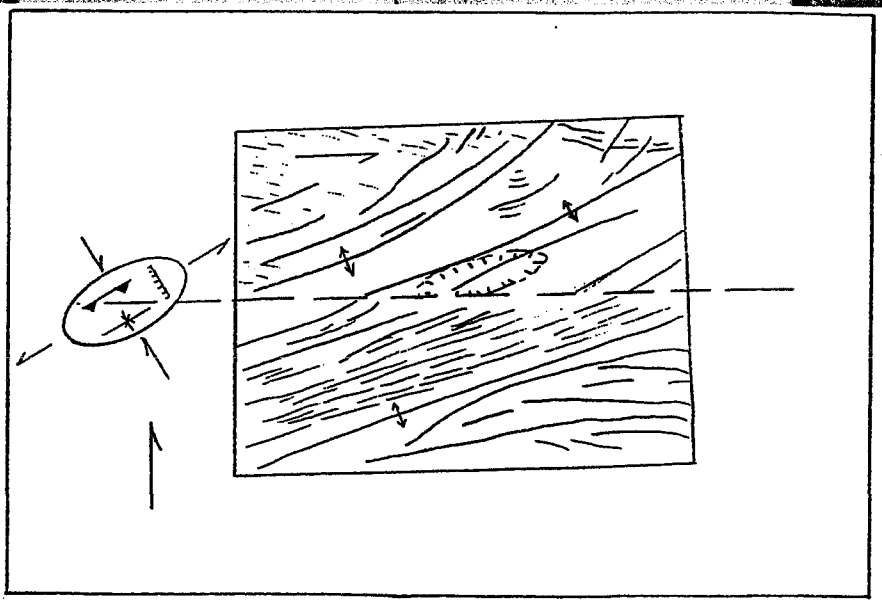

Figures 20b and 20c. b) Advanced stage of deformation shows that folds are rotating toward parallelism (18° to 30°) with the basement fault, and isolated basins are beginning to form roughly parallel with the fold axes. c) The line drawing illustrates the disruption of the folds across the fault trace, the rotation of the principal stress axis, and the formation of the basin parallel to the fold axes.

Experiment 4

A low strength, low friction fault zone is the remaining variable to be added to the experiment in order to accurately incorporate the most recent data regarding SAFZ characteristics. Oil has been placed along the fault interface to reduce the friction between the two gelatin plates. Therefore, modelling Experiment #4 is characterized by two distinct gelatin plates with individual cellophane layers, a low strength, low friction fault zone, and transpressional motion. Each of these modelling parameters has been incorporated to simulate SAFZ characteristics. As transpressional motion is applied to the modelling material, a striking change is evident in the orientation of the resulting structures (figs. 21 and 21a). Continued deformation results in the generation of additional cellophane folds, as well as large amplitude folds and basins in the gelatin (figs. 21b-d). The folds are primarily oriented parallel to the trace of the basement wrench fault, and have similar orientations whether located close to, or far from, the basement fault. This type of structural configuration suggests that the maximum horizontal stress is acting perpendicular to the wrench fault, resembling a compressional fold belt. Fault-parallel folds developed whether the rate of transpressional movement was rapid, slow, or episodic. The angle of convergence between the two plates varied from 5° to 15° in separate experiments, each resulting in similar fault-parallel features.

Interpretation of Experimental Results

The features observed in Experiment #4 are indicative of fault-normal compressional stress. This closely resembles the stress orientation that is

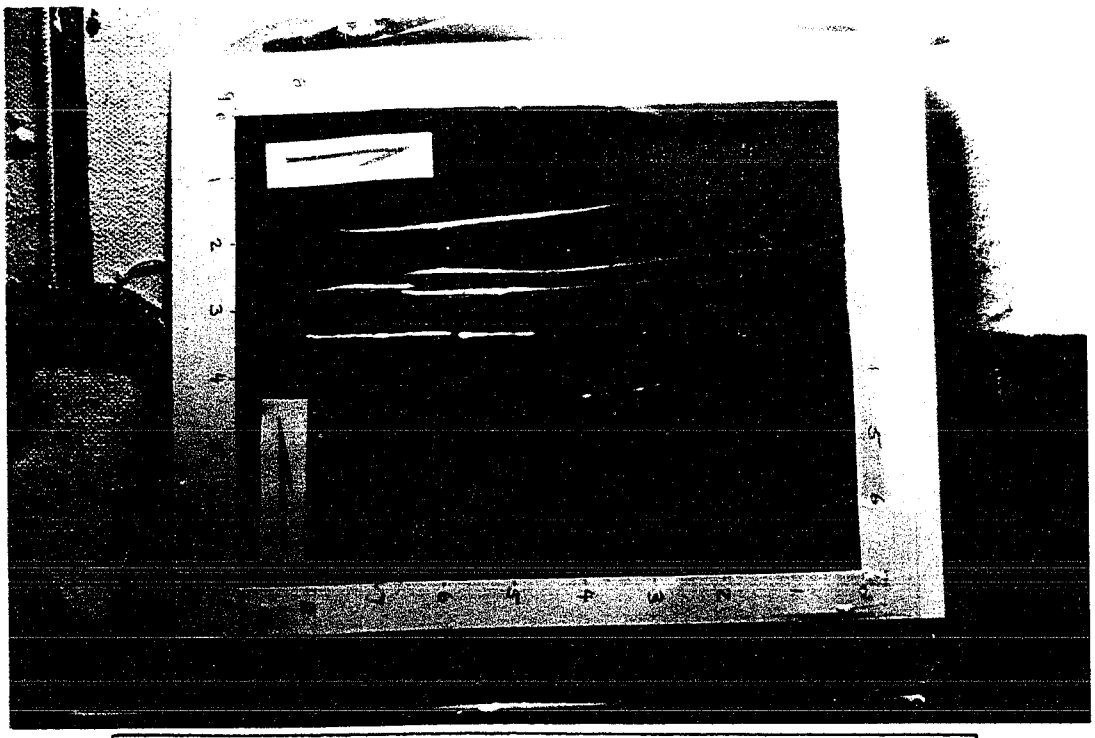

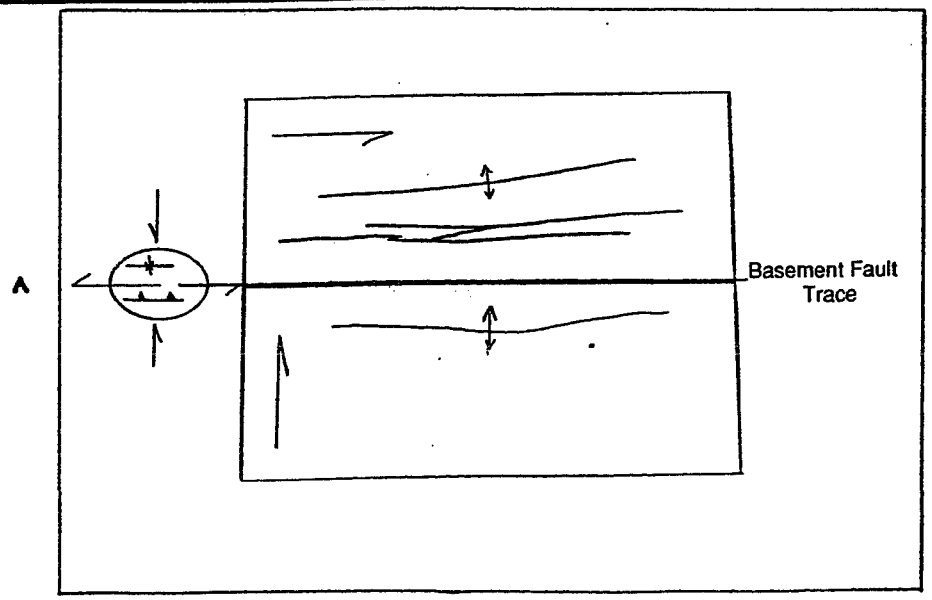

Figures 21 and 21a. Transpressional deformation of separate gelatin plates with separate cellophane layers, and oil lubricating the fault interface to reduce the sliding friction. The incipient folds develop at nearly fault-parallel orientations in response to 1/4 inch of translation, and 10° of transpression. a) The line drawing shows that the maximum horizontal stress is oriented at 90° to the trace of the basement fault.

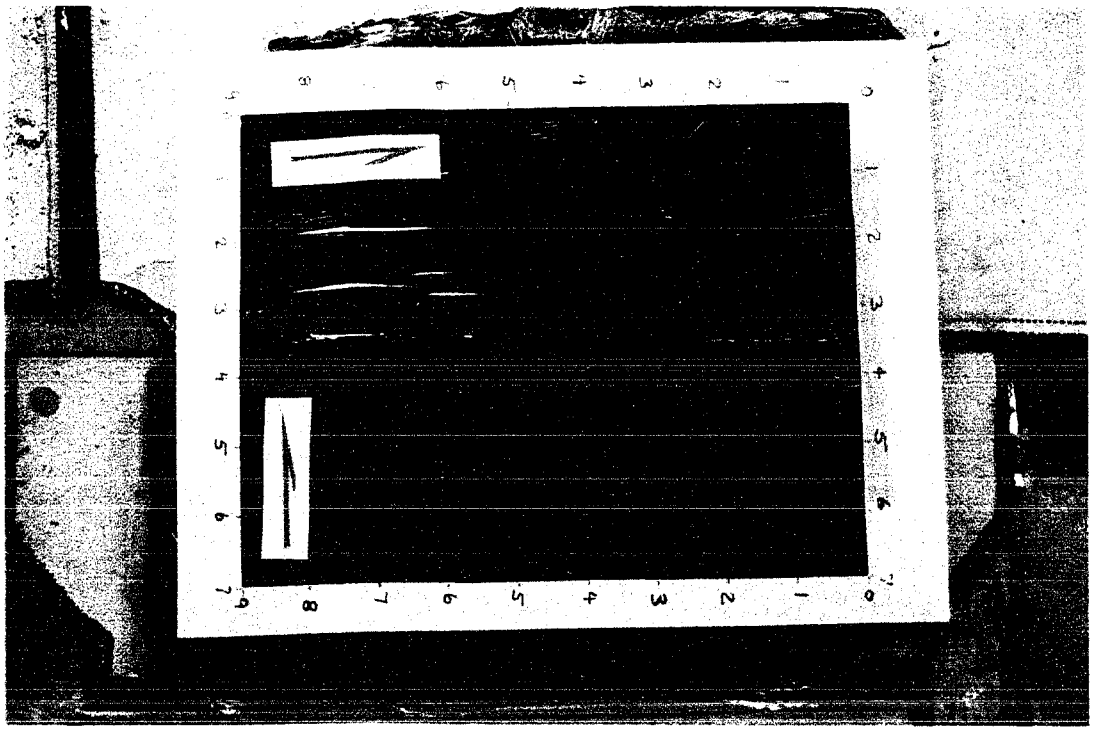

B

Figures 21b-d. b) Deformation continues to produce fault-parallel folds, along the entire width of both gelatin plates; 1/2 inch of translation, 10° of transpression. c) At an advanced stage (1 inch of translation) of deformation, large amplitude folds start to develop with numerous fault-parallel folds superposed atop these features. d) The line drawing illustrates the fault-parallel orientation of the first-order folds (small amplitude), and the second order folds (large amplitude folds) which show up as fault-parallel basins.

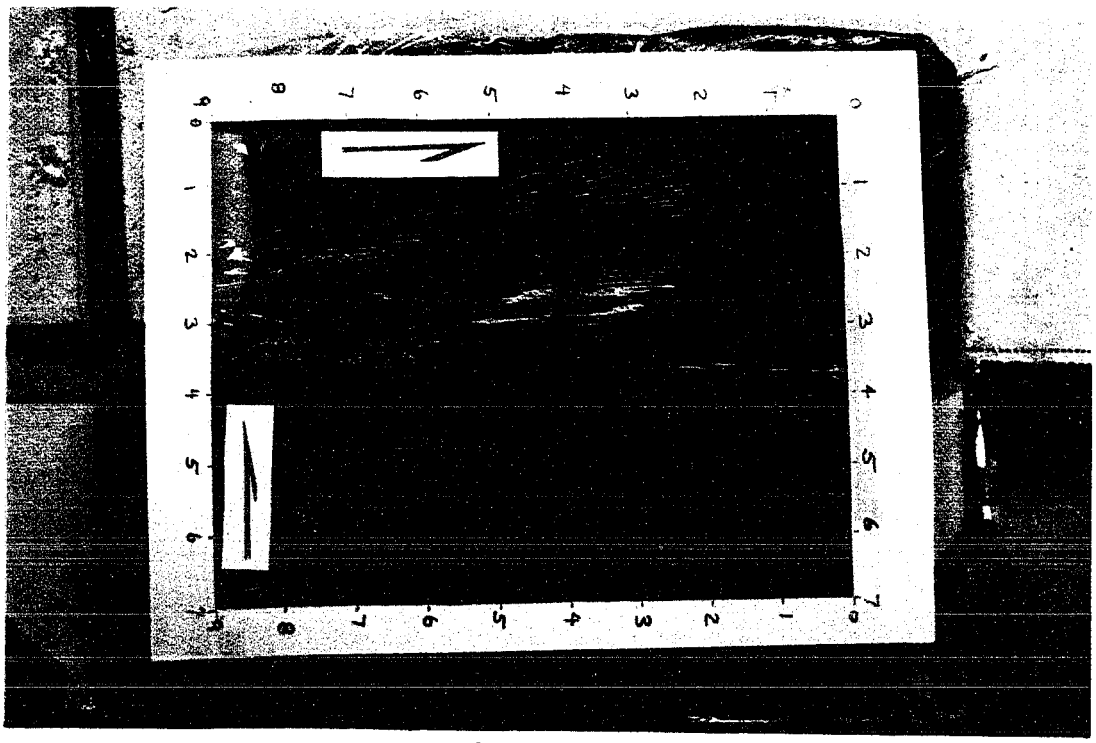

C

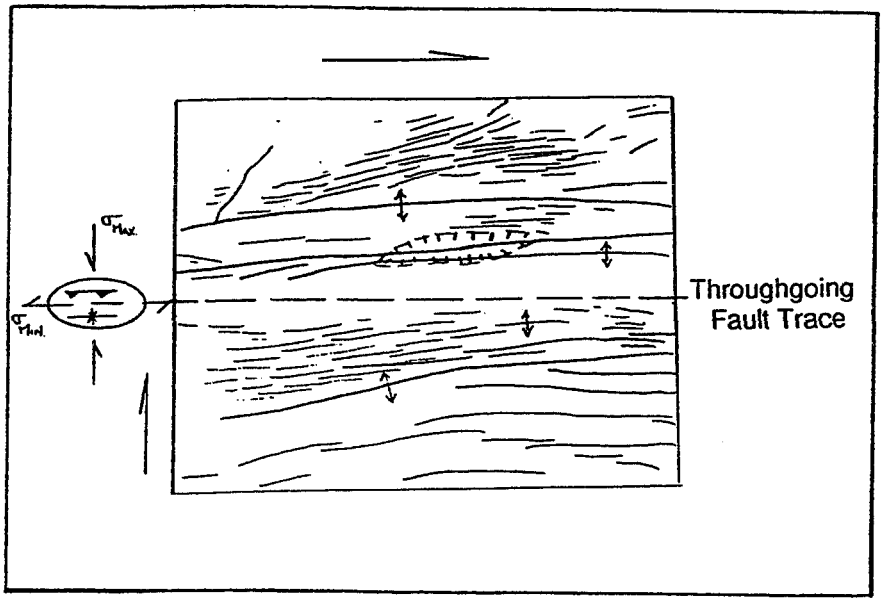

D

thought to be currently acting across the SAFZ (Zoback and others, 1987; Mount and Suppe, 1987). The critical factor influencing the generation of fault-parallel folds in the experimental models is the low-friction fault zone. Zoback and others (1987) showed that the SAFZ materials may, in fact, be weak, and thus responsible for re-orienting the maximum horizontal stress to a fault-normal direction. The similarities between laboratory models and actual field structures flanking the SAFZ cannot be discounted. The fact that fault-parallel contractional features are generated along a model transpressional fault, in which fault zone characteristics have been specifically incorporated to match those in the field, suggests that the variables controlling deformation are at least a physical and mechanical possibility in natural examples. Scaling these modelling parameters up to natural examples may or may not be appropriate, but should at least be considered when analyzing deformational features flanking the SAFZ.

Sand Experiments

Scale modelling with gelatin has been shown to be advantageous for developing and photographing surface folds, due to the rapid transfer of stresses throughout the elastic medium. However, modelling with sand can be performed to illustrate surface fault orientations, the timing of fault deformation, and subsurface fault configurations. Modelling a weak fault zone in gelatin experiments necessitated the use of oil placed between the gelatin plates, which reduced the shear stress and frictional resistance. Since dry sand has no cohesive strength, the fault zone is inherently weak. Reducing the

friction along the interface between the two plates of sand is not necessary because shear stresses are reduced by granular adjustments during deformation.

Experiment 5

Initial modelling experiments with dry sand involve simple strike-slip movement of the wrench fault beneath a homogeneous sand pack. The primary purpose of this experiment is to verify that the modelling materials deform in a manner consistent with previous experimental sand models. Naylor and others (1986) performed extensive strike-slip experiments with sand placed above a model wrench fault. Their study delineated various stages in the evolution of a wrench fault and emphasized the timing of deformation and orientation of secondary fault features, such as Riedel shears, splay faults, and P-shears in relation to the basement wrench fault (fig. 22). Experiment #5, although not aimed at delineating wrench deformation in the detail of Naylor and others (1986), indicates that the experimental model produces similar deformational features and orientations as that of Naylor's experiment.

Initial strike-slip deformation of the sand pack produces synthetic Riedel shears within the zone of distributed shear (fig. 23). The accompanying line drawing illustrates the orientation of the Riedel shears with respect to the basement wrench fault (fig. 23a). As deformation continues, the secondary faults coalesce and a throughgoing fault zone is developed (figs. 23b-e). Initial dilation along the fault zone (fig. 23), created by the translational shear stresses imposed upon the cohesionless sand grains, produced the topographic bulge, or "mole track" that is eventually dissected by the development of the throughgoing fault

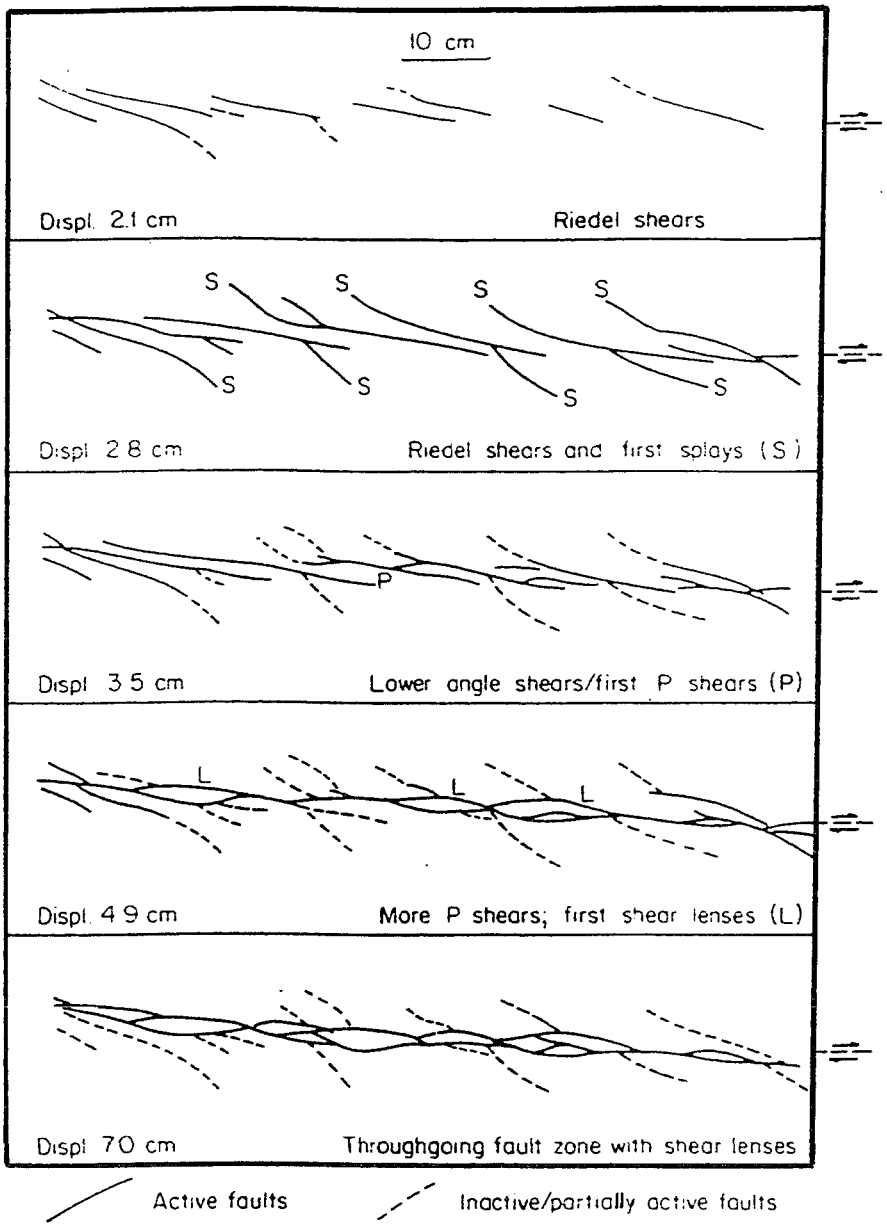

Figure 22. The evolution of a wrench fault zone in experimental sand models, showing the progression from initial Riedel shears to the eventual development of a throughgoing fault zone (modified from Naylor and others, 1986).

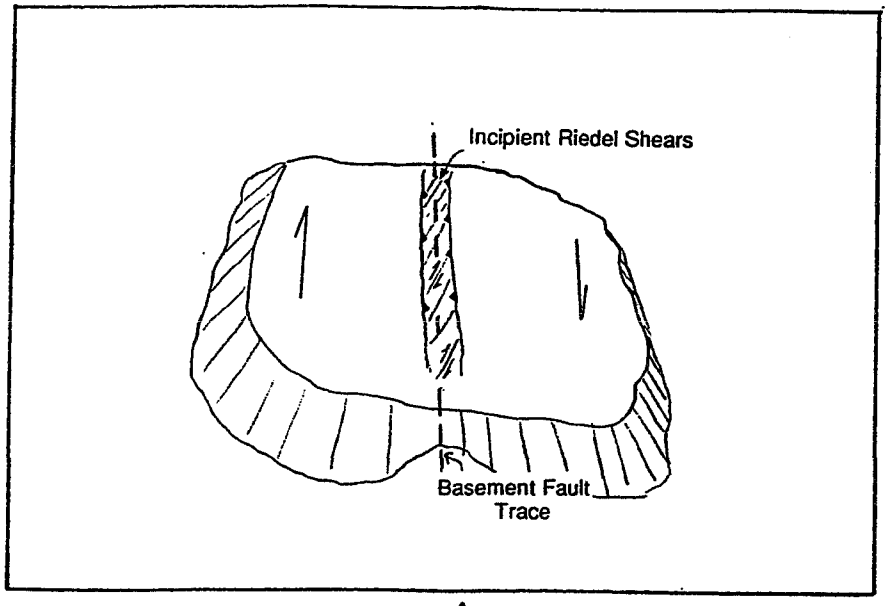

A

Figures 23 and 23a. Initial strike-slip deformation of an unconsolidated sandpack, 1.5 inches thick. a) The line drawing illustrates the Riedel shears that develop across the "mole track".

B

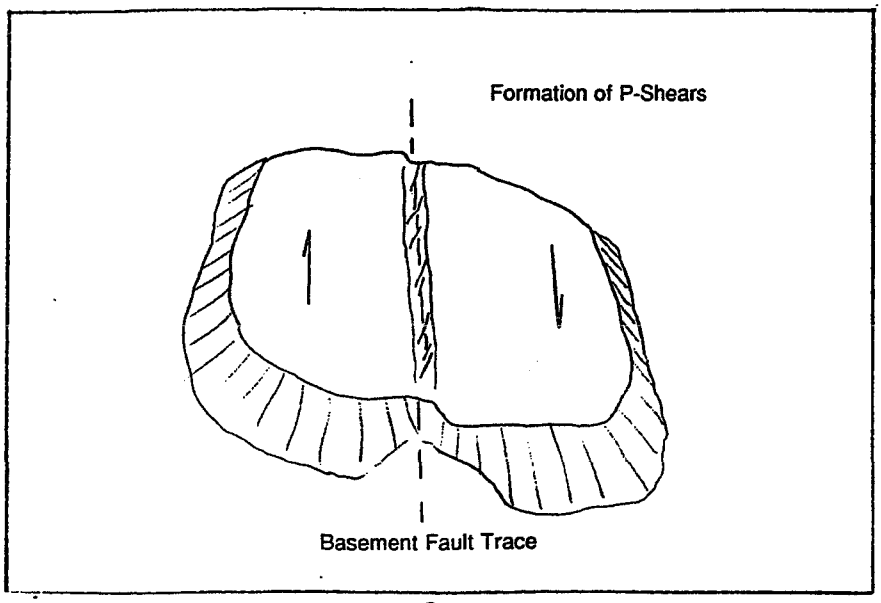

C

Figures 23b and 23c. b) The uplifted "mole track" is being dissected as a throughgoing fault zone is developed. c) Line drawing illustrating the formation of incipient P-shears.

D

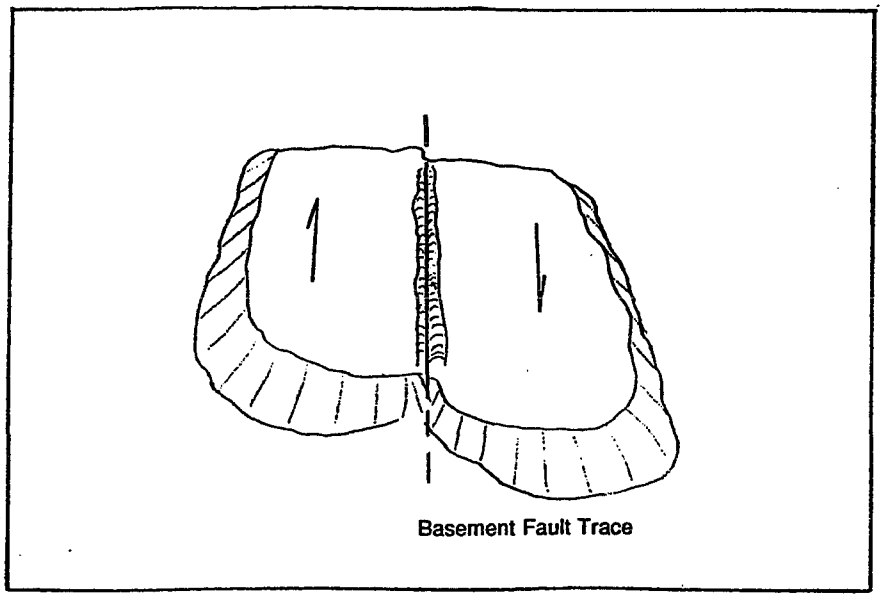

E

Figures 23d and 23e. d) Well-developed throughgoing fault zone with remnant boundary scarps. e) Line drawing.

zone (fig. 23e). This type of fault geomorphology is expressed along the central segment of the SAFZ (fig. 24). Although this experiment is characterized by pure strike-slip movement, while the SAFZ is currently experiencing approximately 5° of convergence, the geomorphology along the narrow fault zone bears a striking resemblance to the model fault zone. The 5° of plate convergence across the SAFZ is responsible for producing the abundant fault-parallel mountain ranges, such as that pictured in Figure 24, taken along the central segment of the SAFZ near the Carrizo Plane. The development of the initial topographic bulge, en echelon Riedel shears, and secondary compressional and extensional features is well documented in natural examples. A classic example is depicted by this young, previously undeformed sedimentary deposit that has been deformed by right-lateral movement of the Coyote Creek fault during the 1968, Borrego Mountain earthquake, which illustrates well-developed deformational features similar to those produced in the experimental models (figs. 25 and 25a) (Wallace, 1990). The structures developed in the sedimentary materials is a natural example illustrating a virtual duplication of model Experiment #5, where a homogeneous, undeformed, brittle material is exposed to strike-slip faulting at depth. The primary difference between the model and the natural example is the amount of cohesive strength in the natural sand deposit. The cohesive strength of the material causes the deformation to be expressed by fractured blocks; however, the observed features are still characterized by brittle deformation in response to similar principal stress orientations as seen in the model experiments. Right-lateral strike-slip deformation beneath this young sedimentary deposit has developed visible en echelon tension fractures, zones of compression, and an obvious "mole track." The cohesive nature of the

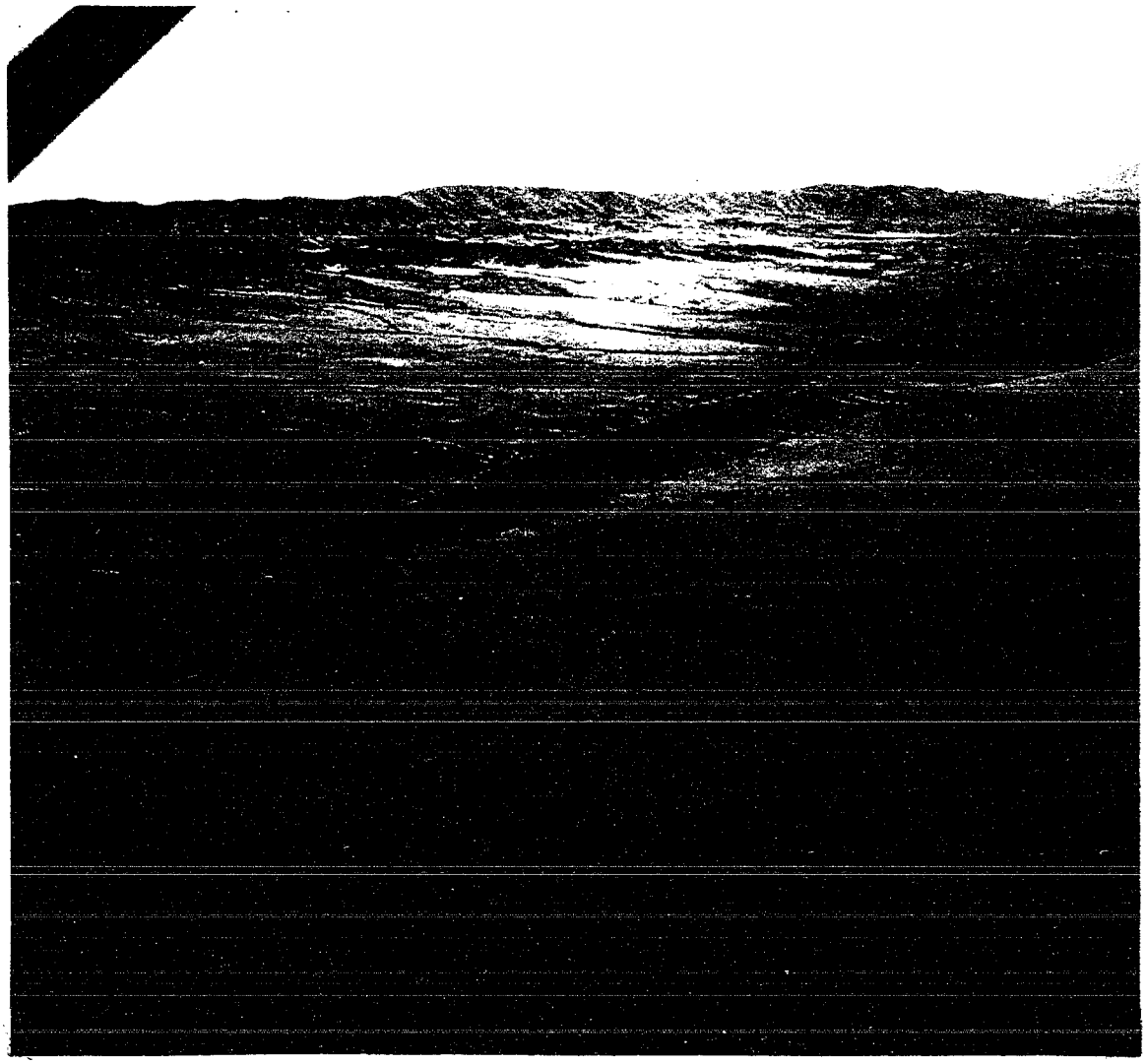

Figure 24. A photograph of the central segment of the San Andreas fault zone near the Carrizo plain. The San Andreas fault is a well-defined, throughgoing fault, bounded by fault-parallel mountain ranges (view to southeast) (Photo by Bob Wallace, U.S.G.S. Library).

Figure 25. Right-lateral motion beneath a young sedimentary deposit produces characteristic en echelon features along the "mole track." This ground rupture occurred along the Coyote Creek fault during the 1968, Borrego Mountain earthquake (from Wallace, 1990).

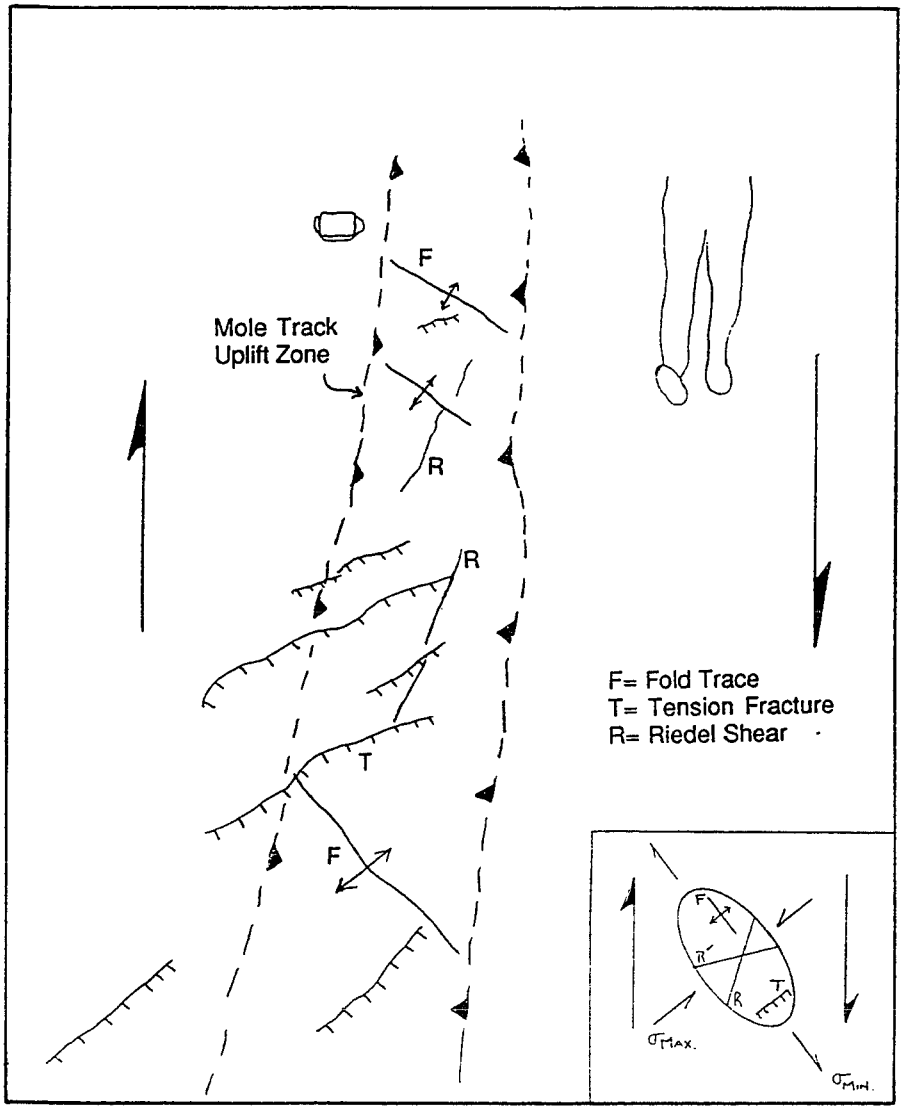

Figure 25a. The deformational features are accentuated in this line drawing. The characteristic frictional faulting orientations of deformational features stemming from dextral slip motion include en echelon tension fractures and zones of compression. The accompanying strain ellipse indicates the theoretical stress directions and the resulting geologic structures developed in a right-lateral slip environment.

deformed material produces block deformation, which is slightly more difficult to discern than the non-cohesive materials used in the model experiments; however, deformational patterns consistent with right-lateral, frictional wrench faulting are illustrated in the accompanying line drawing (fig. 25a).

Experiment 6

Experiment #6 incorporates transpressional movement of the basement wrench fault, rather than strike-slip movement, and uses the same overlying homogeneous sand pack as used in Experiment #5. The primary purpose of this transpressional sand experiment is to analyze surface deformation, both within the zone of distributed shear and outside the wrench fault zone, and compare these structures to natural SAFZ examples. A 15° degree convergence angle has been used for this experiment. The amount of convergence applied in the model corresponds to the angle of convergence currently thought to be acting across the Santa Cruz Mountains segment of the SAFZ, which will be the natural example used for comparison. The Santa Cruz Mountains segment has been referred to as the "little bend," due to the 10° westward bend (N. 50° W.) in the trend of the SAFZ, which, when coupled with the 5° angle of convergence thought to be acting across the central segment (N. 40° W.) of the SAFZ, produces a 15° convergence angle. The increased angle of convergence across the Santa Cruz segment of the SAFZ is responsible for the rapid uplift of the Santa Cruz Mountains. The more well-known "big bend" in the SAFZ, just north of the Los Angeles area, has a trend of N. 75° W., and an angle of convergence of approximately 40°. This large component of compression is responsible for the

development of the Transverse Ranges, a rapidly uplifting mountain range consisting of tightly folded and thrust faulted Tertiary sedimentary strata.

The onset of transpressional deformation is visible under low-light illumination, which helps to expose the deformational features. Immediately, a topographic bulge overlying the wrench fault is apparent, and a faint, linear, fault-parallel topographic scarp is visible outside of the wrench fault zone. En echelon synthetic Riedel fractures are well-developed within the wrench fault zone, as was also seen in the pure strike-slip experiment (figs. 26 and 26a). The synthetic Riedel fractures are overprinted by en echelon tension features, as transpressional motion advances (figs. 26b and 26c). The off-fault scarp with an orientation parallel to the basement wrench fault, does not behave in a manner consistent with frictional faulting theory. This feature is indicative of fault-normal compression, and is similar to the orientation of the folds developed in the weak fault gelatin experiment #4. Continued deformation results in the accentuation of the tensional features within the wrench fault zone and the growth of the thrust sheet, while no obvious throughgoing fault zone is developed. The amount of uplift is apparently great enough, aided by the lack of erosion inherent to all model experiments, that the throughgoing fault zone is gradually buried. The final stage of model deformation is depicted by a topographic bulge marked by en echelon tension fractures, flanked by off-fault thrust sheets diverging from, and parallel to the basement wrench fault, without obvious surface expression of a throughgoing fault zone (figs. 26d and 26e). This deformational configuration may be explained by a weak fault zone at depth, overlain by a shallow, brittle layer, which results in the development of off-fault,

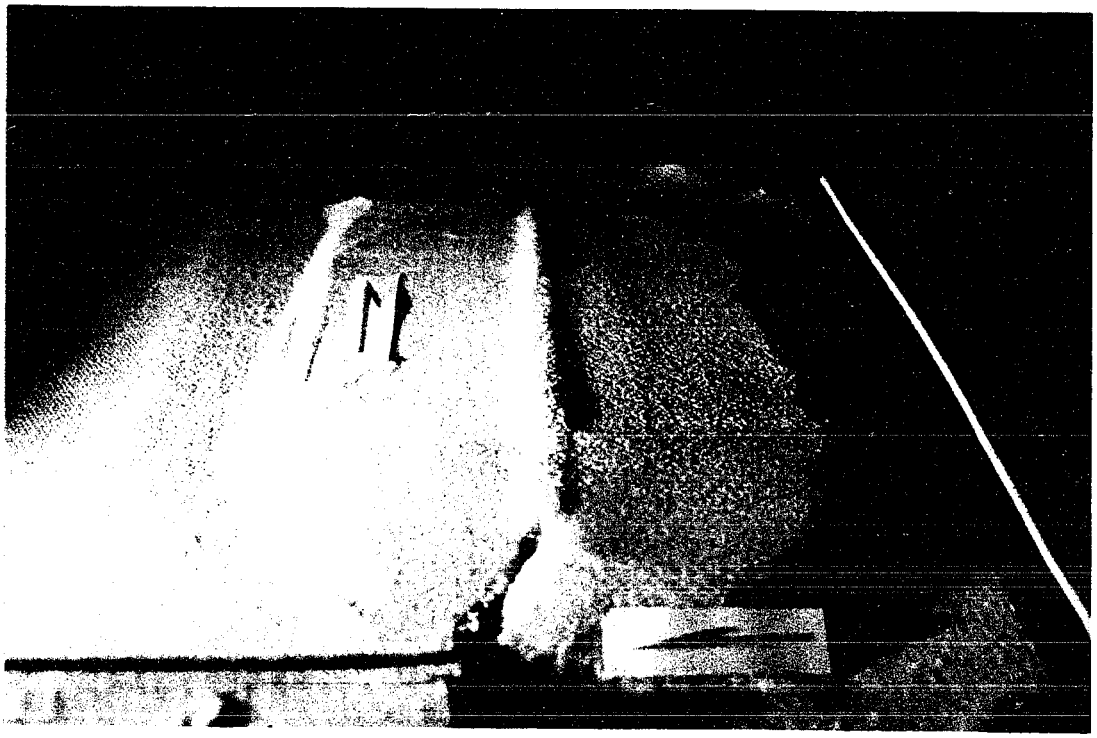

A

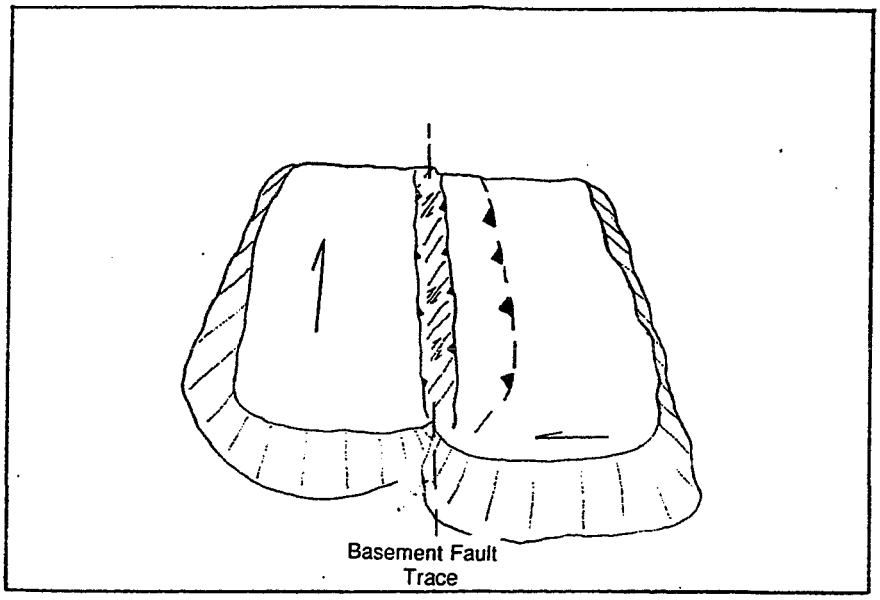

Figures 26 and 26a. A 1.5 inch, unconsolidated sandpack is subjected to 15° of transpressional deformation. The resulting deformational features include a similar mole track as observed in the previous experiment, with en echelon Riedel shears, and a developing fault-parallel thrust sheet. a) The line drawing illustrates the deformational configuration.

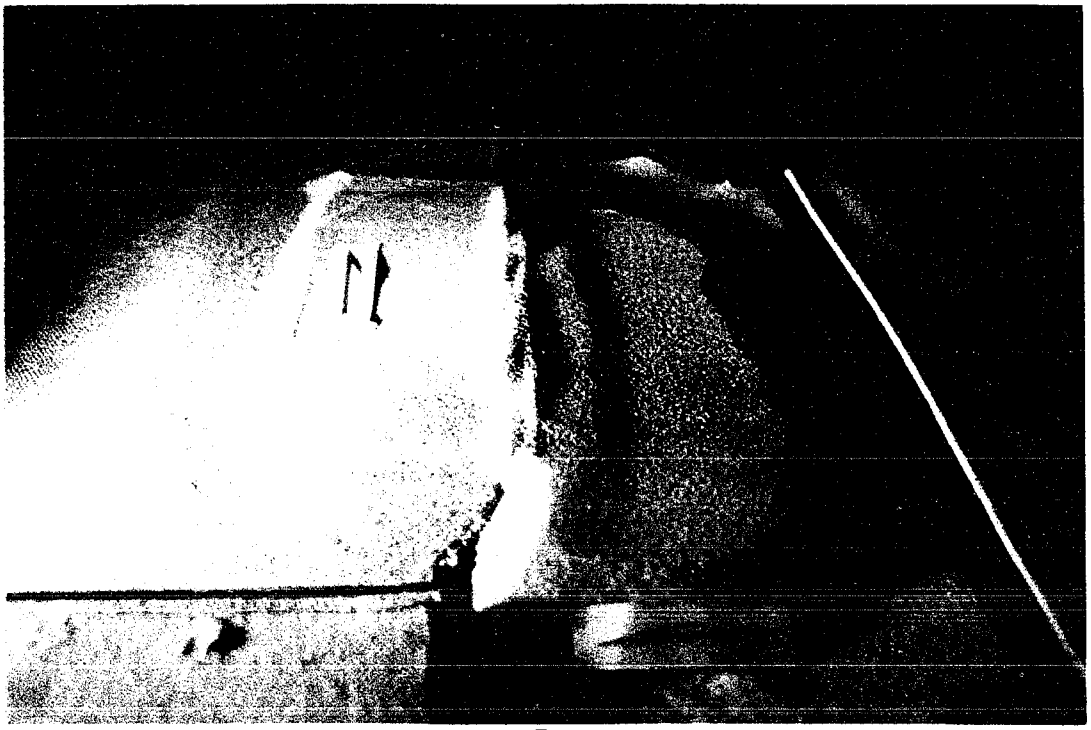

B

C

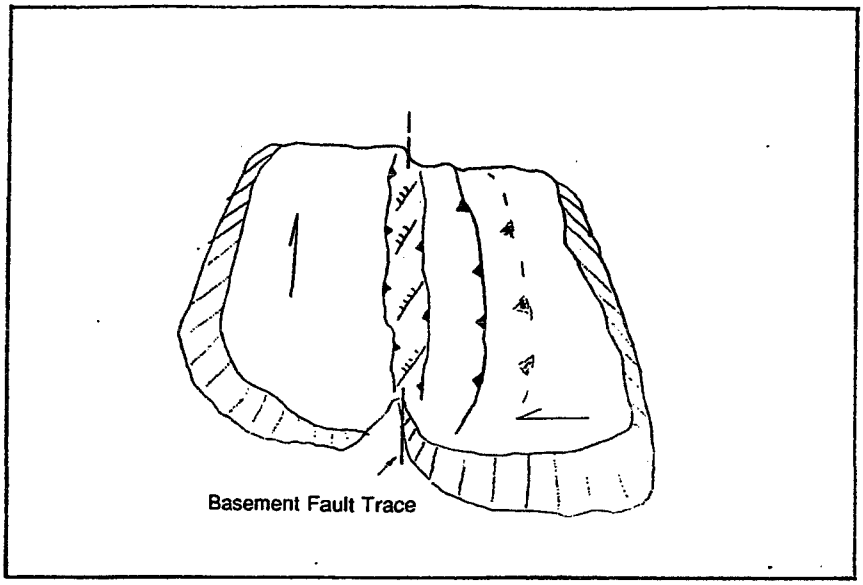

Figures 26b and 26c. b) Continued displacement produced striking en echelon tension features, reactivating along the Riedel shears. The thrust sheet is becoming highly pronounced, and a faint trace of a second thrust fault is developing outside of the first thrust fault. c) The line drawing illustrates the orientation of the en echelon tension features that have overprinted the initial Riedel shears.

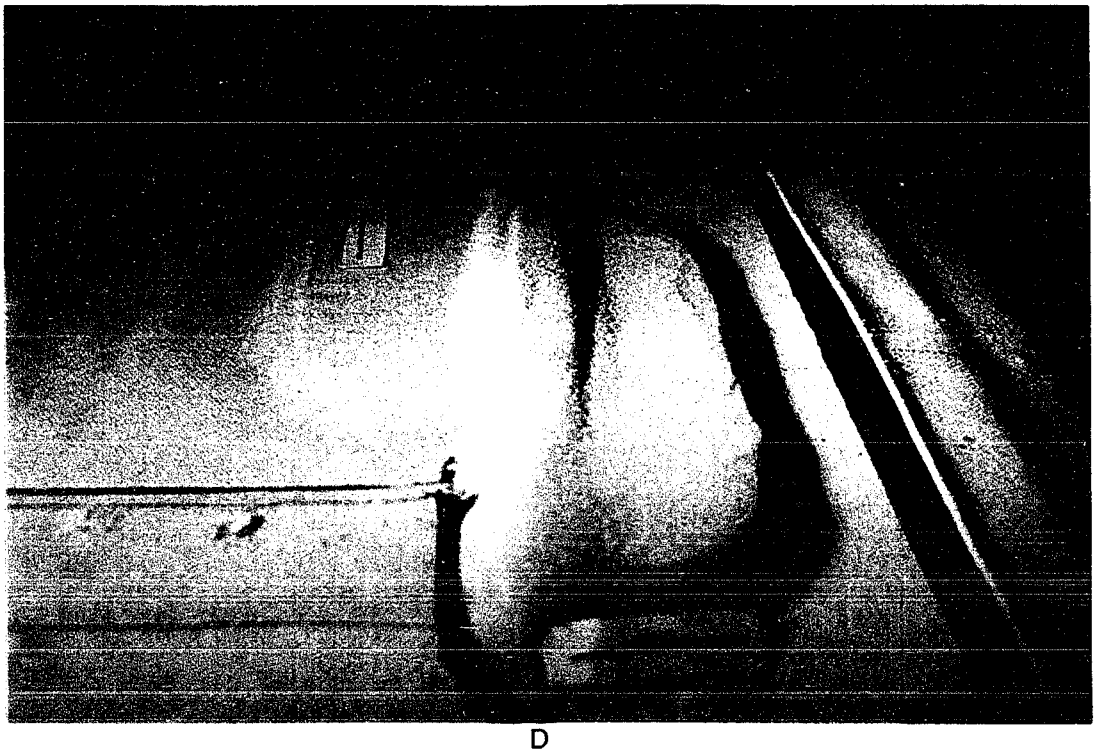

D

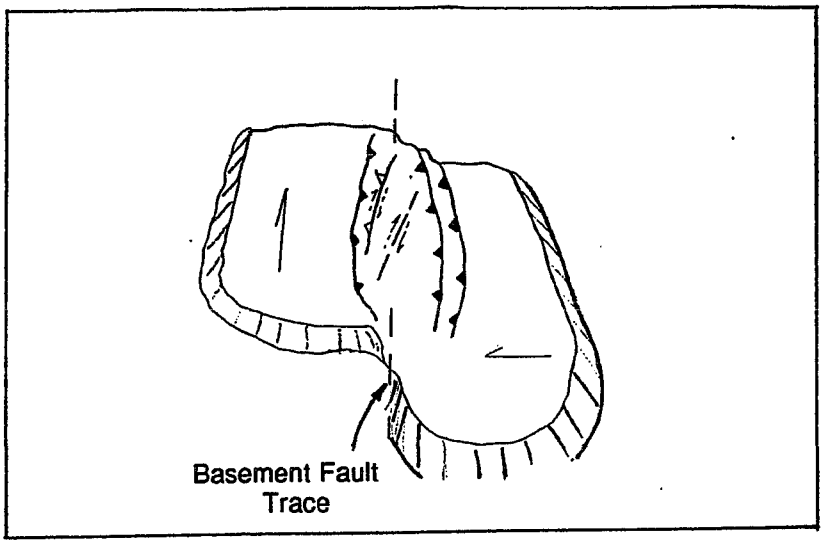

E

Figures 26d and 26e. d) The 15° angle of convergence prevents the development of a throughgoing fault zone, as uplift and thrust development out-pace translational movement. e) Line drawing illustrating fault and fold orientations in relation to the basement wrench fault.

fault-parallel contractional features and en echelon Riedel and tension fractures near the zone of wrench deformation.

The Santa Cruz Mountains segment of the SAFZ bears a striking resemblance to the features observed in Experiment #6. The Santa Cruz Mountains are characterized by rapid uplift, mostly fault-parallel thrust faults, such as the Berrocal and Shannon faults, and en echelon tension fractures located along the trace of the SAFZ. En echelon tension fractures were developed during the 1989 Loma Prieta earthquake, and had orientations consistent with the sand model experiments. Figure 27 is a cartoon depicting the relationship between the earthquake generated en echelon tension fractures, the fault zone at depth, and the fault-parallel thrust faults.

Following the San Francisco earthquake of 1906, Waring (1908) mapped the surface fractures along the Santa Cruz Mountains segment of the SAFZ. He noted numerous tension fractures oriented from N. 3° W. to N. 13° W. These orientations are consistent with the expected orientations of deformational features stemming from movement along a right-lateral strike-slip fault. The en echelon fractures developed in the 1989 Loma Prieta earthquake have orientations ranging from N. 25° W. to N. 45° W., as well as fractures oriented nearly parallel to the inferred trace of the San Andreas fault. The lower angle of the Loma Prieta tension fractures, as opposed to the 1906 event, mostly likely stems from the component of uplift that occurred during the 1989 earthquake. The relatively large component of uplift, approximately 1.4 m (Plafker and Galloway, 1989), without accompanying surface rupture resulted in bending

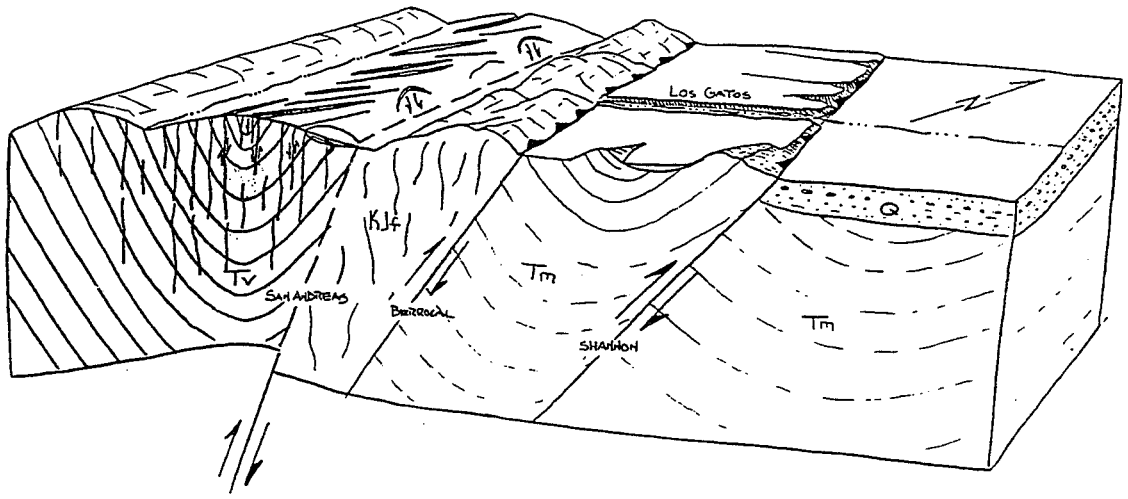

Figure 27. A block diagram depicting the 3-dimensional relationship between the en echelon tension fractures formed during the 1989, Loma Prieta earthquake, the San Andreas fault, and the fault-parallel thrust faults. The cartoon illustrates the Santa Cruz Mountains area near the town of Los Gatos. The sand model in Experiment #6 produced deformational features with striking similarities to geologic structures observed along this portion of the Santa Cruz Mountains (modified from Cotton, 1990, Unpubl.).

moment tension along the crest of the Santa Cruz Mountains. If pure vertical uplift occurs, the orientation of these features, in theory, should be parallel with the rupture zone that is accommodating vertical movement at depth. Since the Loma Prieta earthquake occurred along the SAFZ, or on a splay fault roughly parallel to the SAFZ, and was accompanied by 1.6 m (Working Group, 1990) of horizontal translation, then surficial tension fractures would be expected to be oriented somewhere between the theoretical en echelon (strike-slip deformation) and bending moment (reverse deformation) orientations. The N. 25° W. to N. 45° W. orientations of the en echelon tension fractures are consistent with this hypothesis.

The Santa Cruz Mountains segment lacks a well-defined fault trace like that developed along the central segment of the SAFZ, and no well-defined fault rupture occurred during the Loma Prieta earthquake. This morphology resembles the transpressional sand experiment where the increased amount of convergence prevents the development of a throughgoing fault zone. A broad rift zone does mark the San Andreas fault through the Santa Cruz segment; however, rapid uplift and landsliding may be concealing the upper portions of the fault zone. Therefore, the overlying materials may behave in a similar fashion, but on a larger scale, to the sedimentary materials shown overlying the Coyote Creek fault during the 1968, Borrego Mountain earthquake (figs. 25 and 25a). Convergence, and possibly a weak fault zone at depth, may be responsible for developing the fault-parallel thrust faults, while uplift of the sedimentary cover along the fault trace deforms according to the expected frictional faulting theories. The rapid uplift and profuse landsliding in the Santa Cruz Mountains

along the 'little bend" prevent the development of a narrow, throughgoing fault zone.

Experiment 7

Recent stress indicators, orientations of folds and faults, and earthquake focal mechanisms indicate that the SAFZ and surrounding area more closely resemble a contractional fold and thrust belt rather than a true strike-slip fault zone. Gelatin model experiments have shown that, by simulating fault characteristics such as those currently acting along the SAFZ, surface fold orientations indicate the development of a fault-parallel fold and thrust belt. However, no subsurface data can be obtained from gelatin or clay to verify that thrust faults are being generated. The plastic and elastic behavior of clay and gelatin permit stresses to be transferred through the material without inducing brittle fractures, unless the material is subjected to extreme displacements. The nature of the thin upper layer permits these stresses to be expressed as folds, but not genetically related to underlying thrust faults.

The use of sand in modelling experiments has been shown to be favorable for illustrating surface and subsurface faulting due to the brittle nature of the material. Early sand box experiments performed by Hubbert (1951) illustrated subsurface thrust fault configurations stemming from a purely compressional force. Experiment #7 is a recreation of Hubbert's experiment, using a vertical compressional plate to deform a pile of sand, and transparent side walls to view the subsurface deformation (fig. 28). Compressional forces imposed by horizontal movements of the vertical plate against the sand result in well

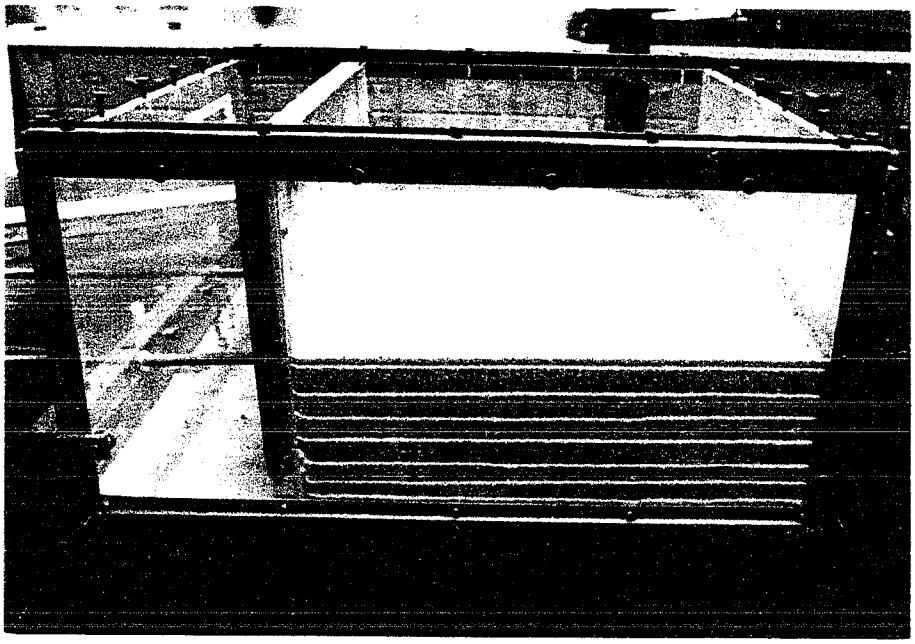

Figure 28. A typical thrust box with glass sides to view the deformation in the layered, unconsolidated sandpack.

defined low-angle thrust faults stemming from the base of the vertical plate. Continued deformation produces first and second order thrust faults with similar orientations, with the later stage thrust fault developing below the initial thrust fault (figs. 28a-f). If deformation is allowed to continue, additional thrust faults develop in succession, each forming below the previously developed thrust fault. The surface of the sand is characterized by a topographic bulge or scarp, roughly parallel to the vertical plate. Each surface scarp is genetically related to the developing thrust faults below. The similarities between natural rock exposures in compressional settings and this type of model configuration are striking.

Sand has been shown to be a good indicator of subsurface brittle deformation, and Naylor (1986) has demonstrated that sand can be valuable for depicting brittle surface deformation. Both surface and subsurface brittle deformation are illustrated in Experiment #8, in which sand is exposed to transpressional motion. The relationship between brittle faulting at depth, orientations of structures at the surface, and the imposed stresses as observed in the gelatin experiment, may help to decipher the nature of the stresses and resulting features seen along the SAFZ.

Experiment 8

The primary purpose of Experiment #8 is to deform a stratified sand pack using the same methods as used in Experiment #6, and to describe the relationship between the imposed stresses, and the surface and subsurface deformational features. Viewing of the subsurface structures is accomplished by

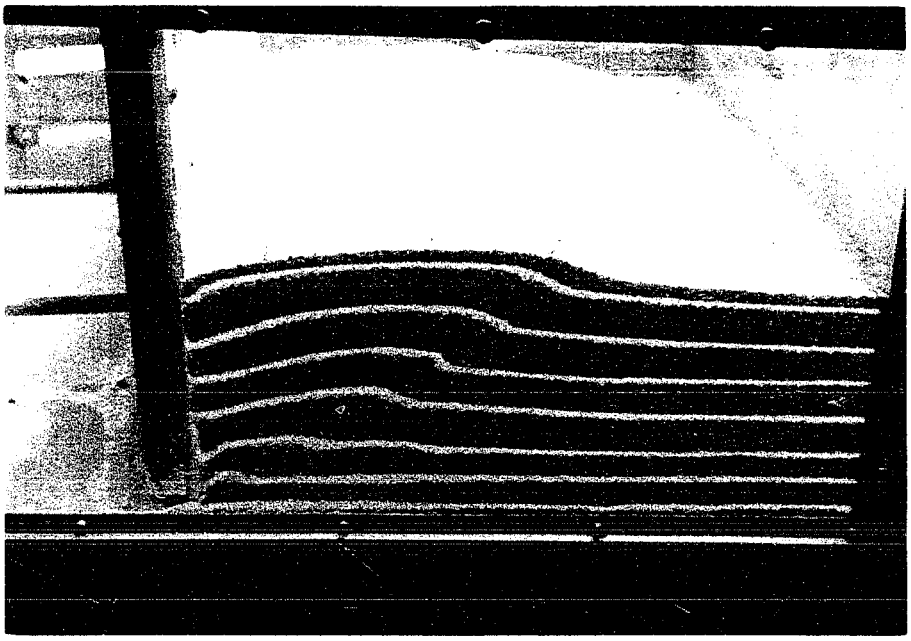

A

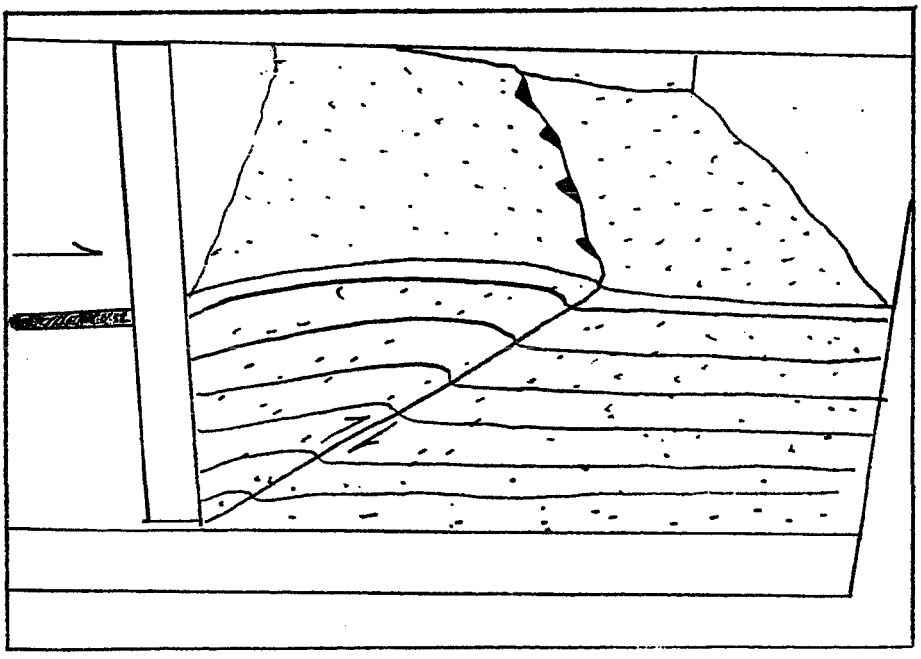

B

Figures 28a and 28b. a) As the vertical plate moves left to right, pure compression is applied to the sandpack. A low-angle (28°) thrust fault is developed that extends to a surface scarp, and produces subsurface drag-folding. b) The line drawing aids in the delineation of the structural features.

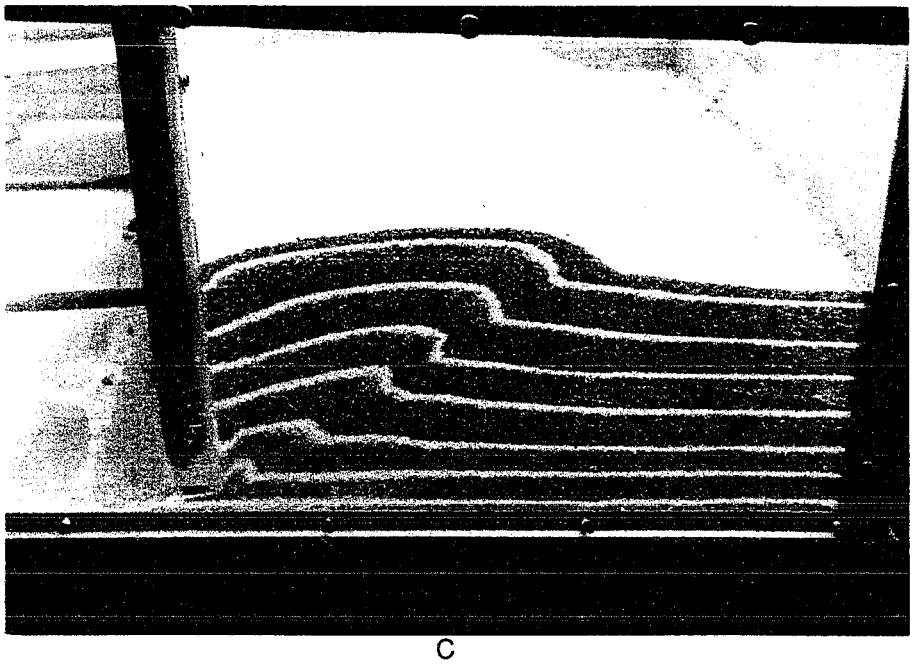

C

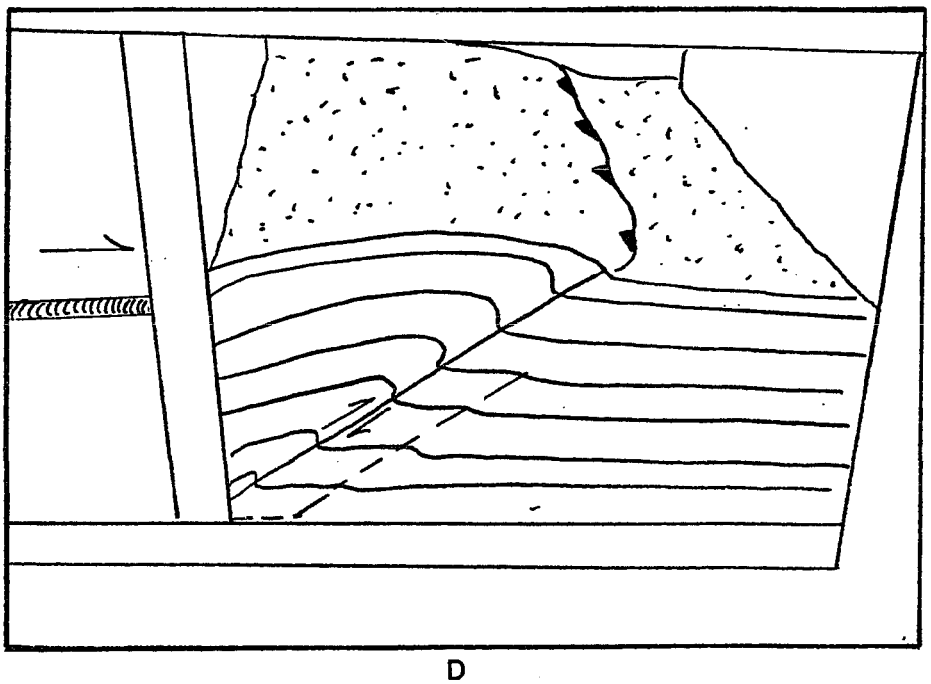

D

Figures 28c and 28d. c) Continued compression produces additional drag-folding, and the early stage of a second order thrust fault developing beneath the initial thrust fault. d) Line drawing to aid in the recognition of deformational structures.

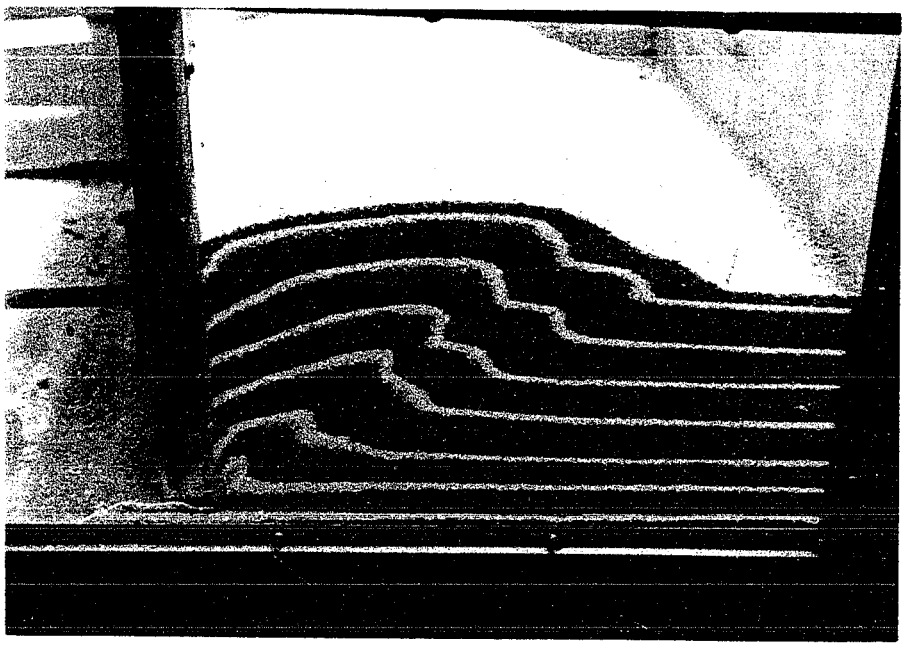

E

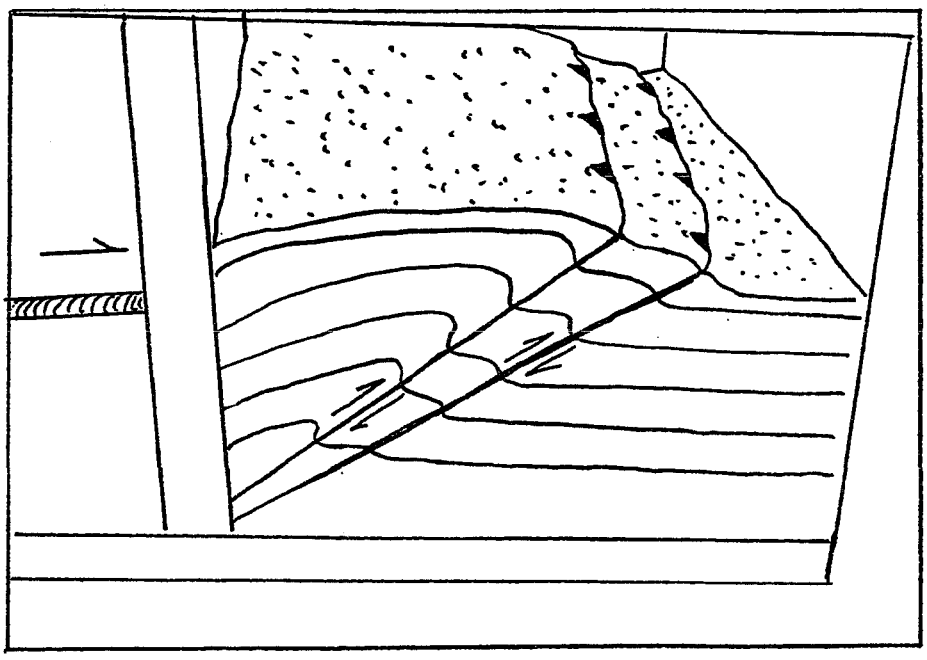

F

Figures 28e and 28f. e) Well-developed first order and second order thrust faults, and pronounced drag-folding. As the second order thrust fault develops, the initial thrust fault becomes dormant. f) Line drawing to aid in the recognition of structures.

impregnating the sand with a small percentage of plaster before placing the layers over the basement fault. The dry sand/plaster material is placed in lifts, alternating with thin dark layers, to better delineate subsurface deformation. Following transpressional deformation, the sand pack is carefully watered and given time to permit partial cementation to occur. The material is carefully sliced into sections and brushed, accentuating the differential cementation between the thin dark layers, which have no plaster, and the sand/plaster material. Thus, each subsurface structure is visible in section and can be correlated with the corresponding surface fault trace.

The presence of the plaster in the sand pack gives a slight cohesive strength to the material. The added cohesion tends to allow fault movement to remain within a singular fault trace for a longer period of time than in a cohesionless material. The faults are highly visible due to the ability of the material surrounding the fault zone to stand at greater angles than the angle of repose of cohesionless sand. Both cohesionless and slightly cohesive sand appear to develop deformational features with similar orientations in response to the imposed transpressional stresses, but the timing of deformation, the width of fault spacing, and the surficial expression occur at different scales. Cohesionless sand deforms on a granular scale, whereas slightly cohesive sand deforms on a block scale. The block scale of deformation probably has greater applicability to natural examples due to the strength disparity between the fault interface and the surrounding material, as is well documented in natural fault zones.

For the purposes of this experiment, a 10° component of convergence is steadily applied across the fault zone, and is consistent throughout the entire experiment. Initial transpressional movement along the basement wrench fault creates a topographic bulge that is dissected by complex, curvilinear, synthetic Riedel surface faults (figs. 29 and 29a). These features are similar to deformational features developed in Naylor's experiments, which have been shown to be curvilinear on the surface and helicoidal in the subsurface. The uplift in the central region is flanked by fault-parallel thrust faults verging away from the throughgoing fault zone. The curvilinear faults initially develop as en echelon synthetic Riedel shears, much the same as in the strike-slip sand experiments. However, further transpressional motion shows that these features have a complex history. Following the initial formation of the Riedel shear, portions of the fault accommodate active uplift as well as translation (figs. 29b and 29c). At this stage, incipient secondary thrust faults, marked by faint fault-parallel topographic scarps, begin to develop outside of the centralized zone of deformation. The component of thrust faulting observed along the upper section of the main throughgoing Riedel shear soon becomes dormant, apparently as the secondary thrust develops beneath this fault and accommodates most of the compressional motion. The secondary thrust fault is now expressed as a well-defined scarp located outside of the shear zone (figs. 29d and 29e). This type of fault behavior matches that of the pure thrust fault experiment, in which newly developed thrust faults, generated beneath the pre-existing thrust, accommodate most of the shortening. Following the termination of thrust displacement along the Riedel shear, purely translational movement is reactivated, and the Riedel shear becomes a well-defined,

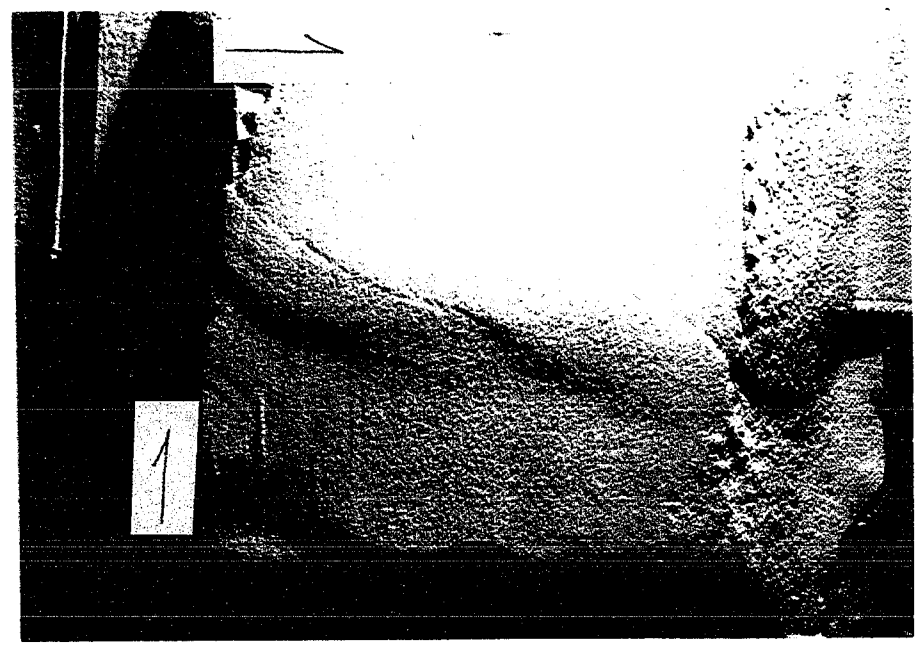

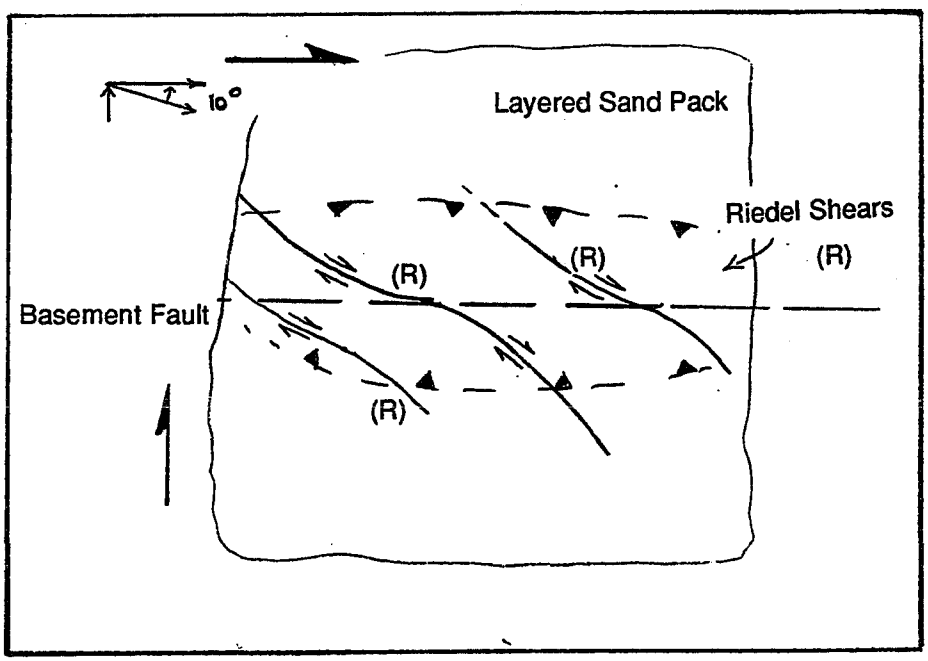

A

Figures 29 and 29a. Incipient transpressional deformation of a 2.5 inch, layered sandpack. En echelon, synthetic Riedel shears are formed, oriented approximately 25° to the basement wrench fault. a) The line drawing shows the orientation of the shears in relation to the basement fault, and to the zone of uplift, which is oriented nearly parallel to the basement fault.

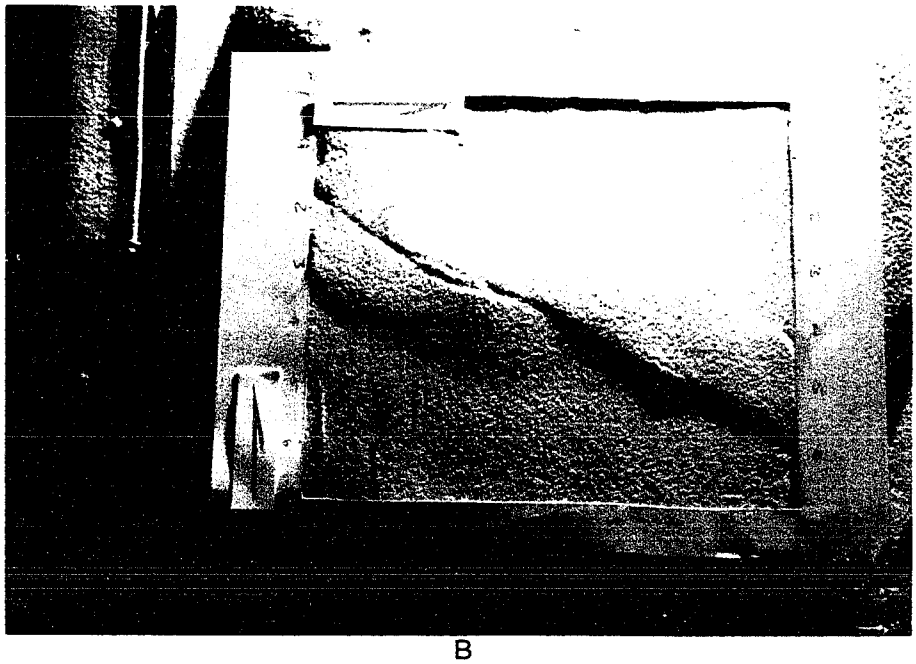

B

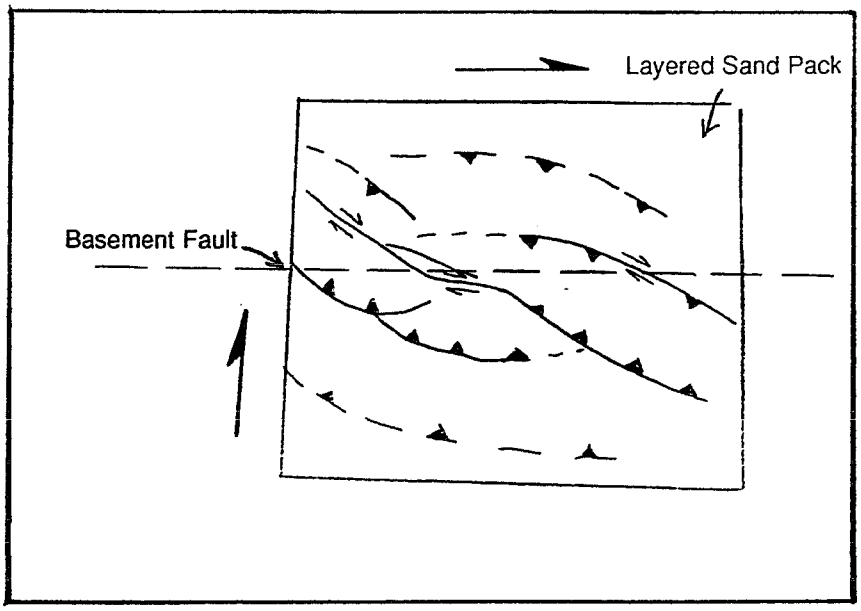

C

Figures 29b and 29c. The sand/plaster mixture has a slight cohesive strength, resulting in block type deformation. Further displacement results in the development of a well-defined synthetic Riedel shear accommodating both horizontal and vertical movement. The flanking Riedel shears have been reactivated as thrust faults, and incipient fault-parallel thrust faults are developing outside of these features, as shown in the line drawing.

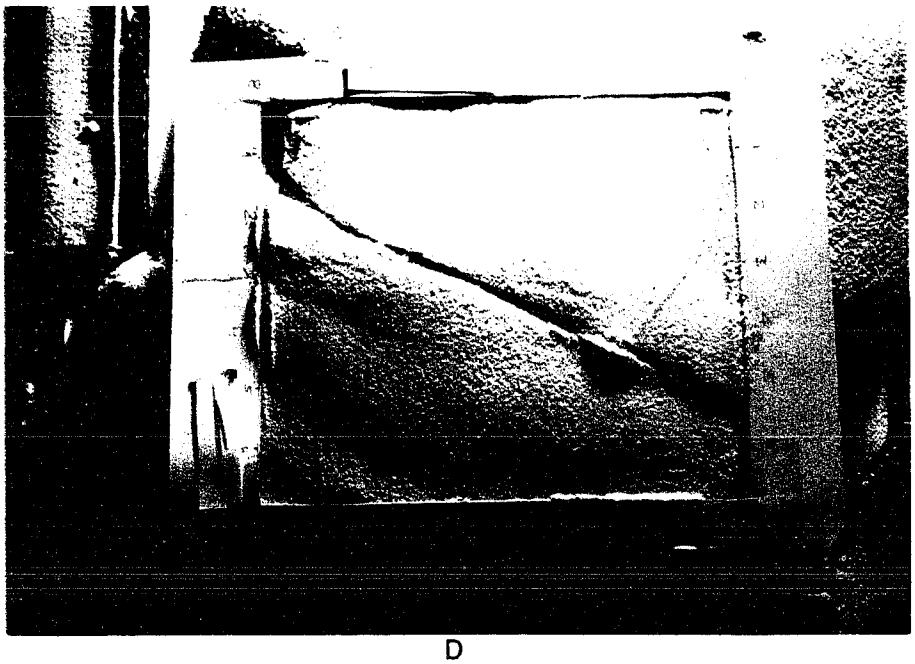

D

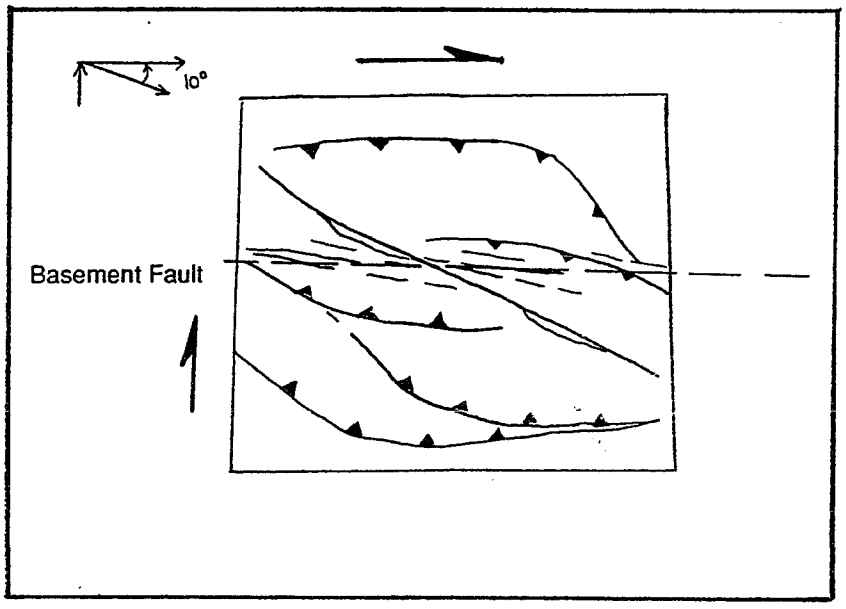

E

Figures 29d and 29e. Continued deformation results in the formation of a throughgoing, synthetic Riedel shear with predominantly translational movement, as the secondary thrust faults have taken up most of the compressive component of deformation. Incipient P-shears are faintly apparent, and suggest that a throughgoing fault zone may be developing. The well-developed thrust faults have orientations nearly parallel to the basement fault. e) Visualization of the deformational features is aided by the accompanying line drawing.

throughgoing fault (figs. 29d and 29e). Faint traces of incipient shear planes can be seen developing at a low angle to, and located directly above, the basement wrench fault. This low angle shear becomes well-defined as deformation proceeds (figs. 29f and 29g). As the low-angle shear zone develops, translational movement along the synthetic Riedel shear gradually decreases as motion transfers to the developing, throughgoing low-angle shear. First and second generation thrust faults, oriented nearly parallel to the trace of the basement fault, are well-defined on both sides of the throughgoing fault (figs. 29f and 29g).

Sand Sections

The deformed sand pack was wetted and allowed to partially solidify prior to slicing into four sections (fig. 30). Lightly brushing the sand sections preferentially eroded the darker layers because they were not mixed with plaster, thus, providing a topographic contrast that accentuates the deformational features. The sand sections are accompanied by line drawings that help to illustrate the subsurface deformational features (figs. 31, 31a-h).

The sand sections provide striking evidence to suggest that low-angle thrust faults and folds are generated along the flanks of a basement wrench fault during transpressional deformation (figs. 31, 31a-i). Low-angle (28° to 33°) thrust faults originate at the base of the throughgoing wrench fault and terminate at the surface, corresponding with the topographic scarps outside of the zone of wrench deformation (fig. 31h, i). The thrust faults are mostly straight, but some are slightly concave upward. No apparent deformation has taken place outside of these thrust fault zones. Deformation between the bounding thrust faults is

F

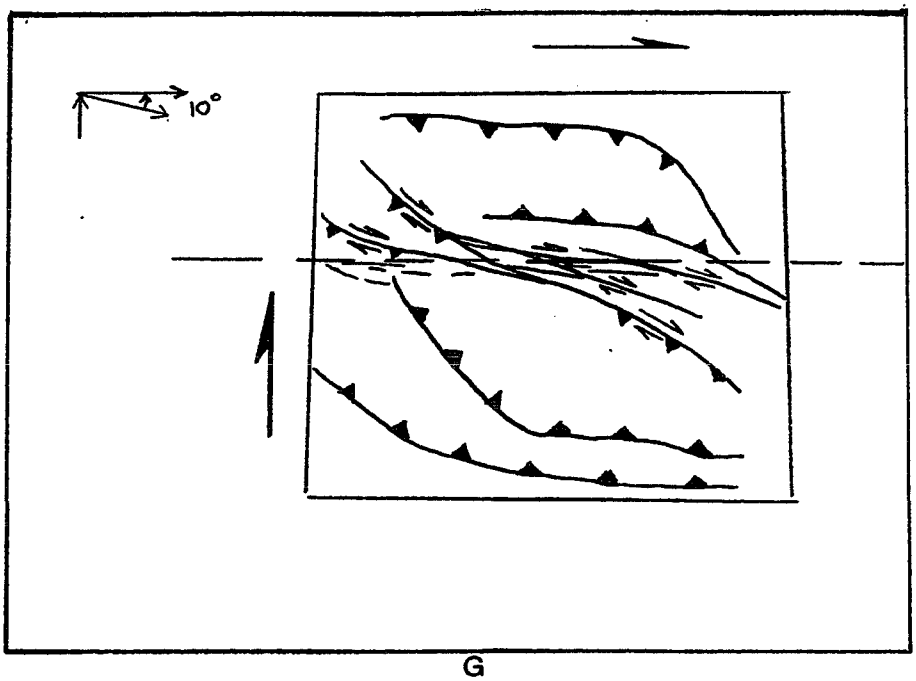

G

Figures 29f and 29g. Further deformation creates additional P-shears that help to form the initial trace of the throughgoing fault zone. g) The line drawing illustrates the orientation of thrust faults and the low-angle shears.

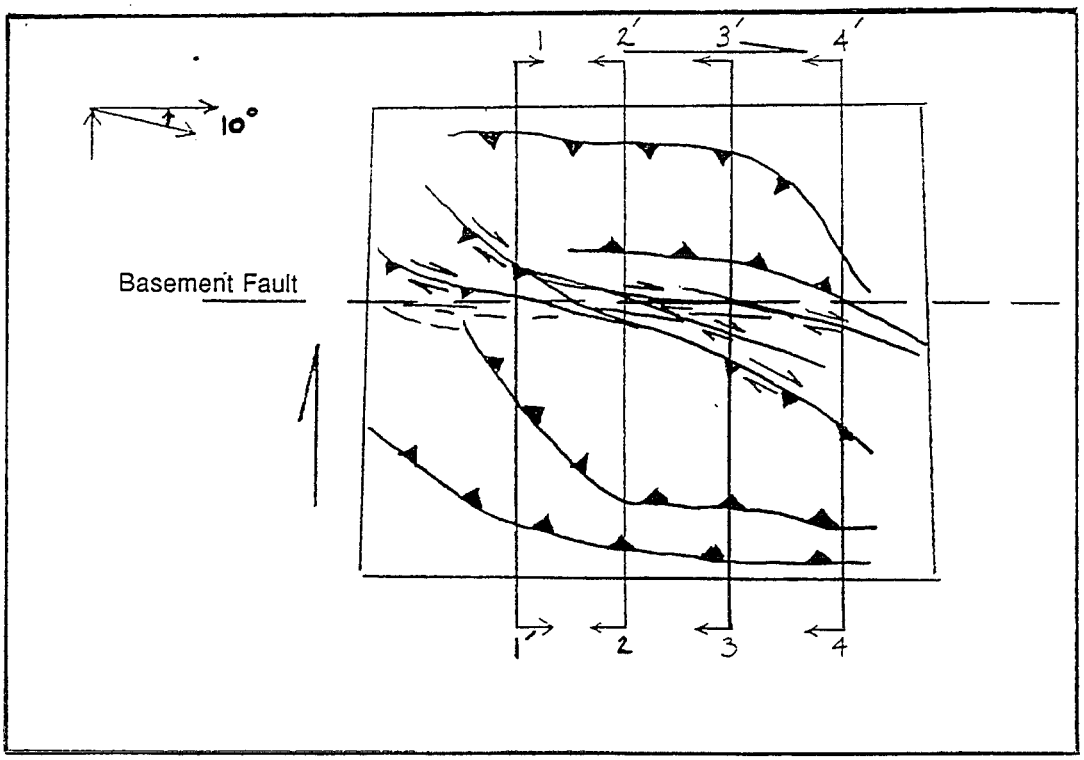

Figure 30. Following deformation, the sand/plaster mixture was wetted and sliced into sections, with the section arrows showing the facing direction.

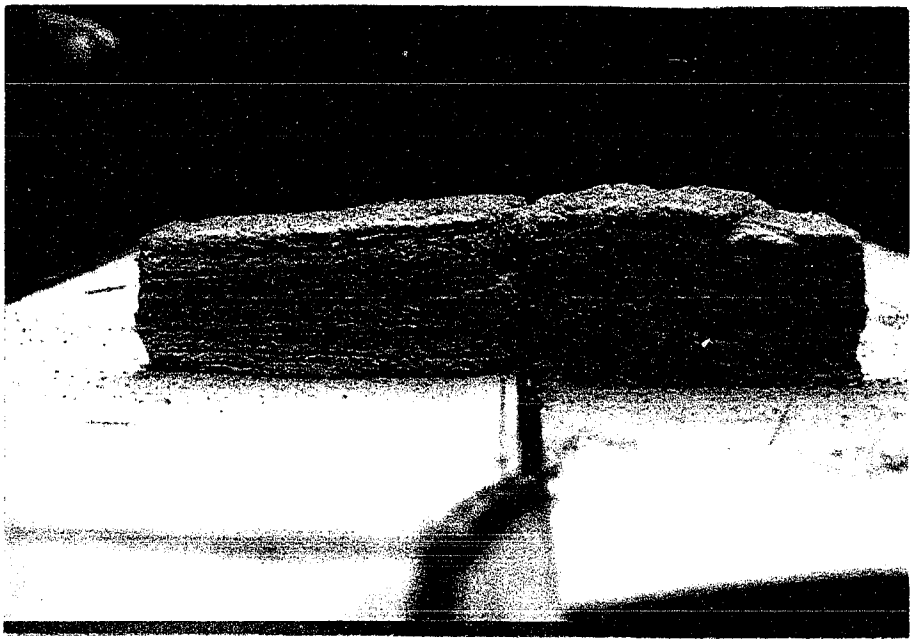

31

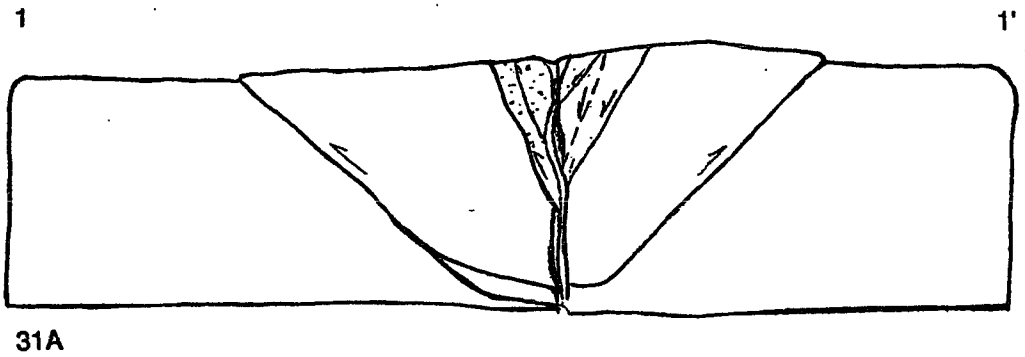

31A

Section 1

Figures 31 through 31g. Sand sections showing well-developed thrust features outside of the zone of wrench deformation. These structures resemble those generated in the pure thrust box experiment. The thrust faults have relatively gentle dips (25° to 38°), pronounced drag folds, and correlate with a topographic surface scarp. The zone of wrench deformation is characterized by a disrupted zone of translated, uplifted, and downdropped blocks.

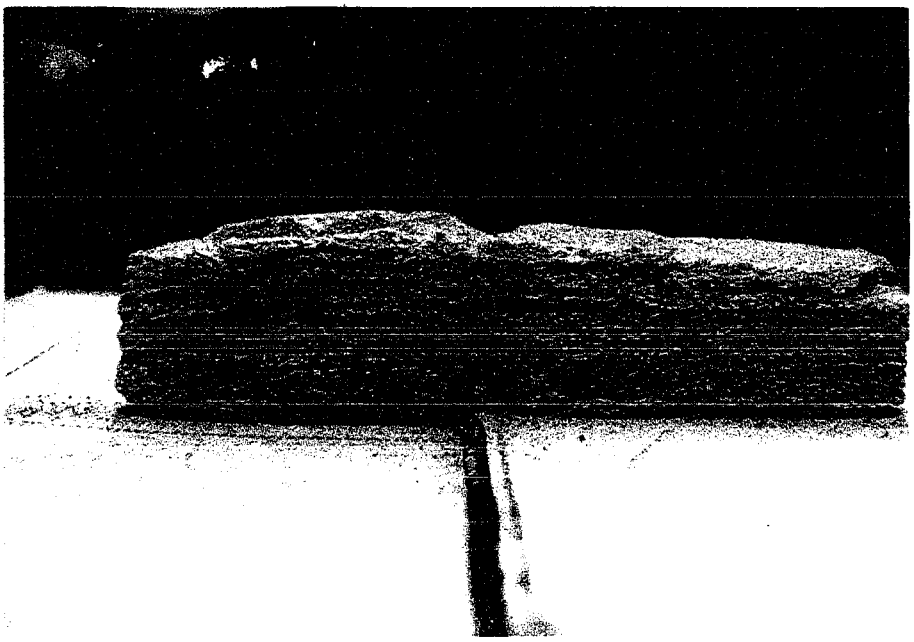

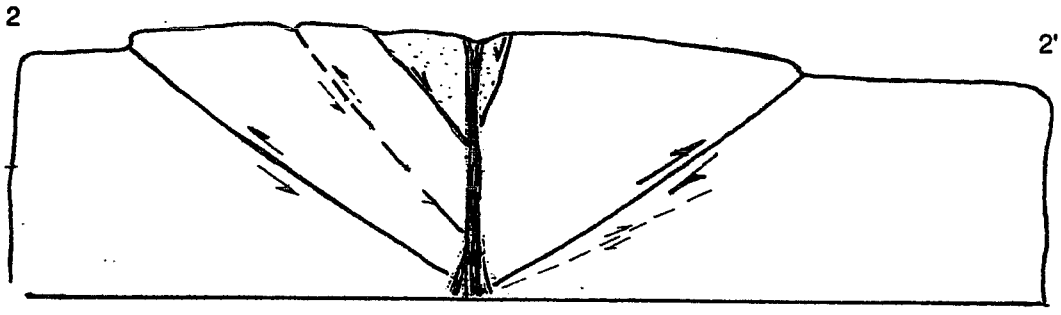

31C

Section 2

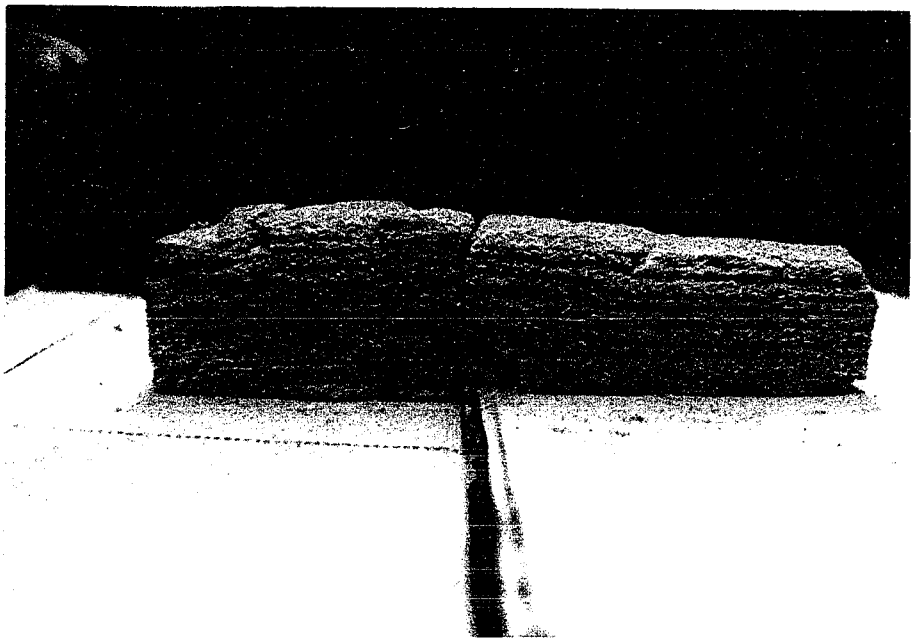

D

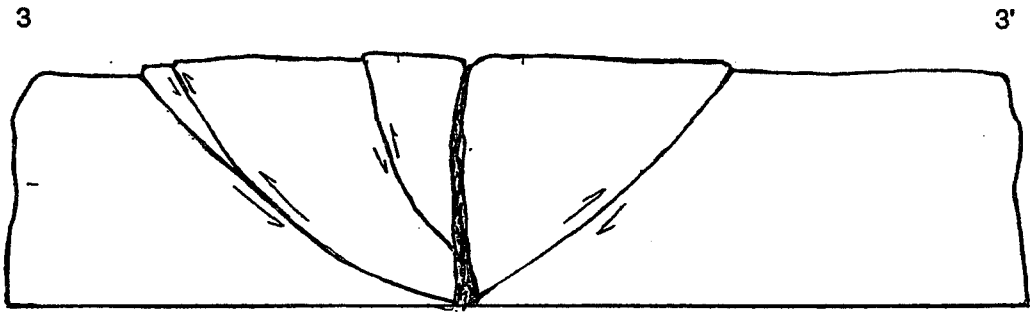

31E

Section 3

F

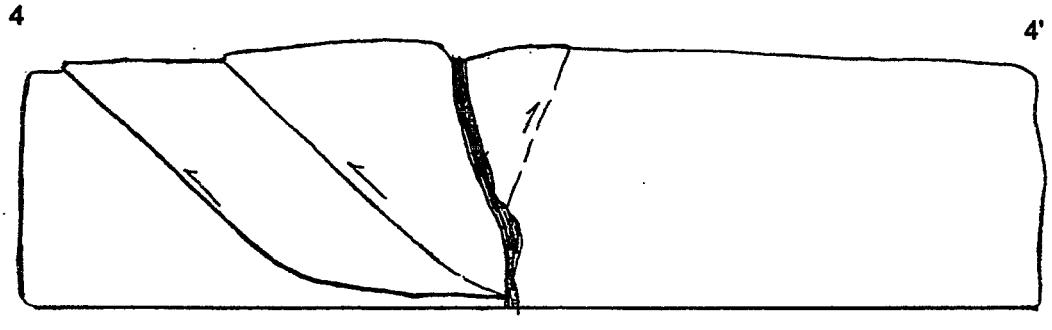

G

Section 4

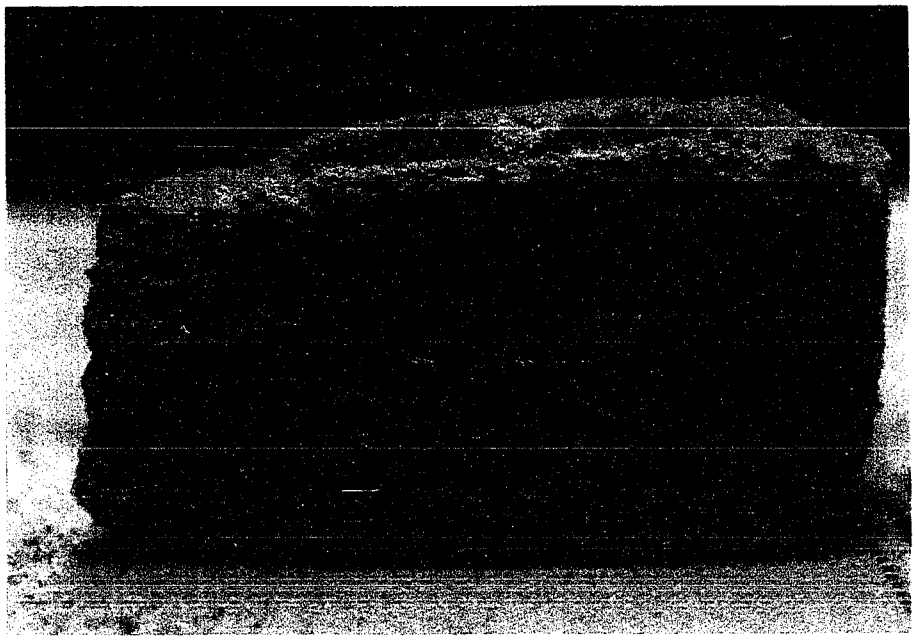

H

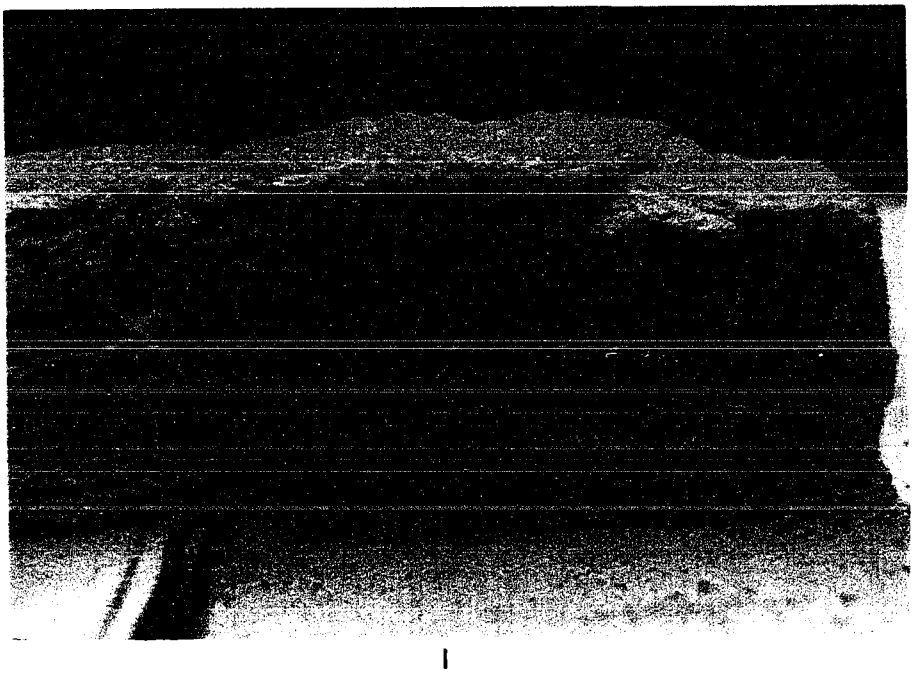

I

Figures 31h and 31i. Two close-up views of these thrust faults. Photos show well-developed drag-folding and connection with surface fault trace.

characterized by drag folding along the thrust faults, warping of the sedimentary layers, and uplifted and downdropped blocks. Translational disruption of the sediments expressed as diffuse areas void of stratigraphic layering, are located near the basement wrench fault. The throughgoing fault zone is expressed mostly as a vertical fracture, except in section #4, where it dips nearly 75°. Naylor and others (1986), in their sand models, identified helicoidal subsurface fault geometries in Riedel shears, similar to the orientation of the throughgoing fault in section #4. Section #1 shows a feature that could have been one end of the helicoidal structure, but translational movement and the development of a throughgoing wrench fault have masked this feature. The overprinting of the Riedel shear was apparent in the plan view of Figure 29f as the majority of the translational movement transferred from the Riedel shear to the throughgoing wrench fault. The throughgoing wrench fault is characterized, in section, by the diffuse central area, void of any stratigraphy that flanks the main vertical fracture. A three-dimensional depiction of the four sand sections indicates fault-normal contraction along low-angle thrust faults oriented nearly parallel to the trace of the master wrench fault (fig. 32).

Summary

Sand experiments have shown that surface and subsurface brittle deformation can be correlated in a transpressional environment. The results indicate that despite the relatively small component of contraction as compared to translation, the dominant structures developed are low-angle thrust faults and folds. The surface and subsurface orientation of these features suggests that the component of compression is acting perpendicular to the basement wrench fault.

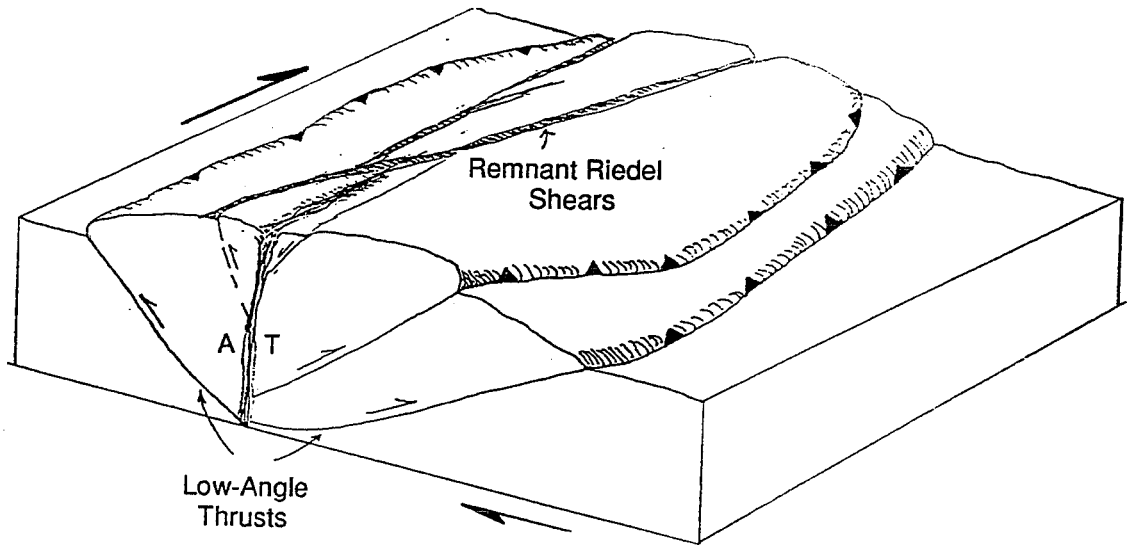

Figure 32. A 3-dimensional diagram developed from the 4 sand sections. This fault geometry is not consistent with a positive flower type of deformation, which predicts helicoidal subsurface configurations, and high angle reverse faults.

Experiments #5, #6, and #8 provide strong evidence that initial deformation of a coherent overburden follows standard frictional faulting theory by developing en echelon Riedel shears and tension fractures. However, as basement wrench faulting continues, a weak, throughgoing fault zone is developed that accommodates translational motion with low shear stresses. The convergent component of transpression acting perpendicular to the basement fault is the deformational mechanism responsible for producing fault-parallel thrust faults and folds. Table 1 summarizes the eight experiments performed for this study.

The experimental results are valuable for generating general, large-scale theories, and should not be used to develop actual scaling parameters in natural settings. The material response to an imposed force, and the orientation of the resulting deformational structures, provides insightful clues for discerning the origin of natural structural features.

Table I

Summary of Experiments

Experiment #	Material	Conditions	Results	Figure #
1	Gelatin	Wilcox Re-creation, Dextral Slip	Wrench Deformation	23-25
2	Gelatin	Separate Plates, Transpression	Wrench Deformation	26, a,b
3	Gelatin	Throughgoing Fault, Transpression	Wrench Deformation	27, a-c
4	Gelatin	Low Friction Fault, Transpression	Decoupled Deformation	28, a-d
5	Sand, Homogeneous	Naylor Re-creation, Dextral Slip	Riedel Shears "Mole Track"	30, a-e
6	Sand, Homogeneous	Buried Fault, Transpression	Riedel Shears, Thrusts	33, a-e
7	Sand, Layered	Pure Compression	Thrust Faulting	35, a-f
8	Sand, Layered	Transpression	Riedel Shears, Thrust Faults	36, a-g

NATURAL EXAMPLES

The lack of a naturally occurring analogue to the San Andreas fault zone prevents direct comparative studies to be carried out on natural examples. The development of any theory based upon only one example would be somewhat short-sighted; therefore, by using a model's controlled, predictable environment, additional physical evidence can be obtained to aid in the elucidation of geologic processes. The combination of field and experimental data has helped increase our knowledge of potentially hazardous fault zones. The following are examples of hazardous fault zones that have deformational tendencies that can be re-created and therefore, predicted in experimental models.

Coalinga, California

The Coalinga earthquake (M = 6.7) of May 2, 1983, occurred 35 km northeast of the SAFZ, in an area characterized by numerous active folds and thrust faults oriented nearly parallel to the trace of the San Andreas fault. Similar active folds and thrust faults exist along the eastern flank of the Coast Ranges, as indicated by the Avenal, Idria, and Kettleman Hills earthquakes, among others (fig. 6) (Eaton and Rymer, 1990). Subsurface data, including focal mechanisms, seismic reflection and refraction, and well-log analysis, indicate that the structural configuration of the Coalinga area, and most likely the eastern Coast Ranges in general, is characterized by fault-bend folding above thrust faults that ramp up from a basal detachment fault (figs. 4 and 33) (Namson and Davis, 1988). This type of structural configuration cannot be explained in terms of

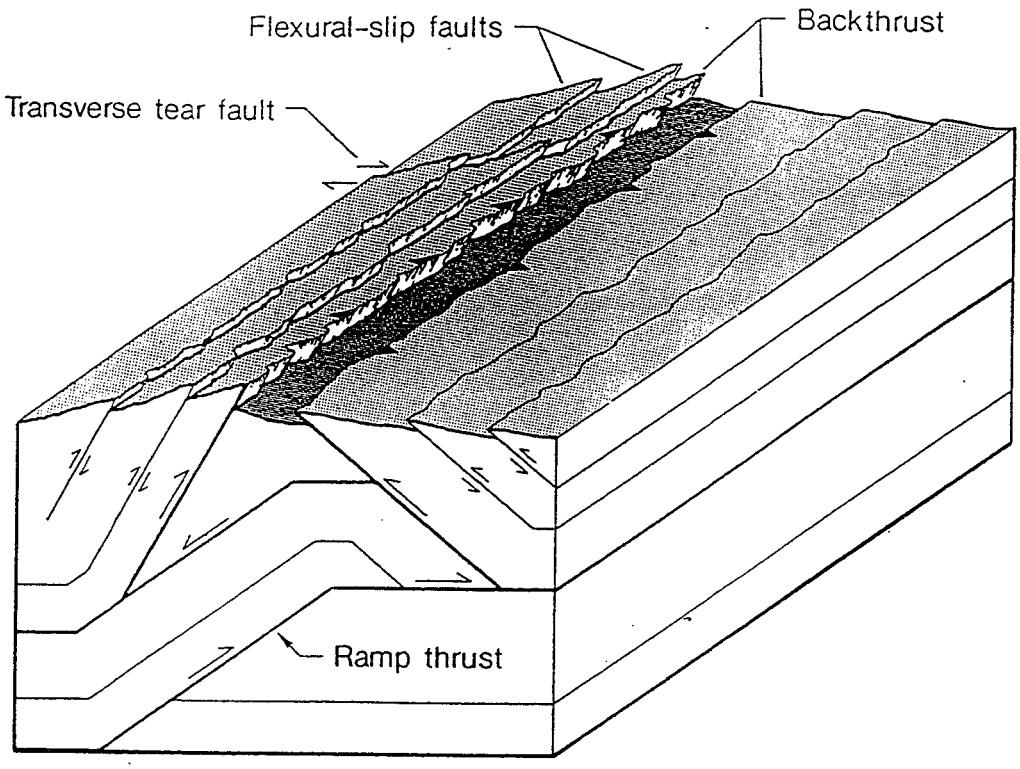

Figure 33. Block diagram illustrating hypothetical ramp-related structural features. This type of deformational structure may explain the deformational features observed stemming from the 1983, Coalinga earthquake sequence (modified from Namson and others, 1990).

wrench deformation along a high friction San Andreas fault. A more appropriate explanation, and one that matches the structural configuration of the low-friction gelatin models, is a low-friction, decoupled SAFZ that reduces shear stresses along the fault, and re-orients the maximum horizontal stress across the fault zone, resulting in a fault-parallel fold and thrust belt.

It is noteworthy that seismicity along the eastern flank of the Coast Ranges essentially terminates adjacent to the southern boundary of the creeping central segment of the SAFZ (fig. 34). Therefore, a genetic relationship may exist between the creeping central segment of the SAFZ and the seismically active fold and thrust belt along its flanks. There is also a marked northern seismic terminus roughly adjacent to the northern end of the creeping central segment of the SAFZ, near San Juan Bautista (fig. 10). However, this area is much more complex because of the presence of the active Calaveras fault. Structures in the San Francisco Bay region flanking the San Andreas, Hayward, Greenville, and Calaveras faults are also characterized by both fault-parallel thrust faults and folds, and structures indicative of high-friction wrench tectonics (fig. 8). It is possible that incipient strain softening along the Santa Cruz and Peninsula segments of the SAFZ, and the Hayward and Calaveras faults, has resulted in the initiation of thrust faults and folds oriented roughly parallel to the SAFZ. If the SAFZ continues to accommodate a large proportion of the movement between the Pacific and North American plates, progressive deformation of fault zone materials may lead to greater stress re-orientation, resulting in off-fault structures becoming gradually more active with time.

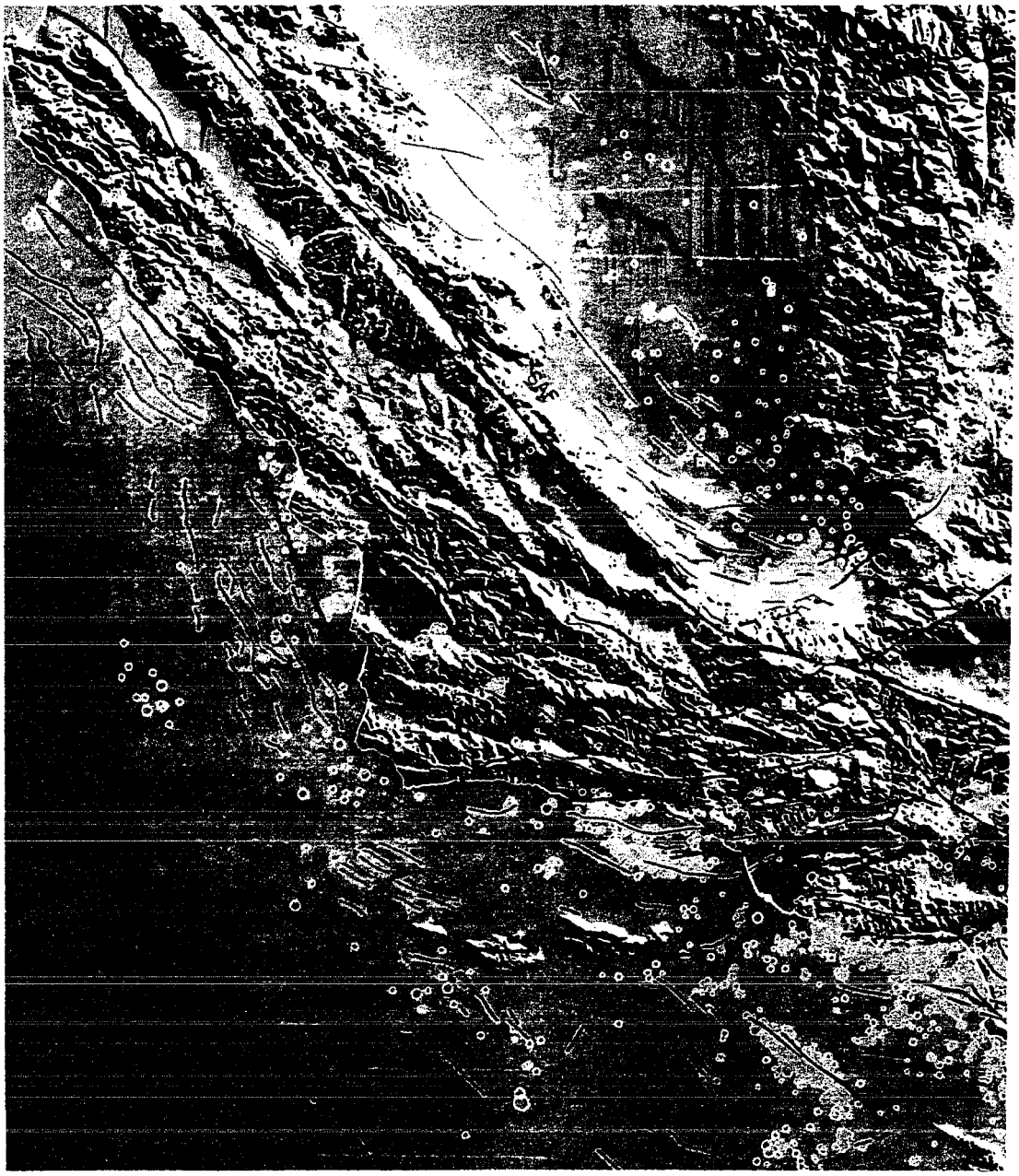

Figure 34. A digital shaded-relief map of central California showing faults (blue), fold axes (red), and seismicity (yellow circles). Note the correlation between the seismically active areas located along the eastern flank of the Coast Ranges, the creeping segment of the SAFZ, and the faults oriented roughly parallel to the trace of the SAFZ (modified from Wallace, 1990).

Newport-Inglewood fault, California

The Newport-Inglewood fault zone is located in the Los Angeles basin, and is considered to record deformation occurring along the Pacific-North American plate boundary. The fault zone is delineated by the alignment of hills and mesas oriented approximately N. 40° W. from Newport Beach to north of Inglewood, rather than by a well-defined, throughgoing fault zone (fig. 35). A discontinuous, en echelon array of active faults and folds has been mapped along the Newport-Inglewood fault zone (fig. 36) (Toppozada et al., 1989) and appears to conform to the Wilcox and others (1973) model experiment in which a clay layer is placed atop a master wrench at depth and deformed by dextral slip. The Newport-Inglewood fault is expressed by a series of oil-bearing anticlines and discontinuous secondary surface faults that appear to resemble surface deformation observed in the Wilcox model experiments (figs. 35 and 36). This fault zone may be a young feature, as implied by the lack of a well-developed surface trace, that is accommodating a portion of the plate boundary motion. A clockwise rotation of the Pacific plate 2.5 to 3.9 million years ago created a large angle of convergence (approximately 35° to 40°) across the southern segment of the SAFZ and may have initiated movement along secondary faults, such as the Newport-Inglewood fault. The trend of the Newport-Inglewood fault zone (N. 40° W.) is more suited to accommodate Pacific plate motion (N. 35° W.) than is the main trace of the San Andreas fault (N. 70° W.) along the nearby "big bend" area to the north. The Newport-Inglewood fault zone has deformational features similar to those seen in model experiments of young fault zones where

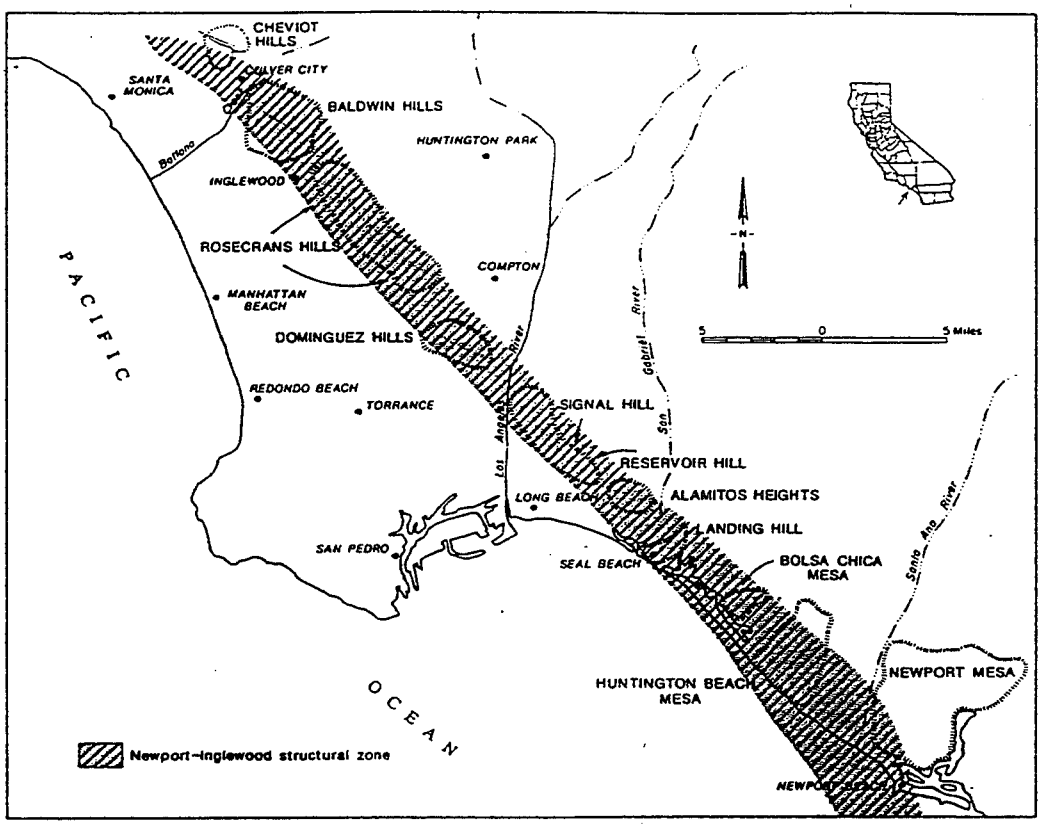

Figure 35. The Newport-Inglewood fault zone, southern California, showing alignment of folds, which are also zones of oil entrapment (modified from Toppozada and others, 1989).

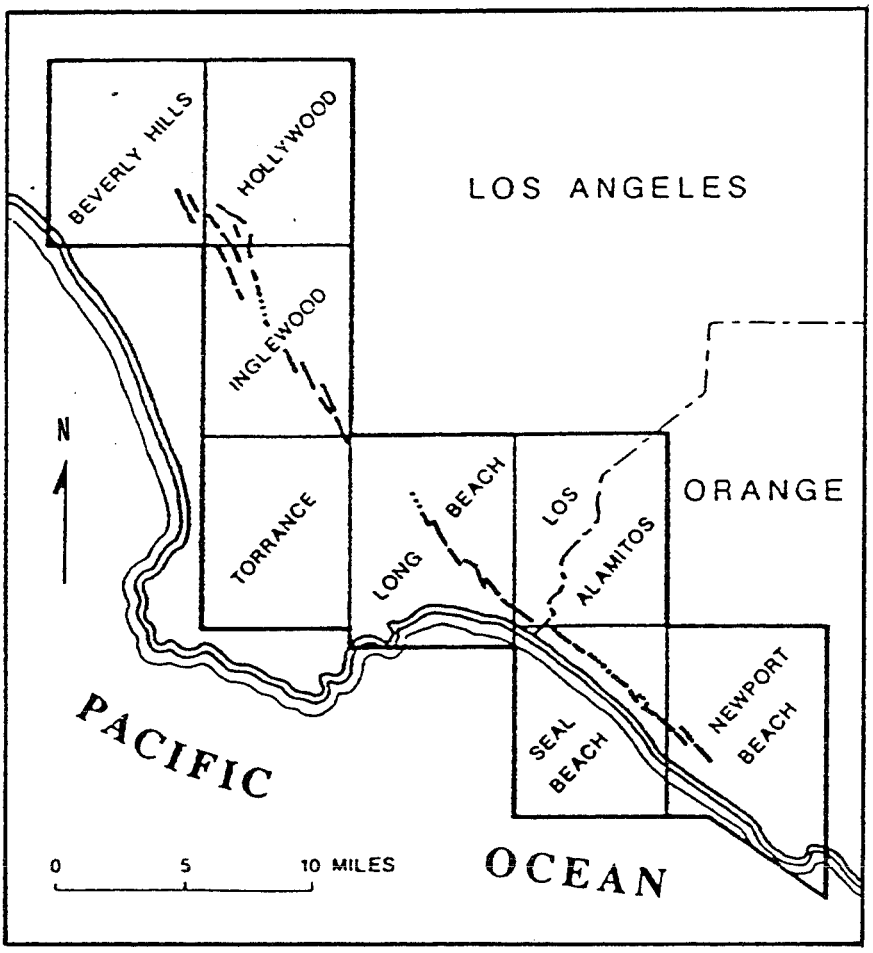

Figure 36. The Newport-Inglewood fault zone is not expressed by a well-defined, throughgoing fault zone, but is delineated the alignment of uplifted and folded hills, and the en echelon, discontinuous alignment of surface fractures, as shown above (modified from Toppozada and others, 1989).

incipient movement creates a "positive flower" type of structure, characteristic of high drag, wrench fault zones.

Alpine Fault, New Zealand

The Alpine fault of New Zealand is the surface expression of a major continental transform fault separating the Indian and Pacific plates. The Alpine fault is characterized by right-lateral, oblique convergence, resulting in large-magnitude earthquakes, similar to those on the SAFZ. Despite the general similarities between the Alpine and San Andreas fault zones, substantial differences exist. Structures surrounding the Alpine fault zone have orientations that suggest the fault zone may be characterized by high friction and drag, as depicted in the Wilcox and others (1973) model for the SAFZ.

The Alpine fault zone is characterized by nearly 20 mm/yr of convergence perpendicular to the fault, and 40 mm/yr parallel to the fault, with an angle of convergence between the Indian and Pacific plates of approximately 27°; the SAFZ has approximately 9 mm/yr of fault-normal convergence, 35 mm/yr of fault-parallel translation, and a 5° convergence angle along the central segment (Johnston and White, 1983; Scholz and others, 1979). The large component of convergence along the Alpine fault zone is responsible for the generation of thrust faults and rapidly uplifting mountain ranges. The amount of convergence is such that the Alpine fault zone is not a vertical fault, but has an easterly dip of approximately 50° to 60° (Allis, 1981) (fig. 37).

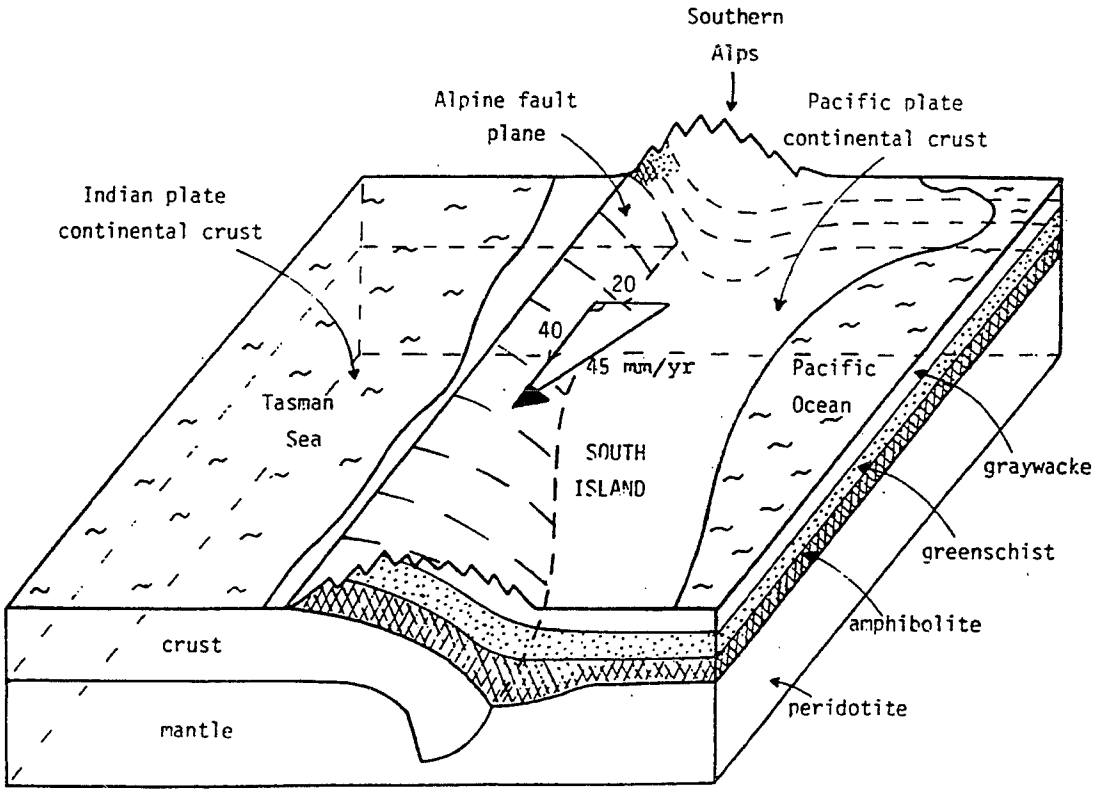

Figure 37. Block diagram illustrating the high-angle reverse nature of the Alpine fault, New Zealand. Motion vectors indicate the components of translational and compressional average yearly movement (modified from Allis, 1981).

The Alpine fault is a classic example of a continental transform fault with both vertical and horizontal components of motion acting across a singular, high-angle reverse fault. During the 1989 Loma Prieta earthquake, both vertical and horizontal (1.2 m vert. and 1.8 m horiz.) movement occurred along a 70° dipping rupture surface at a depth of approximately 18 km (Plafker and Galloway, 1989). The location of the Loma Prieta event along the restraining "little bend" of the Santa Cruz Mountains segment of the SAFZ, which is characterized by approximately 15° of plate convergence, indicates that, much like the Alpine fault zone, continental transform faults may not be exclusively vertical features.

DISCUSSION

The results of the modelling experiments performed in this study strongly support the recent theories of Zoback and others (1987), Mount and Suppe (1987), and Namson and Davis (1988), who have postulated that structures along the central segment of the SAFZ do not conform to frictional faulting theory. A more appropriate mechanism is a low-drag SAFZ that re-orients the convergent component of transpression into the maximum compressive stress. This type of mechanism is consistent with *in situ* stress field data, and is supported by surficial geologic expression and subsurface seismic activity. By applying the most recent San Andreas fault data to a scale model, physical and mechanical evidence can now be used to support the fault-normal compression theory.

This theory appears to be well suited to the central segment of the SAFZ where the presence of numerous fault-parallel folds and thrust faults is undeniable. The specific characteristics responsible for the stress re-orientation have yet to be resolved. However, the creeping nature of this segment of the SAFZ may play a critical role, as illustrated by the correlation of off-fault seismicity. The lack of seismic activity along the western flank of the central segment of the SAFZ indicates that lithologic variations and resultant competency contrasts may control deformation to a certain extent. The Salinian block granitoids appear to be much less susceptible to deformation than the Franciscan complex melange and Great Valley sequence. The relatively straight fault segment eliminates the possibility of "stuck spots" due to restraining bends, as is the case with the big and little bends to the south and north, respectively. In

all likelihood, a combination of these fault parameters creates the characteristic fault-normal compressional stress regime along the central segment of the SAFZ.

Geologic evidence for fault-normal compression is present along the northern portions of the SAFZ, but is not as pervasive as that of the central segment of the SAFZ. The majority of the region's seismicity occurs due to stick-slip movement along the major strike-slip faults. The relatively short seismic record does not indicate that large seismic events occur on thrust faults flanking the northern SAFZ. Most of the thrust faults in northern California are located relatively close to the trace of the San Andreas fault, possibly indicating a different mechanism is responsible for their genesis. The southern section of the Calaveras fault is actively creeping and has been associated with off-fault compressional seismicity. Few other natural examples exhibit characteristics similar to those of the creeping segment of the SAFZ, but this may be due to a lack of detailed studies. Therefore, the application of the model results and the relevance of the fault-normal compression theory remains to be seen.

The ability to apply the model results and the fault-normal compression theory to natural examples will be valuable for delineating seismic hazard zones. On a regional scale, the ability to accurately assess the stress state of a given region will aid in the characterization of potential ground motion. This is illustrated by comparing the 1983 (M = 6.7) Coalinga earthquake, which occurred in a compressional stress regime, to the 1983 (M = 7.1) Idaho earthquake, which was characterized by an extensional stress regime. The earthquakes occurred at similar depths, but there was an enormous inverse relationship between

earthquake magnitude and ground acceleration (McGarr, 1984). The Coalinga earthquake had much greater ground accelerations than that of the Idaho event, and civilian damages were nearly 20 times greater. The ability to recognize and predict regional and local stress regimes and earthquake mechanisms is important, and experimental modelling can be a valuable tool for this purpose. Recognizing structures associated with a decoupled fault zone, such as those adjacent to the central segment of the SAFZ, will aid in the delineation of specific hazardous zones that, until recently, have gone unnoticed.

REFERENCES CITED

Allis, R.G., 1981, Continental underthrusting beneath the Southern Alps, New Zealand: Geology, v. 9, p. 303-307.

Aydin, A., and Page, B.M., 1984, Diverse Pliocene-Quaternary tectonics in a transform environment, San Francisco Bay region, California: Geological Society of America Bulletin, v. 95, p. 1303-1317.

Bartlett, W.L., Friedman, M., and Logan, J.M., 1981, Experimental folding and faulting of rocks under confining pressure: Tectonophysics, v. 79, p. 255-277.

Cloos, H., 1928, Experimenten zur Inneren Tektonik: Centralbl f. Mineralogie, Abt. B. 609-621.

Cloos, E., 1955, Experimental analysis of fracture patterns: Bulletin of the Geological Society of America, v. 66, p. 241-256.

Courtillot, V., Tapponnier, P., and Varet, J., 1974, Surface features associated with transform faults: A comparison between observed examples and an experimental model: Tectonophysics, v. 24, p. 317-329.

Cox, A., and Engebretson, D., 1985, Change in motion of Pacific plate at 5 million years before present: Nature, v. 313, p. 472-474.

Eaton, J.P., 1990, The earthquake and its aftershocks from May 2 through September 30, 1983, *in* Rymer, M.J., and Ellsworth, W.L., eds., The Coalinga, California, earthquake of May 2, 1983: U.S. Geological Survey Professional Paper 1487, p. 113-170.

Eaton, J.P., and Rymer, M.J., 1990, Regional seismotectonic model for the southern Coast Ranges, *in* Rymer, M.J., and Ellsworth, W.L., eds., The Coalinga, California, earthquake of May 2, 1983: U.S. Geological Survey Professional Paper 1487, p. 97-111.

Emmons, R.C., 1969, Strike-slip rupture patterns in sand models: Tectonophysics, v. 7, p. 71-87.

Graham, S.A., Stanley, R.G., Bent, J.V., and Carter, J.B., 1989, Oligocene and Miocene paleogeography of central California and displacement along the San Andreas fault: Geological Society of America Bulletin, v. 101, p. 711-730.

Harbert, W., 1991, Late Neogene relative motions of the Pacific and North America plates: Tectonics, v. 10, no. 1, p. 1-15.

Harding, T.P., 1976, Tectonic significance and hydrocarbon consequences of sequential folding synchronous with San Andreas faulting, San Joaquin Valley, California: American Association of Petroleum Geologists Bulletin, v. 60, p. 356-378.

Hempton, M.R., and Neher, K., 1985, Experimental fracture, strain and subsidence patterns over en echelon strike-slip faults: Implications for the structural evolution of pull-apart basins: Journal of Structural Geology, v. 7, p. 597-605.

Henyey, T.L., 1968, Heat flow near major strike-slip faults in central and southern California: Pasadena, California Institute of Technology , Ph.D., thesis, 421 p.

Horsfield, W.T., 1977, An experimental approach to basement controlled faulting, *in* Frost, R.T.C., and Dikkers, A.J., eds., Fault tectonics in norhtwest Europe: Geologie Mijnb., v. 56, p. 363-370.

Hubbert, M.K., 1937, Theory of scale models as applied to the study of geologic structures: Bulletin of the Geological Society of America, v. 48, p. 1459-1521.

_____, 1951, Mechanical basis for certain familiar geologic structures: Bulletin of the Geological Society of America, v. 62, p. 355-372.

Johnston, D.C., and White, S.H., 1983, Shear heating associated with movement along the Alpine fault, New Zealand: Tectonophysics, v. 92, p. 241-252.

Kennedy, W.Q., 1946, The Great Glen fault: Geological Society of London Quarterly Journal, v. 102, p. 41-76.

Lachenbruch, A.H., and McGarr, A., 1990, Stress and heat flow, *in* Wallace, R.E., ed., The San Andreas fault system, California: U.S. Geological Survey Professional Paper 1515, p. 261-283.

Lachenbruch, A.H., and Sass, J.H., 1973, Thermomechanical aspects of the San Andreas fault system, *in* Kovac, R.L., and Nur, A., eds., Proceedings of the conference on tectonic problems of the San Andreas fault system: Stanford, California, Stanford University Publications in the Geological Sciences, v. 13, p. 192-205.

Lowell, J.D., 1972, Spitzbergen Tertiary orogenic belt and the Spitzbergen fracture zone: Geological Society of America Bulletin, v. 82, p. 3091-3102.

Mandl, G., De Long, L.N.J., and Maltha, A., 1977, Shear zones in granular material: Rock Mechanics, v. 9, p. 95-144.

McClay, K., 1976, The rheology of plasticine: Tectonophysics, v. 33, p. T7-T15.

McGarr, A., 1984, Scaling of ground motion parameters, state of stress, and focal depth: Journal of Geophysical Research, v. 89, p. 6969-6979.

Minster, J.B., and Jordan, T.H., 1984, Vector constraints on Quaternary deformation of the western United States east and west of the San Andreas fault, *in* Crouch, J.K., and Bachman, S.B., eds., Tectonics and sedimentation along the California margin: Society of Economic Paleontologists and Mineralogists, Pacific Section Annual Convention, San Diego, v. 38, p. 1-16.

_____, 1987, Vector constraints on western United States deformation from space geodesy, neotectonics, and plate motions: Journal of Geophysical Research, v. 92, p. 4798-4804.

Mount, V.S., and Suppe, J., 1987, State of stress near the San Andreas fault: Implications for wrench tectonics: Geology, v. 15, p. 1143-1146.

Namson, J.S., and Davis, T.L., 1988, Seismically active fold and thrust belt in the San Joaquin Valley, central California: Geological Society of America Bulletin, v. 100, p. 257-273.

Namson, J.S., Davis, T.L., and Lagoe, M.B., 1990, Tectonic history and thrust-fold deformation style of seismically active structures near Coalinga, *in* Rymer, M.J., and Ellsworth, W.L., eds., The Coalinga, California, earthquake of May 2, 1983: U.S. Geological Survey Professional Paper 1487, p. 113-170.

Naylor, M.A., Mandl, G., and Sijpesteijn, C.H.K., 1986, Fault geometries in basement-induced wrench faulting under different initial stress states: Journal of Structural Geology, v. 8, p. 737-752.

Odonne, F., and Vialon, P., 1983, Analogue models of folds above a wrench fault: Tectonophysics, v. 99, p. 31-46.

Oertel, G., 1965, The mechanism of faulting in clay experiments: Tectonophysics, v. 2, p. 343-393.

Oldenburg, D.W., and Brune, J.N., 1972, Ridge transform fault spreading pattern in freezing wax: Science, v. 178, p. 301-304.

Plafker, G., and Galloway, J.P., eds., 1989, Lessons learned from the Loma Prieta, California, earthquake of October 17, 1989: U.S. Geological Circular 1045, p. 7.

Riedel, W., 1929, Zur Mechanik geologischer Brucherscheinungen, Zb. Miner. Geol. Palaeont. Abh. B, 354-368.

Scholz, C.H., Beavan, J., and Hanks, T.C., 1979, Frictional metamorphism, argon depletion and tectonic stress on the Alpine fault, New Zealand: Journal of Geophysical Research, v. 84, p. 6770-6982.

Stanley, R.G., 1987, New estimates of displacement along the San Andreas fault in central California based on paleobathymetry and paleogeography: Geology, v. 15, p. 171-174.

Stesky, R.M., and Brace, W.F., 1973, Estimation of frictional stress of the San Andreas fault from laboratory measurements, *in* Kovac, R.L., and Nur, A., eds., Proceedings of the conference on tectonic problems of the San Andreas fault system: Stanford, California, Stanford University Publications in the Geological Sciences, v. 13, p. 206-214.

Sylvester, A.G., 1988, Strike-slip faults: Geological Society of America Bulletin, v. 100, p. 1666-1703.

Tapponnier, P., Peltzer, G., Le Dain, A.Y., and Armijo, R., 1982, Propagating extrusion tectonics in Asia: New insights from simple experiments with plasticine: Geology, v. 10, p. 611-616.

Tchalenko, J.S., 1970, Similarities between shear zones of different magnitudes: Geological Society of America Bulletin, v. 81, p. 1625-1640.

Toppozada, T.R., Bennett, J.H., Borchardt, G., Saul, R., and Davis, J.F., 1989, Earthquake planning scenario for a major earthquake on the Newport-Inglewood fault zone: California Geology, v. 42, p. 75-84.

Working Group On California Earthquake Probabilities, 1990, Probabilities of large earthquakes in the San Francisco Bay region, California: U.S. Geological Survey Circular 1053, 51 p.

Wallace, R.E., 1990, Geomorphic expression, *in* Wallace, R.E., ed., The San Andreas fault system, California: U.S. Geological Survey Professional Paper 1515, p. 15-58.

Waring, G.A., 1908, Congress Springs to San Juan, *in* Lawson, R.B., chairman, California earthquake of April 18, 1906: Report of the State Earthquake Investigation Commission: Carnegie Institution of Washington Publication 87, 2 vols., p. 109-111.

Wilcox, R.E., Harding, T.P., and Seely, D.R., 1973, Basic wrench tectonics: American Association of Petroleum Geologists Bulletin, v. 57, p. 74-96.

Zoback, M.D., and Zoback, M.L., 1980, State of stress in the conterminous United States: Journal of Geophysical Research, v. 85, p. 6113-6156.

Zoback, M.D., Moos, D., Mastin, L.G., and Anderson, R.N., 1985, Wellbore breakouts and in situ stress: Journal of Geophysical Research, v. 90, p. 5523-5530.

Zoback, M.D., Zoback, M.L., Mount, V.S., Suppe, J., Eaton, J.P., Healy, J.H., Oppenheimer, D., Reasenberg, P., Jones, L., Raleigh, C.B., Wong, I.G., Scotti, O., and Wentworth C., 1987, New evidence on the state of stress of the San Andreas fault system: Science, v. 238, p. 1105-1111.